Numerical Simulation of Road Salt Impact at the Greenbrook Well Field, Kitchener, Ontario

by

Michelle L. Bester

A thesis
presented to the University of Waterloo
in fulfilment of the
thesis requirement for the degree of
Master of Science
in
Earth Sciences

Waterloo, Ontario, Canada, 2002

© Michelle Lynne Bester, 2002

I hereby declare that I am the sole author of this thesis. This is a true copy of the thesis, including any required final revisions, as accepted by my examiners.

I understand that my thesis may be made electronically available to the public.

Michelle Lynne Bester

Abstract

Chloride concentrations at the Greenbrook well field in Kitchener, Ontario, have been steadily increasing over the past several decades and may soon pose a threat to drinking water quality. Drinking water limits at some wells have already been exceeded.

The Regional Municipality of Waterloo (RMOW) relies mainly on local groundwater resources for its drinking water supply, and the Greenbrook well field is the oldest of 50 municipal well fields contributing to this supply. Urban growth and the expansion of city limits over the years has surrounded the well field, placing it in a high risk area in need of protection. As such, protection of this water supply is essential until alternative sources can be found.

Road salt has been identified as the prime source of the chloride contamination, and various management alternatives and remediation strategies are currently being studied. In order to characterize the behaviour of chloride in the subsurface, an understanding of the mechanisms that control travel of chloride to the water table and through the groundwater system is needed. For the first phase of this work, a 2-D variably-saturated flow and transport model (SWMS-2D) was used to evaluate the effect of seasonal fluctuation in chloride loading to a generic aquifer system. Chloride was applied over the surface of the model in seasonal pulses that correlated with temperature and precipitation. The model showed a dampening of the seasonal response with depth that lead to the conclusion that long-term transport models can neglect seasonal changes in solute loading.

For the second phase of this work, a proven 3D finite element transport model (Waterloo Transport Code: WTC) was used to simulate road salt impacts to the well field. Road salt was applied over selected roads throughout the steady-state capture zone via a type 3 (Cauchy) boundary that varies both temporally and spatially with road type and location. After calibrating the model from 1945 to 2002 to chloride concentrations using the weighted average of 5 Greenbrook production wells, the model was run to the year 2041 to assess future implications. Remediation strategies were also investigated via 6 predictive scenarios in which chloride applications were reduced by varying degrees. The results of this phase will be used by the RMOW in cost-benefit analyses of alternative de-icing approaches versus de-chlorination treatment of the well water.

Acknowledgments

I would like to thank my advisors, Dr. Emil Frind, Dr. John Molson and Dr. Dave Rudolph for the unique opportunity to do interesting and real-life applicable research. Aside from supporting me academically, Emil has become like a father to me and I will be forever grateful for him introducing me to the world of modelling and renewing my appreciation for science. His advice and patience has not gone unappreciated.

Special thanks of course to John, who provided his vast technical expertise, countless theoretical explanations and debates and became a great friend throughout the process (and was almost tempted to sign up for the "How to Deal with Difficult People" seminar because of it). His friendship was key to this thesis being accomplished, and I will miss him beyond words. Also thanks to Dave, who provided insight and focus to this work and was always available for encouragement or direction.

A large thank-you goes to the modelling group (past and present) which includes, Michael Mößner, Dawood Muhammad, Tony Radcliffe (for getting my blood pressure up with our constant arguments) and Tessa Di Iorio, for providing me with precipitation data and letting me use her computer. Special thanks to Tessa and Jen Hurley for helping me with preparation in the final stages of this work, as well as to Sue Fisher, who never stopped smiling and never hesitated to help me through many administrative issues in the last two years.

Financial support was provided to me through NSERC in collaboration with the Water Services Division of the Regional Municipality of Waterloo. Additional thanks to Jim Robinson and Eric Hodgins, for kindly allowing me to work in their office, and Craig Johnston and Jayme Campbell of Stantec for helping with data needs, direction and focus in the overall Chloride Reduction Project.

Finally, I couldn't have finished this thesis without the non-stop support from all of my family in the past two years: Dad, Mom & Rob, Jay, Robbie & Naomi, Joyce, Randy, Don & Judy, Grandma & Grandpa, Grandpa B, Terra, Tess, Holly, Missy and Travis and all the others. And of course, Christoph♡, for always knowing what to say.

The most beautiful experience we can have is the mysterious. It is the fundamental emotion which stands at the cradle of true art and true science.

- *Albert Einstein (1879-1955)*

Water, water everywhere, Nor any drop to drink.

- *Samuel Coleridge*

Contents

List of Figures

List of Tables

Chapter 1

Introduction

1.1 Study Background

As urban populations continue to grow, greater demand is being placed on water resources to supply drinking water. In many cases, drinking water supplies are compromised as anthropogenic contamination of urban well fields becomes more likely with urban development. In recent years, the protection of critical aquifers has become essential as municipalities are starting to re-evaluate various land-use practices that threaten drinking water quality.

As a leading municipality in the field of groundwater protection and management, the Regional Municipality of Waterloo (RMOW) has undertaken a comprehensive approach through the development of the Water Resources Protection Strategy (WRPS). The WRPS is aimed at reducing the risk of contamination to surface water and groundwater from historic and existing land use practices, as well as future land uses. An element of this program is to conduct an extensive research program to delineate well head protection areas and to identify and map sensitive areas as well as identify potential threats and sources of contamination to sensitive areas.

As one of Canada's fasting growing regions with a current population of about 430,000 covering approximately 1360 km^2 (Figure 1.1), the RMOW encompasses four townships: Wellesley, Wilmot, Woolwich and North Dumfries and three cities: Waterloo, Kitchener, and Cambridge. Municipal water supply for the RMOW is provided by an integrated system of groundwater and surface water supplies; approximately 75% of the RMOW water supply is currently provided by groundwater and the remaining 25% is provided by surface water. The groundwater component

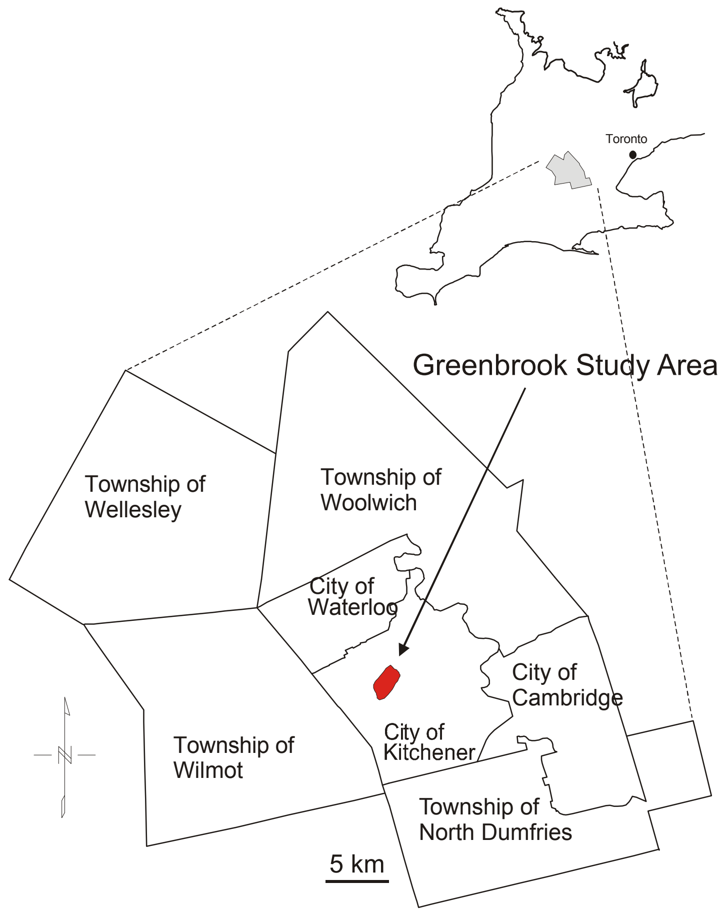

Figure 1.1. Location of the Regional Municipality of Waterloo and the Greenbrook study area.

of the total water supply is provided by 126 pumping wells, grouped into about 50 municipal well fields.

Given the importance of groundwater from a water supply perspective and as part of the WRPS program, the RMOW has recently reviewed trends in water quality at a number of its municipal well fields. As part of this review, elevated chloride and sodium concentrations have been identified at a number of well fields. While only a few wells have chloride concentrations exceeding Ontario Drinking Water Standards (ODWS), of greater concern is the increasing trends at most of the wells, particularly in urban cores.

The Greenbrook well field in the city of Kitchener is one such case where city limits have expanded within and beyond the well field, placing it in a high contamination risk urban environment. It extracts water from a complex multi-aquifer system called the Waterloo Moraine, which historically has provided an excellent source of drinking water in terms of both quantity and quality. The Greenbrook well field produces about 15 million litres of water a day or about 12% of the water supply for the RMOW. As such, it provides the second largest source of groundwater to the cities of Kitchener and Waterloo, next to the Mannheim South well field which is located outside of city limits in a rural environment. Interestingly enough, these two well fields show contrasting situations at present; the Greenbrook well field was originally situated outside city boundaries but is now considered an urban well field, surrounded by development, and chloride concentrations are increasing rapidly. The Mannheim well field, on the other hand, is on the verge of being enveloped by the same urban annexation that Greenbrook had experienced 20 years earlier. A sound understanding of the water resources at Greenbrook and its susceptibility to contamination must be obtained and applied for future land-use planning and protection of other well fields such as Mannheim.

Water pumped from the Greenbrook well field has been showing steadily increasing chloride concentrations for several years. In an unpublished report, *Farvolden and Weitzman* [1980] were the first to observe elevated levels of chloride in the well field. Possible sources of the chloride include leachate from the nearby Ottawa Street Landfill, mineralized water from a deeper aquifer underlying the pumped aquifers, or road salt. Several previous studies have suggested that the high chloride content found in most of the wells originates from a nearby salt dump and/or local road salting [*Farvolden and Weitzman*, 1980][*Woeller and Farvolden*, 1989][*Fritz et al*, 1991]. In light of these findings, the RMOW has recognized the need to better evaluate the potential impacts of winter road salting on groundwater supplies. They are also estimating future chloride trends and are testing road salt reduction measures at the Greenbrook well field. In 2001, the Road Salt Management and Chloride Reduction Study, an element of the WRPS program, was initiated by the RMOW to determine the preferred option for stabilizing or reducing the concentrations of chloride in drinking water. The overall objective of this study is to determine the preferred option for stabilizing or reducing the concentration of chloride in drinking water at the RMOW well fields that are close to or exceeding the ODWS for chloride.

In order to fill the current and future demands for drinking water, proper management including enhancement and protection of the existing well fields is essential. Consequently, management of the Greenbrook well field will play a key role in the future supply of groundwater to the Kitchener-Waterloo area. Before effective management strategies can be developed, an understanding of the potential sources, such as road salt, and their impacts to water quality at the well fields must be determined. A study of these impacts, particularly of chloride contamination in the Greenbrook well field, may also serve to assess future impacts on other well fields in the area that may not yet have been subjected to such dramatic urban growth.

1.2 History and Operation of the Greenbrook Well Field

The Greenbrook well field has been in operation since the late 1800s and was originally located within a swampy area where artesian springs fed into the adjacent Shoemaker pond at the northern edge of the site (Figure 1.2). In 1888, Shoemaker Pond was developed as the first major municipal water source for Kitchener. Within ten years, wells were installed and during this time, the water being extracted was under artesian conditions and flowed freely without pumps. As water levels declined, pumping was soon required to meet the demand of the growing city.

Considerable testing and developing has been completed over the years and the field now comprises five production wells (K1, K2, K4b, K5a, K8) and some 54 observation wells, of which 19 have been installed in conjunction with research projects at the University of Waterloo. In addition, records are available for a number of other test holes drilled by the University which are now abandoned. Because the University of Waterloo researchers have focused their efforts on the Greenbrook well field, this area has the best stratigraphic and hydrological control of all the well fields around Waterloo.

The production wells pump into adjacent reservoirs at varying rates; from there water is delivered from the reservoirs into the municipal water mains. Production of the well field is scheduled to maintain a safe level in the reservoirs. From October to April, the demand is relatively low, and wells are normally pumped from early morning to early evening about 12 hours per day. During the rest of the year, demand is higher and wells are sometimes continuously pumped for several days. The schedule is not firmly fixed because demand varies considerably through the week and is lowest on weekends and holidays. Demand also varies according to weather conditions and production from other well fields.

The well field is located within parklands in a residential area but may be vulnerable to contamination by past and present industrial, commercial, road maintenance, and waste disposal activities. Contamination by road salt, by trace amounts of volatile organic compounds (VOCs) and by poor quality water from the bedrock has been noted in previous studies [*CH2M-Hill Ltd., 1995*]. Leachate from the former Kitchener Landfill site (about 0.9 km southeast of the well field) may also be migrating northward and affecting water quality.

Figure 1.2. Greenbrook well field with current production wells.

1.3 Physiography and Climate

The Greenbrook well field lies on the eastern flank of the Waterloo Moraine (750 km^2), which is believed to have formed by the complex interlayering of till sheets deposited by the Huron and Georgian Bay lobes from the northwest and north, and the Erie and Ontario lobes from the south and southeast. The Waterloo Moraine consists of glacio-fluvial deposited sands and gravels with interfingering till units. These till units are sometimes discontinuous, due to erosion during periods of glacial retreat. The topography of the area is characteristic of a moraine environment with an undulating hummocky surface and isolated swampy areas and ponds where the water table intersects the ground surface. Glacial sediments overlying the Salina formation consist of locally discontinuous tills and coarse glacio-fluvial material. Texturally, the glacial sediments range from fine clay to coarse-cobbled gravels, and this heterogeneous distribution of texture in the Greenbrook well field is reflected in zones of highly variable hydraulic conductivity, ranging from 8.5×10^{-4} to 10^{-10} m/s [*Béland*, 1977].

The study area is underlain by layers of soft, sedimentary limestones, shales and sandstones, deposited in the Paleozoic era [*Chapman and Putnam*, 1984]. Locally, two formations, the Guelph formation and the Salina formation, are present at the bedrock surfaces [*Sanford*, 1969]. According to Sanford, the contact line between these two formations is located almost directly below the Greenbrook well field.

There is some natural protection for the Greenbrook wells afforded by aquitards (primarily glacial till units) which separate and confine the sand and gravel aquifers. However, “windows”, which are located where the till units are absent, provide pathways for contaminants to enter the lower two aquifers.

Local relief in the vicinity is 12-15 metres and the upper slopes on the sandy soil are well drained. Springs are common on the lower slopes which give rise to small marshes and streams such as Schneider Creek which drains to the Grand River, several miles to the southeast. The streams occupy well-defined channels that follow depressions in the topography. Generally these lowlands are broad and flat and underlain by outwash and gravel. The natural drainage was poor with extensive springs, swamps and ponds, but the main channels have now been improved. Borden Greenway and Voisin Greenway drain urbanized areas to the south and southwest, and meet near the center of the well field to form Shoemaker Creek. Shoemaker Pond is in a deep, closed depression, and drains only at high water stages into Shoemaker Creek.

Winter weather conditions within the area are highly variable with a winter weather system travelling through Ontario every 3 to 5 days. The Waterloo Region climate is semi-humid with the average winter daily temperatures typically around -5°C and annual precipitation of 917 mm. Of the precipitation that falls in the area, 158 mm/year falls as snow and ice. On average, 65 days of the year have measurable snowfall [*Environment Canada*, 1993].

1.4 Road Salt Use

The application of road-de-icing chemicals to urban and rural roads in southern Ontario during the last 50 years has become a standard solution to keeping winter driving conditions safe. Residents living in these areas have come to expect bare-road driving conditions throughout the winter and consequently millions of tonnes of road salt have been applied freely to the highways and city streets. It is estimated that approximately 4.75 million tonnes of sodium chloride were used as road salt in the winter of 1997-98 and that 110,000 tonnes of calcium chloride are used on roadways in a typical year [*Environment Canada, 2001*]. Based on these estimates, about 4.9 million tonnes of road salt is released to the environment in Canada every year, accounting for about 3.0 million tonnes of chloride. The highest annual loadings of road salt on a road-length basis are in Ontario and Quebec. In the past, the general assumption has been that most of the applied road salt is flushed through overland flow and into sewers and the environmental impact is minimal.

In the vicinity of Kitchener-Waterloo, road salting began by the townships in the late 40s. During this time, road salts were used as de-icing and anti-icing chemicals for winter road maintenance, with some use as summer dust suppressant on dirt roads. Until the late 50s, a 95:5 sand to salt mixture was used for de-icing purposes. As the benefits of driving on bare pavement became clear, mixtures ranging from 2:1 to 5:1 sand to salt were used. This ratio is still used on paved rural areas throughout Ontario. When the RMOW was established in 1973, almost all primary roads within the urban areas were receiving pure salt. Currently, a standard rate of application of road salt is 141 kg/km of 2-lane highway. Salting normally begins in the RMOW on November 15th, and ends March 31st.

Road salt can enter the groundwater system via three sources: salt storage areas, disposal sites for salt-contaminated snow removal from roadways, and salt applied to pavements as a de-icing agent. Across North America, there are numerous documented cases of groundwater contamination from all three sources of road salt [*Pollock*, 1992][*Pilon and Howard*, 1987][*Locat and Gélinas*, 1989][*Howard et al*, 1993][*Howard and Haynes*, 1993][*Gutiw and Jin*, 1998][*Novotny et al*, 1999][*Stantec,* 2001]. However, salt applied to roadways represents by far the largest and most damaging source of anthropogenic salt contamination in groundwater [*Jones et al, 1986*][*Perchanok et al*, 1991].

Road salts that enter the environment through application to roadways enter surface water, soil and groundwater after snowmelt and are dispersed through the air by splashing and spray from vehicles and as wind-borne powder. One of the primary concerns associated with inorganic sodium chloride road salts is their high solubility in water. The dissociated ions will migrate with infiltrating precipitation to the water table. This is not always the case for cations such as sodium, which can be affected by cation exchange reactions in certain geological environments. Chloride ions are conservative, and migrate with water without being retarded. Accordingly, all chloride ions that enter the soil and groundwater can ultimately be expected to reach surface water, although this may take from a few years to several decades.

Natural background concentrations of chloride in non-bedrock aquifers are generally no more than a few milligrams per litre, with some local or regional instances of higher natural salinity. High chloride concentrations are most often associated with road salt application, releases from storage yards or snow dumps. For example, chloride concentrations over 18,000 mg/l were observed in runoff from roads [*Environment Canada*, 2001]. Chloride concentrations up to 82,000 mg/L were also observed in runoff from uncovered blended abrasive/salt piles in a patrol yard [*Environment Canada*, 2001]. Chloride concentrations in snow cleared from city streets (measured in equivalent volume of water) can also be quite variable. For example, the average chloride concentration in snow cleared from streets in Montreal was 3000 mg/L for secondary streets and 5000 mg/L for primary streets. Waters from roadways, patrol yards or snow dumps can also be diluted to various degrees when entering the environment. Adjacent to storage yards, chloride concentrations have been measured as high as 2800 mg/L in groundwater, 4000 mg/L in ponds and wetlands, 4300 mg/L in watercourses, 2000-5000 mg/L in urban impoundment lakes and 150-300 mg/L in rural lakes [*Environment Canada*, 2001]. While the highest concentrations are usually associated with winter or spring thaws, high concentrations can also be measured in the summer, as a result of the travel time to surface waters and the reduced water flows in the summer.

Groundwater contamination by road salt chemicals has been studied extensively in "snow belt" regions such as southern Ontario, Finland and the northeastern corridor of the U.S.. A study in the Boston area found that if 20 tonnes of salt were applied per 2-lane km during a winter season, chloride levels in groundwater near major highways could exceed 250 mg/L [*Huling and Hollocher*, 1972]. One of the earliest studies in Canada was that done by *Paine* [1979], who performed a chloride mass balance on the Don River watershed in Toronto, Ontario, and found that as little as 50% of the NaCl being applied to the watershed was being removed by surface water flow. *Frost et al* [1981] estimate that 20% of the chloride applied during de-icing procedures in Massachusetts re-entered surface waters through the ground water system. *McConnell and Lewis* [1972] estimate that between 25% and 50% of the salt used on a road infiltrates the groundwater.

Also within the Greater Toronto Area, *Pilon and Howard* [1987] reported chloride concentrations as high as 14,000 mg/L in shallow sub-surface waters adjacent to a salted urban Toronto highway. This study also found that contamination resulting from application of road salt had been detected at a depth of 3.3 m and at a distance of 100 m from major urban roads.

Applied research on the impact of road salt has been ongoing in the state of Massachusetts [*Pollock*, 1992]. This study found that reduced application rates, the use of alternative de-icing materials and the redesign of road drainage systems have been very effective in reducing the concentration of chloride in local groundwater systems. In Finland, several innovative measures have already been implemented as a result of extensive studies and subsequent recommendations [*Nystén, per. comm.*, 2001] including sealing ditches with bentonite and weather controlled speed limits. The Finnish Water and Environment Districts along with the Road Districts in Finland have been engaged in a national risk assessment project since the early 90s with the aim to establish the magnitude of the risk faced by groundwater areas of becoming polluted by road salting [*Kivimäki*, 1994].

Data on concentrations of salts in groundwater are frequently discussed in literature in terms of exceeding drinking water quality guidelines. In Canada, these are set on the basis of taste thresholds at 200 mg sodium/L and 250 mg chloride/L [*CCME*, 1998]. Recently in Canada, road salts have been recommended by the Environment Minister to be added as a priority substance under the Canadian Environmental Protection Act [*CEPA*, 1999]. If passed, Environment Canada will begin looking at risk management measures to reduce environmental impacts associated with the use of winter road salts.

1.5 Study Objectives

This study focuses on two key areas and is divided into 4 chapters. Chapter 1 provides background information and an introduction to the problem at hand. In Chapter 2, the first phase of this study, a 2D vertical variably-saturated flow and transport model is developed to study transport of road salt from ground surface through the unsaturated zone to the water table. The objective of this phase is to quantitatively assess the physical mechanisms and time frame for salt transport through the unsaturated and saturated zones. This phase of the modelling component is completed using an existing code for variably saturated flow and transport, with the salt mass-flux input treated as a transient function, with the highest loading rates in the spring. The results are also used to validate a key assumption in

Chapter 3 in which salt transport through the unsaturated zone is assumed to be a steady state process where seasonal transients can be neglected. By studying the dampening of the transient input pulses with depth in the 2D model, the validity of the steady-state approach in Chapter 3 can be assessed.

In Chapter 3, the second phase of the research, transport of chloride from the road network within the Greenbrook area is simulated within a fully 3D multi-aquifer system. This phase is a continuation of previous work by *D. Muhammed* [2000] which showed that road salt was the most likely source for the increase in chloride seen at the wells. These previous simulations, however, assumed simplified source functions and an accurate calibration was not attempted. In this phase, the model is extended to include a more realistic source function which includes growth of the road network over the past 50 years, and variable chloride loading rates based on road type and year. The model is calibrated using observed chloride data at the Greenbrook pumping wells and predictive simulations with remediation scenarios are presented. The overall objective of this phase is to determine the general behaviour of chloride plumes developing from road salt sources, to analyze their impact at the Greenbrook wells, and to assess the impact of a variety of salt load reduction scenarios.

Chapter 4 presents a summary of findings, concluding remarks and future recommendations for remediation of the well field.

Overall, the objective of this study is to implement advanced numerical simulation tools to further investigate the mechanisms of chloride transport and will provide the RMOW with the tools to understand the scope of the chloride contamination at Greenbrook. In particular, this study can be used as a catalyst to conduct a cost-benefit analysis of the remediation options presented and to develop a sound strategy for reducing chloride impacts on urban well fields.

Chapter 2

2D Model - Effect of Seasonal Loading

2.1 Introduction

The degree to which road salts may have an impact on the groundwater environment will vary significantly depending on the road salt loading, climatic conditions, surface and subsurface soil conditions, and the location of the site within the overall hydrogeological environment. Although there has been some work completed on chloride contamination in groundwater, as well as chloride retention in the unsaturated zone, very little work has focussed on the seasonal fluctuations of road salt throughout the unsaturated zone.

Chloride concentration profiles in the unsaturated zone show very different trends depending on the season the profile was taken. In field work completed by *Stantec* [2001], profiles in the unsaturated zone show a consistent chloride "bulge" in the centre of profiles taken from a Kitchener well field in the late summer and fall. *Locat and Gélinas* [1989] found that profiles showed the highest concentrations at ground surface and at the water table; however, the date of these profiles is unknown. The same study also found that about one year's worth of salt was retained in the unsaturated zone. Some discrepancies are also due to the material distribution of the profile. For instance, in *Toler and Pollock* [1974], it was found that chloride concentrations increased with an increase in finer-grained materials, in accord with the assumption that the chloride is in solution in pellicular water in the soil. It was also found that the amount of chloride retained in the unsaturated zone reached a plateau soon after the first salting season and did not increase significantly afterward.

In previous modelling studies, it has been assumed that seasonal chloride pulses entering the subsurface dampen with depth, therefore seasonal loading variations can be neglected and replaced by a steady-state source, distributed evenly throughout the year. This assumption has been reinforced in the Kitchener-Waterloo area by the fact that chloride concentrations in the local wells do not seem to reflect seasonal road salting events.

In this chapter, a conceptual flow and transport system is simulated to determine travel times of chloride in the unsaturated zone and to examine the effect of seasonal source loading events characteristic of those in the Kitchener-Waterloo area. The purpose of this chapter is to verify the assumption that seasonal variations in road salt application and transient precipitation events can be neglected in long-term 3D modelling approaches. Although some observed data are available for areas within the RMOW, the focus will be on developing an understanding of the general hydraulic and transport processes rather than to calibrate a site-specific conceptual model.

2.2 Numerical Model

The past several decades have seen considerable progress in the conceptual understanding and mathematical description of water flow and solute transport processes in the unsaturated zone. A variety of analytical and numerical models are now available to predict water and/or solute transfer processes between the soil surface and the groundwater table. For this work, SWMS_2D [*Šimúnek et al.*, 1994] has been used. This program numerically solves the Richards' equation for saturated-unsaturated water flow and the convection-dispersion equation for solute transport. The code can be used to analyze water and solute movement in unsaturated, partially saturated, or fully saturated porous media. The flow solution considers prescribed head and flux boundaries, as well as boundaries controlled by atmospheric conditions.

The governing flow and transport equations are solved numerically using Galerkin-type linear finite element schemes. Assuming that the air phase plays an insignificant role in the liquid flow process, the governing flow equation is given by the following modified form of the Richards' equation:

$$\frac{\partial \theta}{\partial t} = \frac{\partial}{\partial x_i}[K(K_{ij}^A \frac{\partial h}{\partial x_j} + K_{iz}^A)] - S \tag{2.1}$$

where θ is the volumetric water content [L^3L^{-3}], h is the pressure head [L], S is a sink term [T^{-1}], x_i ($i = 1, 2$) are the spatial coordinates [L], t is time [T], K_{ij}^A

are components of a dimensionless anisotropy tensor K^A, and K is the unsaturated hydraulic conductivity function[LT^{-1}] given by:

$$K(h, x, z) = K_s(x, z)K_r(h, x, z) \tag{2.2}$$

where K_r is the relative hydraulic conductivity and K_s is the saturated hydraulic conductivity [LT^{-1}}. The anisotropy tensor K_{ij}^A is used to account for an anisotropic medium.

Depending on the size of the problem, the matrix equations resulting from discretization of the governing equations are solved using either Gaussian elimination for banded matrices, or the conjugate gradient method for symmetric matrices and the ORTHOMIN method for asymmetric matrices [*Mendoza et al, 1991*]. The program is an extension of the variable saturated flow code of *Vogel* [1987], which in turn was based in part on the early numerical work of Neuman and colleagues [*Neuman*, 1972],[*Neuman*, 1973],[*Neuman et al*, 1974],[*Neuman*, 1975],[*Davis and Neuman*, 1983].

The unsaturated soil hydraulic properties in this code are described by a set of closed-form equations resembling those of *van Genuchten* [1980] who used the statistical pore-size distribution model of *Mualem* [1976] to obtain a predictive equation for the unsaturated hydraulic conductivity function. The soil retention, $\theta(h)$, and hydraulic conductivity, $K(h)$, functions in SWMS-2D are given by the following in reduced form:

$$\theta(h) = \begin{matrix} \theta_r + \frac{\theta_s + \theta_r}{(1+|\alpha h|^n)^m} & h < 0 \\ \theta_s & h \geq 0 \end{matrix} \tag{2.3}$$

$$K(h) = \begin{matrix} K_s K_r(h) & h < 0 \\ K_s & h \geq 0 \end{matrix} \tag{2.4}$$

where:

$$K_r = S_e^{\frac{1}{2}} \left[1 - (1 - S_e^{\frac{1}{m}})^m \right]^2 \tag{2.5}$$

$$m = 1 - \frac{1}{n}, n > 1 \tag{2.6}$$

$$S_e = \frac{\theta - \theta_r}{\theta_s - \theta_r} \tag{2.7}$$

in which θ_r and θ_s are the residual and saturated water contents, respectively, and K_s is the saturated hydraulic conductivity. A linear scaling procedure (using n and α) is implemented to approximate the soil hydraulic characteristics in a given area. The water content term in the numerical formulation ($\Delta\theta/\Delta t$) is evaluated using the mass-conservative method proposed by *Celia et al.* [1990] [*Šimúnek et al*, 1994].

The solution of Eqn. 2.1 requires knowledge of the initial distribution of the pressure head within the flow domain, for t=0:

$$h(x, z, t) = h_0(x, z) \tag{2.8}$$

where h_0 is a prescribed function of x and z.

SWMS_2D has the option of three different types of boundary conditions. These boundary conditions are specified pressure head (Dirichlet, Type 1) given by:

$$h(x, z, t) = \phi(x, z, t) \tag{2.9}$$

specified flux (Neumann, Type 1), given by:

$$-[K(K^A_{ij}\frac{\partial h}{\partial x_j} + K^A_{iz})]n_i = \phi_1(x, z, t) \tag{2.10}$$

and specified gradient, given by:

$$(K^A_{ij}\frac{\partial h}{\partial x_j} + K^A_{iz})n_i = \phi_2(x, z, t) \tag{2.11}$$

where ϕ $[L]$, σ_1 $[LT^{-1}]$, and σ_2 $[-]$are prescribed functions of x, z,and t; and n_i are the components of the outward unit vector normal to the boundary.

The governing equation for two-dimensional chemical transport during transient water flow in a variably saturated porous medium is:

$$\frac{\partial \theta c}{\partial t} + \frac{\partial \rho s}{\partial t} = \frac{\partial}{\partial x_i}(\theta D_{ij}\frac{\partial c}{\partial x_j}) - \frac{\partial q_i c}{\partial x_i} + \mu_w \theta c + \mu_s \rho s + \gamma_s \rho - Sc_s \tag{2.12}$$

where c is the solution concentration [ML^{-3}], s is the adsorbed concentration [-], q_i is the i-th component of the volumetric flux [LT^{-1}], μ_w and μ_s are first-order rate constants for solutes in the liquid [$ML^{-3}T^{-1}$] and solid [T^{-1}] phases, respectively; γ_w and γ_s are zero-order rate constants for the liquid [$ML^{-3}T^{-1}$] and solid [T^{-1}] phases, respectively; ρ is the soil bulk density [ML^{-3}], S is the sink term in the water flow equation (2.1), c_s is the concentration of the sink term [ML^{-3}], and D_{ij} is the dispersion coefficient tensor [L^2T^{-1}]. The components of the dispersion tensor for two-dimensional transport are as follows:

$$\theta D_{xx} = D_L\frac{q_x^2}{|q|} + D_T\frac{q_z^2}{|q|} + \theta D_d \tau \tag{2.13}$$

$$\theta D_{zz} = D_L \frac{q_z^2}{|q|} + D_T \frac{q_x^2}{|q|} + \theta D_d \tau \tag{2.14}$$

$$\theta D_{xz} = D_L - D_T \frac{q_x q_x}{|q|} \tag{2.15}$$

where D_d is the molecular diffusion coefficient in free water [L^2T^{-1}], τ the tortuosity [-], $|q|$ is the absolute value of the fluid flux [LT^{-1}]; and D_L and D_T are the longitudinal and transverse dispersivities, respectively [L].

The solution of Eqn. 2.12 requires an initial condition within the flow region, given by

$$c(x, z, 0) = c_i(x, z) \tag{2.16}$$

where c_1 is a prescribed function of x and z.

SWMS_2D has the option of two different types of transport boundary conditions. These boundary conditions are specified concentration (Dirichlet, Type 1) given by:

$$c(x, z, t) = c_o(x, z, t) \tag{2.17}$$

and specified solute flux (Cauchy, Type 3), given by:

$$-\theta D_{ij} \frac{\partial c}{\partial x_j} n_i + q_i n_i c = q_i n_i c_0 \tag{2.18}$$

in which $q_i n_i$ represents the outward fluid flux, n_i is the outward unit normal vector, and c_0 is the concentration of the incoming fluid.

During the work for this thesis, the code was modified to allow transient flow and transport boundaries. Daily fluctuations in road salt applications could therefore be accommodated. The code was further modified to accept both a type 3 transport boundary and a type 2 flow (atmospheric) boundary on the same node, and also to write output files that are compatible with a post-processor (TECPLOT[1]) to enable rapid visualization.

2.3 Conceptual Model

A simple conceptual model was developed which included chloride transport from a road surface to the water table and down-gradient through the saturated zone (Figure 2.1). This test case consists of a 2D vertical section, with atmospheric

[1]TECPLOT; V9.0; Amtec Engineering, Inc. (1988-1996)

and hydrogeological parameters chosen based on a general representation of the Waterloo Moraine area. For simplicity, the porous medium is considered to be both homogeneous and isotropic. A fine sand was selected as the material type, with the material and transport properties modified within reasonable limits to improve plume definition. The hydraulic conductivity is 0.298 m/day and the porosity is 0.30. The uniform grid has element dimensions of 0.5 m in both directions, extending 25 metres in length and 15 metres in elevation. This grid spacing was sufficient to satisfy the Peclet stability criteria at $1.3 < \mathrm{Pe} < 1.6$, well within reasonable limits. Similarly, the Courant criteria of $\mathrm{Cr} < 1$ was also satisfied with a maximum time step of 0.01 days.

The boundary conditions consist of a constant head boundary at the left (Type 1; $\phi = 10.2$ m), a constant head boundary at the right (Type 1, $\phi = 9.8$ m) and an initial head of 10 m throughout the saturated domain which positions the water table at an elevation of 10 m. An impermeable boundary is prescribed at the bottom of the domain.

Along the top of the domain, a variable recharge boundary (Type 2, average flux $(\overline{q_n}) = 0.3$ m/yr) is used to simulate seasonal recharge fluctuations. The amount of precipitation that infiltrates to the water table depends on a number of factors, including the duration and intensity of the rainfall event, the initial soil moisture content and the soil moisture characteristics. Based on the general temperature and precipitation patterns in Canada, the majority of groundwater recharge in a year is expected to occur in the late winter and early spring, as a result of winter snowmelt and spring rains [*Gerber and Howard*, 1997].

Daily recharge was calculated using Waterloo Region precipitation normals, combined with daily temperature readings. Runoff and evaporation were subtracted from the precipitation data using an annual average to give a yearly net infiltration (which becomes available for recharge) of 300 mm, a value that is representative of the Greenbrook area. Because precipitation that occurs during the winter months remains in snow-bank storage until the spring thaw, precipitation from such times was carried over each day until temperatures rose. For long-term storage, this “release” of precipitation into the ground was lagged to simulate melting of the accumulated snow pack over several days or weeks, depending on the accumulated amount. This was done by directly correlating ground temperature with precipitation events, releasing snowmelt according to suitable infiltration rates during periods of ground thaw. Figure 2.2 shows the resulting daily recharge incorporated into the model.

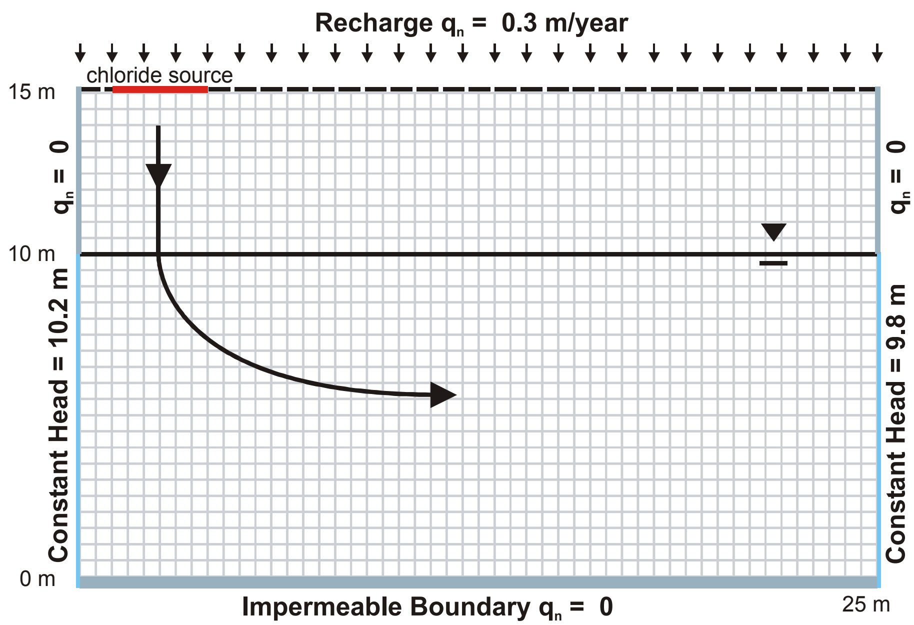

Figure 2.1. Hypothetical base case conceptual model

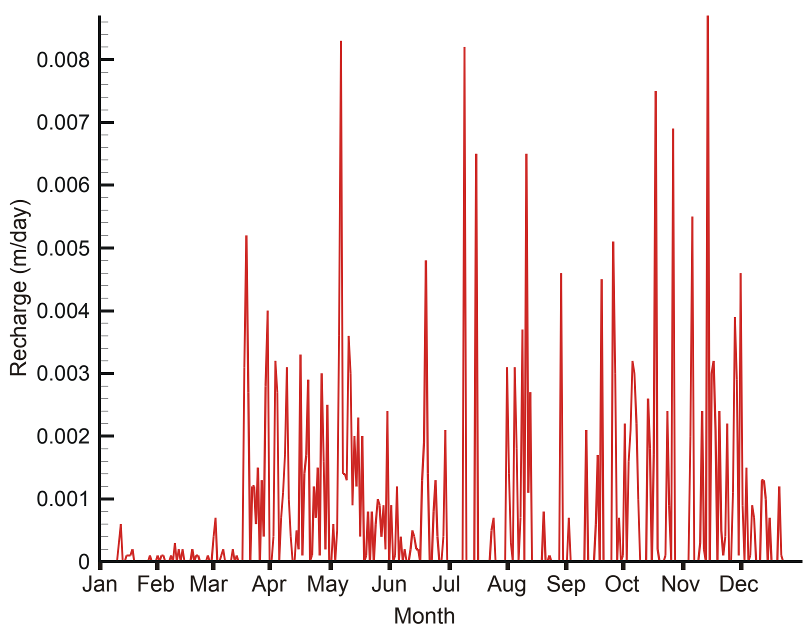

Figure 2.2. Estimated daily recharge for the Greenbrook study area

Simple moisture retention and hydraulic conductivity functions that describe the relationships between moisture content, potential and hydraulic conductivity for a soil in the unsaturated zone are given by *van Genuchten* [1980] and have five fitting parameters, as seen in Section 2.2. The hydraulic parameters for this conceptual model are shown in Table 2.1 and are based on that of a typical sandy medium [*Šimúnek et al.*, 1994]. The soil moisture curve for these parameters is presented in Figure 2.3.

$K_k = K_{sat}$	$= 0.298$	m·day^{-1}
θ_r	$= 0.02$	
$\theta_k = \theta_{sat}$	$= 0.3$	
α	$= 0.1$	m^{-1}
n	$= 0.3$	

Table 2.1. Hydraulic parameters

To simulate chloride transport, a longitudinal dispersivity of 0.6 m and a transverse dispersivity of 0.04 m was used, as well as a diffusion coefficient of $5 \times e^{-5}$ m^2/ day. Literature values for the same aquifer material and scale were reviewed, and a sensitivity analysis was preformed using the range of dispersivities given in the literature. The final values were then chosen to produce a well-defined plume in both the unsaturated and saturated zones.

A Cauchy boundary (Type 3) was placed at the top surface of the domain, from $x = 1$ m to $x = 4$ m. The daily loading rate for this boundary was obtained by using a total annual road salt application typical of a primary roadway of 50 tonnes per 2-lane kilometre per season [*Stantec, 2001*] distributed throughout the year according to a weekly distribution for a typical year in southern Ontario (Figure 2.4)[*Howard and Haynes*, 1993]. With this distribution of road salt loading combined with daily 10-year average ambient temperatures in the study area, the daily chloride loading was estimated taking into consideration that chloride is not suddenly loaded into the subsurface at first application, but is loaded gradually during the spring months (Figure 2.5) as the snowpack thaws. Accordingly, chloride loading was lagged based on a) the concept that precipitation does not enter the subsurface as recharge until ambient air temperature is sufficient to melt the snowpack and b) the concept that chloride-laden recharge will enter the subsurface at a slightly lower temperature than normal due to its thawing characteristics. It should be noted however, that the oscillatory behaviour of the chloride loading function in the winter months in Figure 2.5 are due to the three stages of snowmelt on roads [*Novetny et al*, 1999] and were neglected for this work. These calculations also incorporate the estimation that as much as 50% of road salt applied onto the roads is available to enter the subsurface [*Paine*, 1979]. The resultant masses were divided by the daily recharge (R) to acquire a daily nodal concentration according to the following equation, assuming a unit nodal influence area of 1 m^2:

$$C = \frac{M}{R \cdot A}$$

where M is the mass (kg/day), C is the concentration (kg/m^3) and A is the nodal influence area (m^2). The estimated daily application of chloride to the subsurface is presented as mass in Figure 2.6 and as a concentration in Figure 2.7.

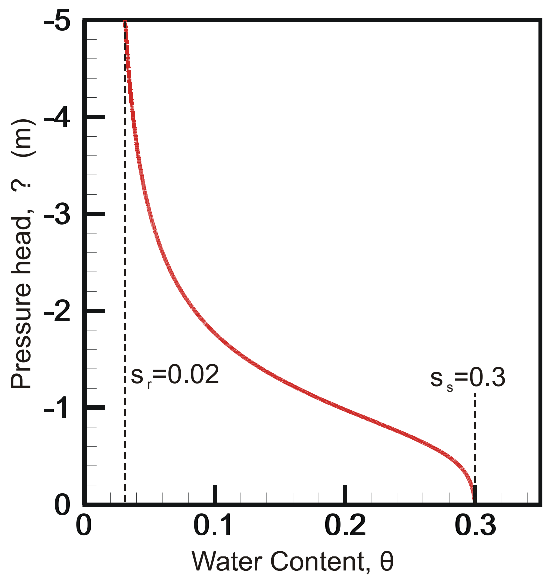

Figure 2.3. Soil moisture curve for base case scenario.

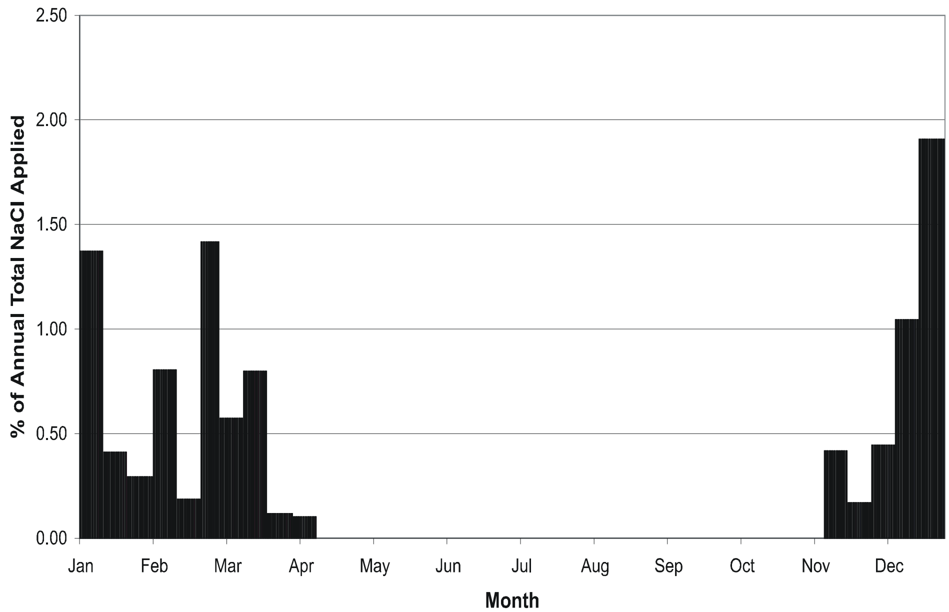

Figure 2.4. Weekly NaCl distribution (after *Howard and Haynes*, 1993).

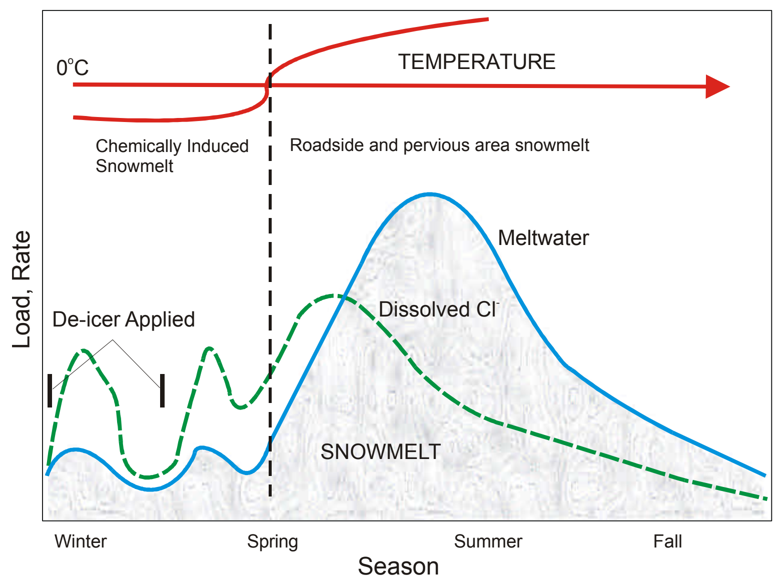

Figure 2.5. Time elapsed snow melt and subsequent chloride load (adapted from *Novetny et al, 1999*).

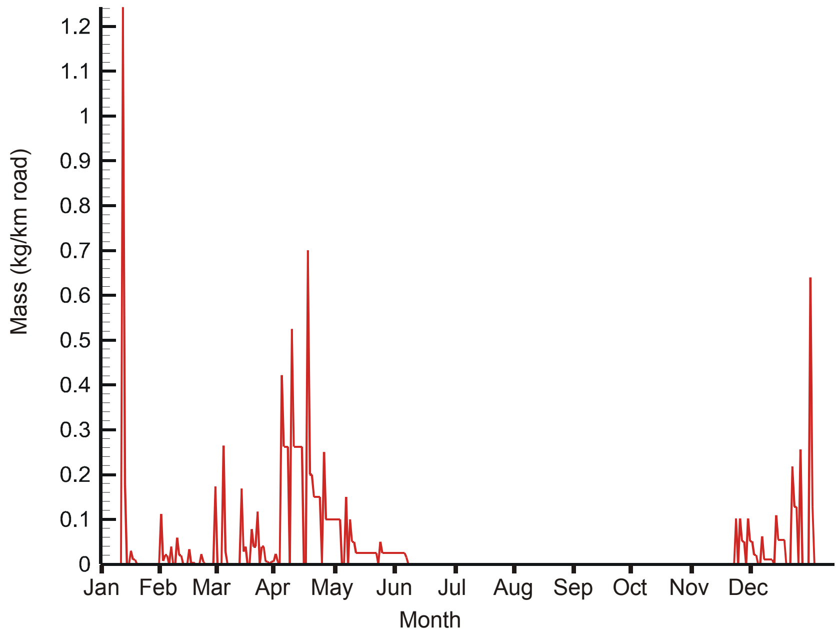

Figure 2.6. Estimated daily chloride loading in mass applied per 2-lane km of road.

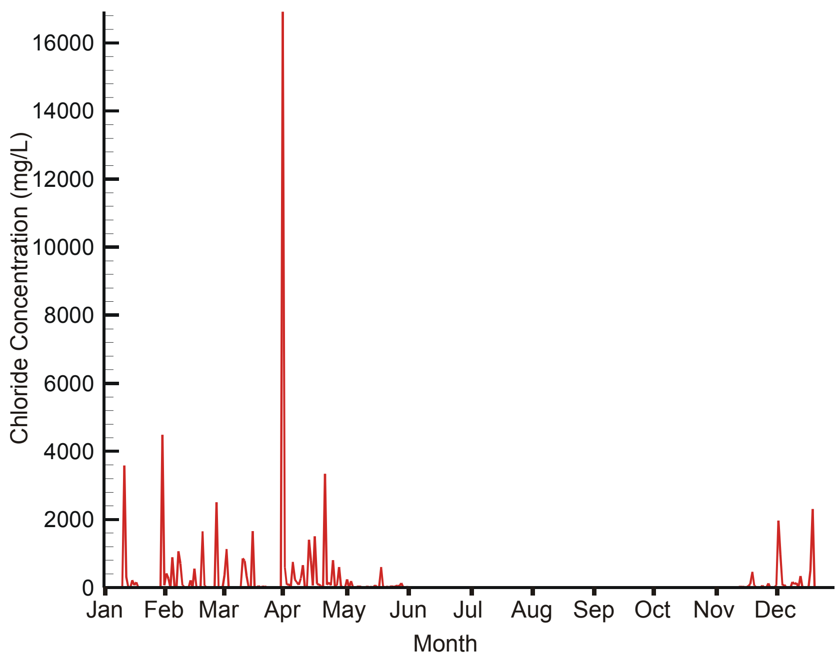

Figure 2.7. Estimated daily chloride concentrations applied to source boundary.

It should be noted that density effects are not considered in the flow calculations for this model. With a preliminary simulation, it was found that the source concentrations used in Figure 2.7 resulted in concentrations in the subsurface to be significantly less than the limit at which density effects occur. For reference, sea water normally has a chloride concentration of 25,000 mg/L.

The main objective in this chapter is to estimate the extent of seasonal effects on the behaviour of chloride migration in the unsaturated zone. Different types of hydrogeological conditions were selected to represent variations of aquifers in the Greenbrook area, and chloride loading variations. The scenarios in Table 2.2 were simulated.

Scenario	**v (m/day)**	**Water Table Depth (m)**	**Source Input**
Base Case	0.015	5	gradual loading
A	0.007	5	gradual loading
B	0.030	5	gradual loading
C	0.015	2.5	gradual loading
D	0.015	5	sudden pulse
E	0.015	5	uniform loading

Table 2.2. 2D variably-saturated scenarios.

The flow velocity was changed by adjusting the constant head boundaries on the sides of the domain to increase or decrease the hydraulic gradient. All of the scenarios used the same total annual mass for the source input; however, the distribution of the mass was varied over time. In scenario D, the sudden pulse was distributed over 14 days from April 6th to April 20th of each simulation year. In scenario E, the chloride loading was distributed uniformly over 365 days of each simulation year. This last scenario most closely reflects conditions assumed in the 3D model.

2.4 Results - Base Case

The base case scenario was simulated to 3650 days (10 years), which was sufficient to reach steady state conditions, as indicated by the stabilization of the chloride plume. The simulated piezometric contours for the parameter set described in Section 2.3, at 3650 days, is presented in Figure 2.8. The effect of the atmospheric boundary (top) is evident as the hydraulic head is high at the top of the domain and decreases towards the water table. Similarly, the constant head boundaries result in a flow direction from left to right. The pressure head distribution at 3650 days (Figure 2.9) shows a slight pressure gradient from left to right, in the direction of flow. The saturation of the system (Figure 2.10) indicates a clearly defined water table at about 11 m, which is 1 m above the water table prescribed in the initial conditions. The water table rise is due to the atmospheric (recharge) flux entering in through the top boundary. The slight curves above the water table at the sides of the domain are the results of a boundary effect, where water mounds slightly due to the impermeable boundary.

The migration of the chloride plume throughout the seasons for the base case scenario (Figure 2.11) illustrates that chloride becomes significantly diluted once it reaches the water table. This is due to concentration being directly related to water content. For example, a volume of porous medium in the unsaturated zone containing the same mass of salt as a corresponding volume in the saturated zone will have a higher concentration than the latter due to the lower water content. This figure also shows the difference in the nature of the plume in the spring, when chloride loading is high and recharge is high, and the fall, where chloride from the previous spring is being diluted by fresh water. When the winter's snow begins to thaw during the spring season, chloride in the meltwaters starts to infiltrate into the subsurface (Figure 2.11, left column). Infiltration continues with each precipitation event until all the chloride has been flushed from the ground surface. By fall, enough fresh water has infiltrated to flush the chloride well below the ground surface (Figure 2.11, right column). Travel time from the first major loading event until the chloride reaches the water table is about 150 days.

Many factors contribute to the phenomenon of the remaining residual plume in the unsaturated zone. Foremost, both in the simulations and in the field, concentrations are calculated as a mass per volume of water. In the unsaturated zone, a certain mass of solute will have a higher concentration in a less-saturated medium than in a higher saturated medium. Further, the residual chloride plume is diluted from water both above, due to incoming precipitation, and below, due to fluctuations in the water table and possible mixing in the capillary fringe. When the water table depth is shallow, this residual plume is less pronounced. In nature, the same principle can be applied. In addition, other factors not modelled in this study could reinforce this phenomenon such as evapotranspiration processes which would result in chloride being precipitated upwards with dry, warm weather. Root uptake as summer vegetation grows can also result in chloride plumes being "pulled" upwards, however it is unlikely that this would have a large effect.

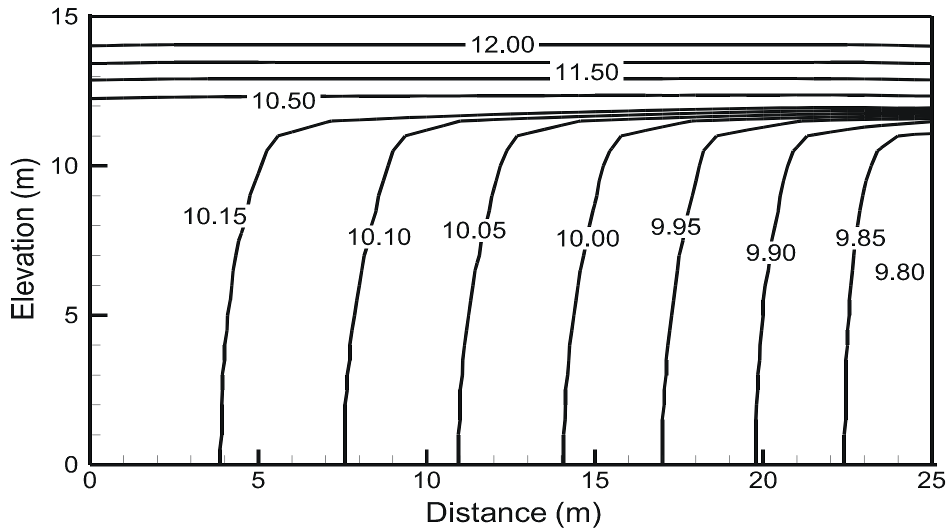

Figure 2.8. Piezometric contours (m) at 3650 days; base case scenario.

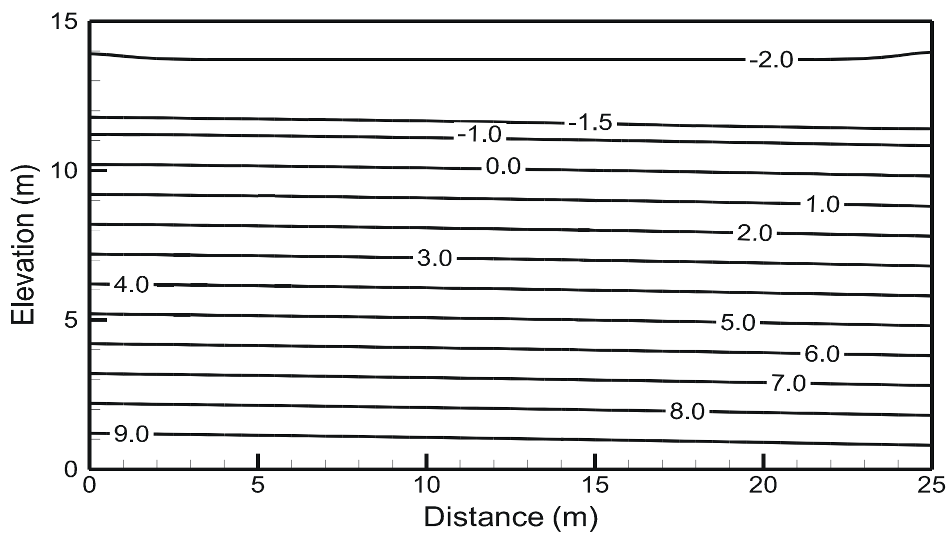

Figure 2.9. Hydraulic pressure distribution at 3650 days; base case scenario. Contours in metres.

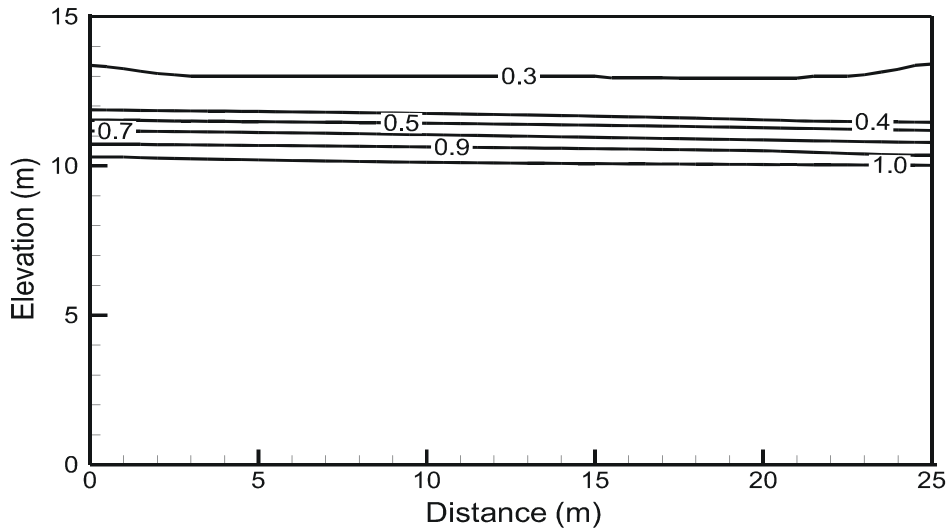

Figure 2.10. Saturation profile at 3650 days; base case scenario.

Breakthrough curves at the observation points labelled in the cross sections can be seen in Figure 2.12. These breakthrough curves clearly show seasonal effects above the water table, and dampening of the source pulse with depth. The breakthrough curve at the top node near the surface sharply reflects the source loading as seen in Figure 2.7, especially during the first season of chloride loading since there is limited fresh water entering the system to further dilute the concentration. After the first season of chloride loading, fresh water enters the system and allows flushing of chloride towards the water table resulting in a residual plume in the midsection of the unsaturated zone.

Initially, dispersivities were adjusted to gauge sensitivity of the plume and the dampened response. In these preliminary simulations, it was found that the final values of 0.6 m and 0.04 m for the longitudinal and transverse dispersivities, respectively, gave the best plume definition at this scale. However, when the dispersivities were increased it was found that the seasonal pulses were further dampened by the increase in mixing, and vice versa.

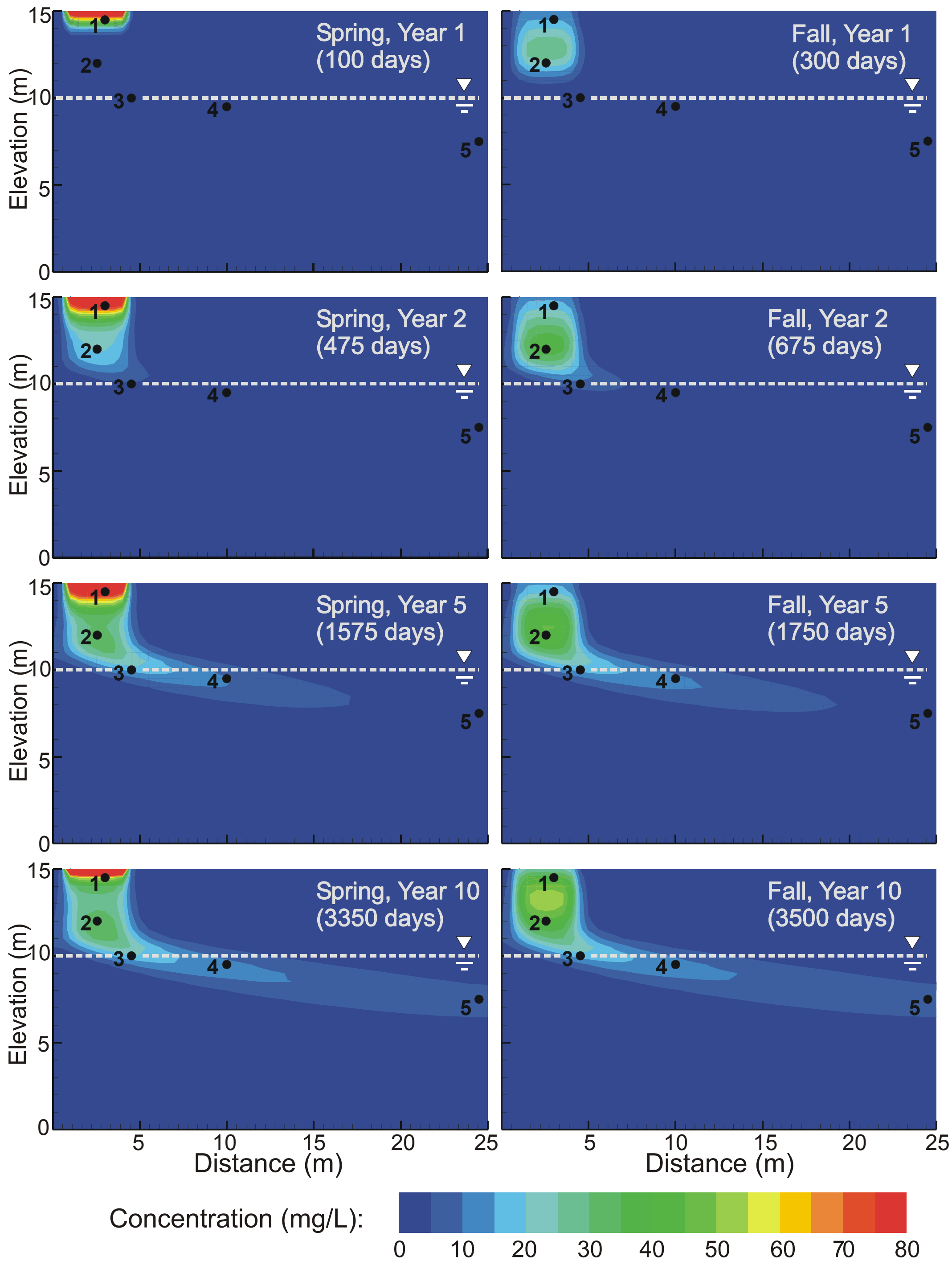

Figure 2.11. Concentration profiles for the base case, numbers refer to breakthrough point locations.

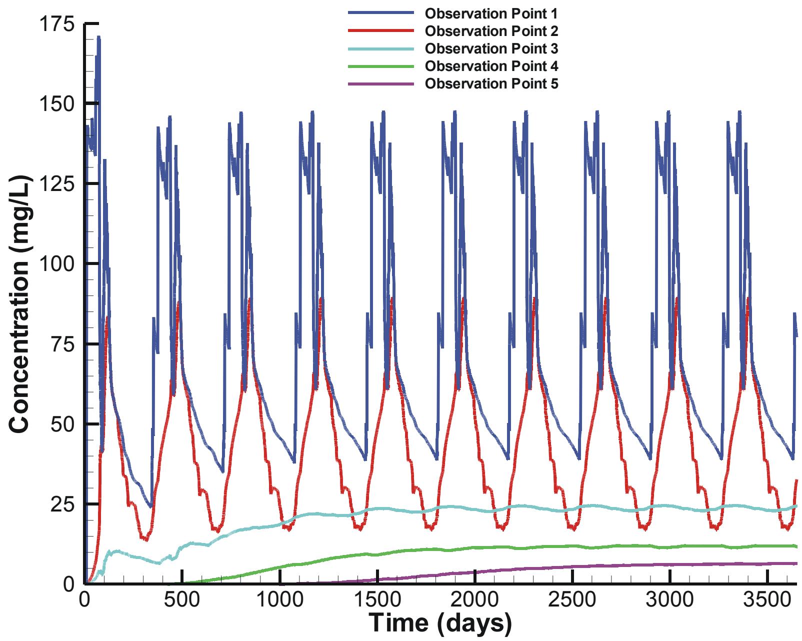

Figure 2.12. Base case breakthrough curves at observation points (labelled on figure 2.11).

2.5 Results - Scenario Analysis

The concentration profiles for both the base case and scenarios A through C at 3560 days (December 31st, 10th year) show that the maximum concentration within the subsurface is approximately 75 mg/L (Figure 2.13). The range of concentration is similar in all four plots. The residual chloride of previous seasons' plumes can be seen above the water table, having been diluted from the capillary fringe below the residual plume and by recharge above the residual plume.

The decreased flow field scenario (Scenario A; Figure 2.13) results in a more prominent plume developing, illustrating that the solute can not dilute as quickly as in the base case. Conversely, Scenario B (Figure 2.13) shows the plume diminishing as it reaches the water table as a result of the increase in average velocity in the saturated zone. Although the plot appears to have less chloride mass than that of Scenario A, this appearance is due to the fact that fresh water is diluting the concentrations to a degree that cannot be resolved by the contour levels shown. In the situation where the water table is comparatively shallow (Scenario C; Figure

2.13), the residual plume from past seasons is less defined as there is more of a "smearing" effect near the centre of the residual plume due to dilution caused by the proximity of the water table.

Figure 2.14 shows the results of two scenarios in which the source loading was adjusted. In the first (Scenario D), the annual chloride loading remained the same as for the base case but was distributed over 14 days throughout the beginning of each spring season, resulting in a sudden pulse of chloride each year, rather than a gradual pulse throughout the winter thaw. This scenario shows very little deviation from the base case, except for the average overall concentration of the plumes resulting from mixing with spring recharge. This deviation occurs because chloride loading in Scenario D was halted just before the main spring season, whereas the base case had more of a "delayed" loading of chloride throughout the spring season.

Scenario E (Figure 2.14) is the result of a simulation using the same annual loading, but distributed uniformly over 365 days. In this scenario, the plume characteristics in the vicinity of the water table are very similar to those of the base case, however, above the water table, there is a steady influx of chloride with no clearly defined dilution near ground surface. This scenario best represents the approach taken in Chapter 3 of this thesis, in which a uniform recharge and source loading is applied over a one-year time span. In both scenarios in Figure 2.14, the residual plume is clearly defined and smears as it reaches the water table. The concentration is relatively the same at the water table at Observation Point #3, but with higher concentrations smeared along the length of the water table. This difference varies depending on which season the cross-section is viewed in.

Figure 2.15 shows the breakthrough curves of all scenarios at observation point #3, which can be seen on Figures 2.13 and 2.14, just above the water table. As with the base case scenario, all of the breakthrough curves sharply mirror chloride loading in the first spring thaw (0-150 days), and to a lesser extent in the second spring thaw (400-550 days). After this point, the average concentration continues to rise until about the 4th or 5th season ($\sim$1600 days), at which point steady-state is reached.

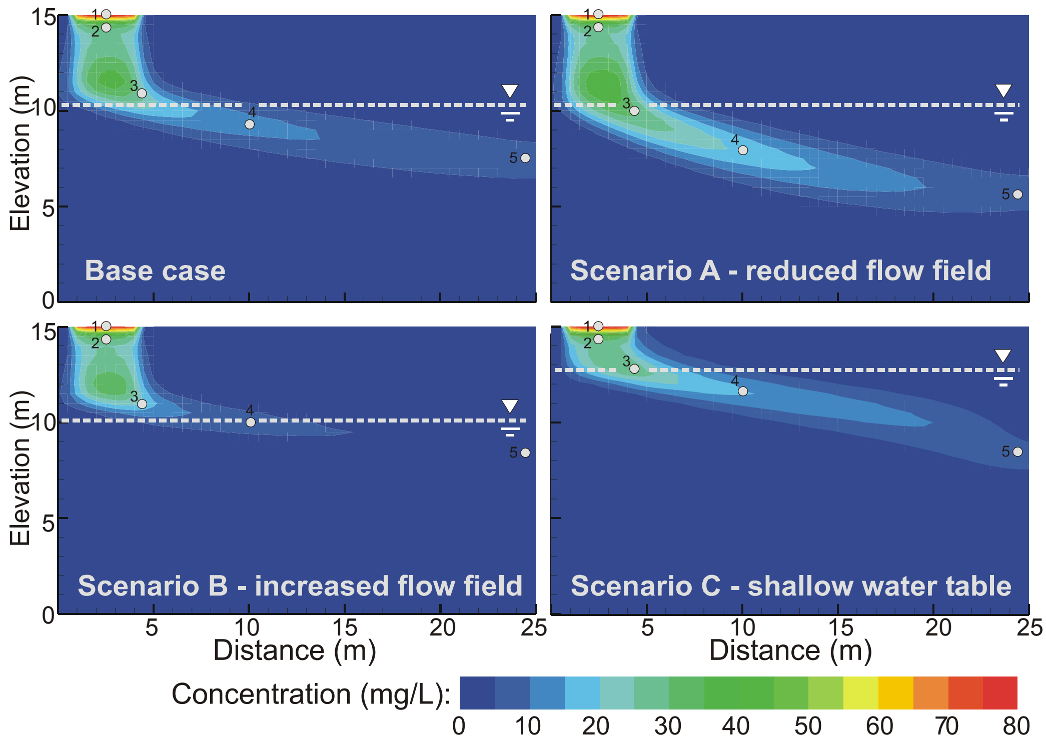

Figure 2.13. Concentration profiles at 3650 days for the base case scenario, scenarios A (reduced flow field), B (increased flow field) and C (shallow water table).

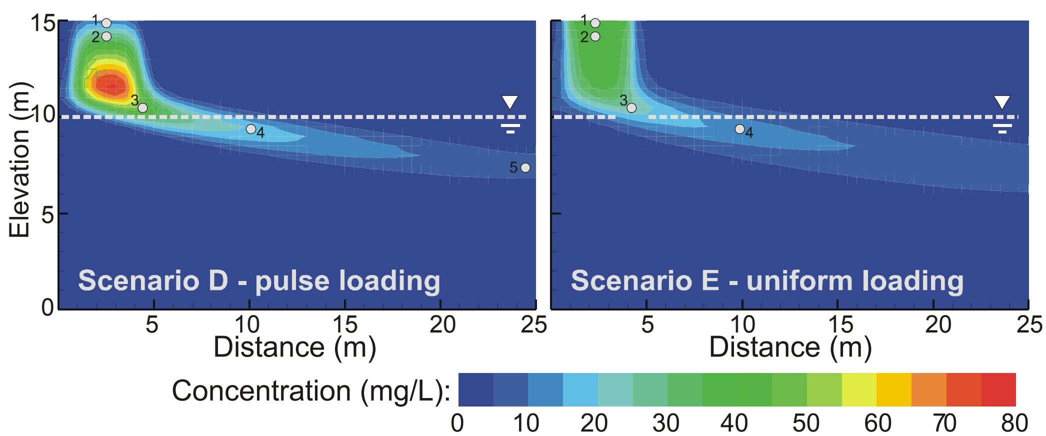

Figure 2.14. Concentration profiles at 3650 days for chloride loading scenarios; D (pulse chloride loading) and E (uniform chloride loading).

Figure 2.16 shows the breakthrough curves at all scenarios at observation point #4, located just below the water table (see Figure 2.13). In these curves, seasonal fluctuations in recharge and chloride loading are significantly dampened compared to Figure 2.15, which is further upstream within the plume. Scenario B illustrates the largest extent of dampening since the increased velocity below the water table causes the plume to be notably diluted, and consequently, the chloride concentration rises towards steady state with minimal effect from seasonal changes. The other scenarios show less than a 6% change in concentrations between seasons. Breakthrough curves at observation points #1, #2, and #5 are not shown here as they are similar to those of the base case.

2.6 Discussion

The simulations performed in this phase of the study have made it possible to observe the effect of seasonal fluctuations in chloride loading and recharge both above and below the water table. For all scenarios with a water table at 5 m depth, it was found that the chloride plume from one spring thaw does not necessarily flush out of the unsaturated zone within the year, but instead accumulates in the midsection of the unsaturated zone as fresh water dilutes the chloride above and below. This phenomenon is clearly seen in the fall season, after enough recharge from the summer months has significantly flushed the chloride from the surface and before the new winter salting season. When the water table is more shallow (2.5 m) this accumulation of chloride in the midsection of the unsaturated zone is less defined.

The effect seasonal fluctuations are considerably less pronounced beneath the water table compared to above the water table. Dilution is strong just above the water table in the capillary fringe where mixing of the solute-laden water with fresh water results in a dampening of seasonal fluctuations. This phenomenon has been explored recently in *Silliman et al*, [2002] who found that the capillary fringe may play a far more active role than traditionally thought in the transport of solutes and mixing of water from the vadose zone with that below the water table. It should also be noted that dampening of the seasonal fluctuations is further caused by dispersion of the solute in water, which would be even further enhanced in a 3D system. The dampening of the response leads to the conclusion that long-term transport models can neglect seasonal changes in solute loading.

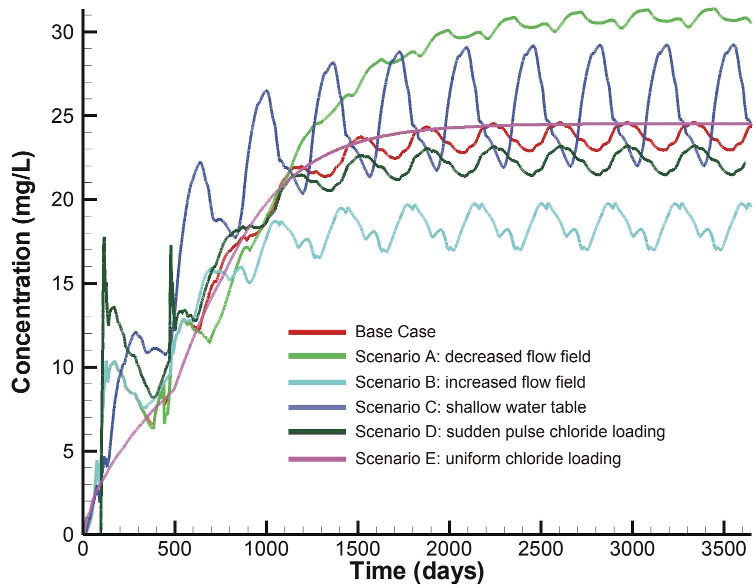

Figure 2.15. Breakthrough curves for all scenarios at observation point 3.

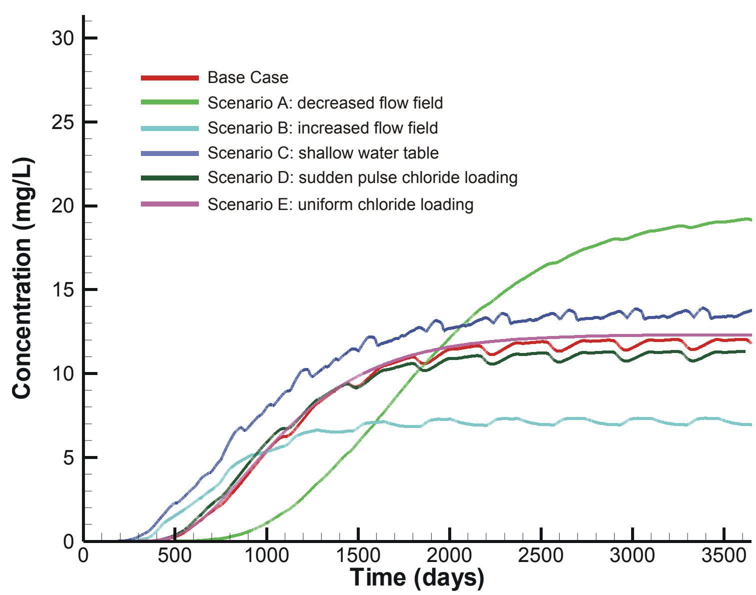

Figure 2.16. Breakthough curves for all scenarios at observation point 4.

Chapter 3

3D Greenbrook Transport Model

3.1 Introduction

The protection of urban well fields has recently become a top priority, particularly in light of recent concerns about drinking water in southern Ontario and throughout Canada. In some areas, road salt use is seriously threatening our water supply and possibly community health. As a result of the complexity associated with evaluating impacts due to non-point sources of contamination such as road salt, a cost effective and defensible management tool is needed to evaluate the impact and risk to groundwater supply sources from winter road salting. In this chapter, the 3D transport of chloride from road salt applications around the Greenbrook well field is simulated. Predictive scenarios are also presented to assess the impact of remediation measures on the water supply. The flow chart in Figure 3.1 outlines the necessary steps for the development of the model.

Source loading was estimated from 1945-2002 in order to simulate road salt contamination and to reproduce current chloride observations in the pumping wells. Since this entails estimating spatial source loading as well as temporal source loading, a reconstruction of the historical road network in the vicinity of the Greenbrook well field was needed. Further, the temporal source loading was adjusted for the purposes of calibrating the model to the target chloride concentrations in the 5 production wells.

Once calibration was achieved, the model was used to simulate another 40 years (2003-2045) into the future to predict chloride trends in the Greenbrook wells. This "forecasting" was carried out using the current (2002) road network and road salt loadings. The addition of future roads within the capture zone is neglected for the purpose of this study. Remediation scenarios are presented and their results are compared to the base case predictions. These simulations are not meant to be interpreted as absolute predictions, but should be used to gain insight to the relative differences of each remediation solution, and give a sense of the response time for improving the water quality from the wells.

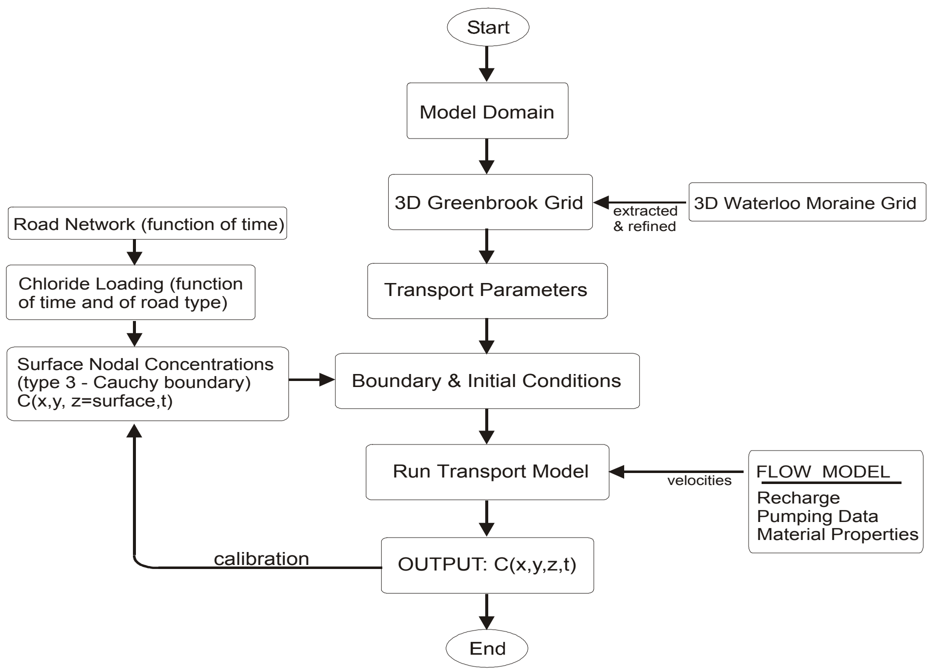

Figure 3.1. Preparation steps for developing transport model.

3.2 Model Development

3.2.1 Theory

The transport model is based on the advection-dispersion equation governing mass transport in the porous matrix is [*Bear*, 1972]:

$$\frac{\partial}{\partial x_i}(D_{ij}\frac{\partial c}{\partial x_j}) - v_i\frac{\partial c}{\partial x_i} = R\frac{\partial c}{\partial t} \tag{3.1}$$

where $c = c(x, y, z, t)$ is the dissolved concentration of solute; x, y, and z are spatial coordinates, D_{ij} is the hydrodynamic dispersion tensor, $v_i = q_i/\theta$ is the average groundwater velocity, and R is the retardation.

The transport model is coupled to a finite element flow model which includes both unsaturated and saturated flow; the unsaturated zone is approximated by a pseudo-unsaturated flow formulation [*Beckers and Frind*, 2000]. For a detailed description of the flow model and the numerical solution that was used to obtain the velocity field for the transport model, the reader is referred to *Frind et al*, 2001.

In three dimensions, the components of the hydrodynamic dispersion tensor for an isotropic medium are given by [*Burnett and Frind*, 1987]:

$$D_{xx} = \alpha_L \frac{v_x^2}{v} + \alpha_{TH} \frac{v_y^2}{v} + \alpha_{TV} \frac{v_z^2}{v} + D^* \tag{3.2}$$

$$D_{yy} = \alpha_L \frac{v_y^2}{v} + \alpha_{TH} \frac{v_x^2}{v} + \alpha_{TV} \frac{v_z^2}{v} + D^* \tag{3.3}$$

$$D_{zz} = \alpha_L \frac{v_z^2}{v} + \alpha_{TH} \frac{v_x^2}{v} + \alpha_{TV} \frac{v_y^2}{v} + D^* \tag{3.4}$$

$$D_{xy} = D_{yx} = (\alpha_L - \alpha_{TH}) \frac{v_x v_y}{v} \tag{3.5}$$

$$D_{xz} = D_{zx} = (\alpha_L - \alpha_{TV}) \frac{v_x v_z}{v} \tag{3.6}$$

$$D_{yz} = D_{zy} = (\alpha_L - \alpha_{TV}) \frac{v_y v_z}{v} \tag{3.7}$$

where α_L, α_{TH}, and α_{TV} are the longitudinal, transverse horizontal, and transverse vertical dispersivities, respectively; $v = \sqrt{v_x^2 + v_y^2 + v_z^2}$; and $D^* = D_d \tau$ is the effective diffusion coefficient in the porous medium with D_d being the free solution diffusion coefficient of the solute; and τ is the tortuosity of the medium.

The transport equation (3.1) requires boundary conditions all around the domain. This may be a *Type 1* or *Dirichlet* boundary condition on boundary segment Γ_1,

$$c = c_o(t) \tag{3.8}$$

a *Type 2* or *Neuman* boundary condition on boundary segment Γ_2,

$$\frac{g_o(t)}{\theta} = -D_n \frac{\partial c}{\partial n} \tag{3.9}$$

or, the boundary condition can be specified in the form of a known mass flux, known as a *Type 3* or *Cauchy* boundary condition on boundary segment Γ_3 which takes the form:

$$\frac{q_o c_o(t)}{\theta} = vc - D_n \frac{\partial c}{\partial n} \tag{3.10}$$

where D_n is the dispersion coefficient in the direction normal to the boundary, g_o and q_o are normal components of the dispersive vector and the Darcy fluid flux, respectively, and c_o is a specified concentration.

3.2.2 Conceptual Model

The Greenbrook model boundary (Figure 3.2) was selected to be sufficiently large so that it fully contained the steady state capture zone for all the wells in the Greenbrook well field. The domain incorporates the northwest corner of Kitchener, the southwest corner of Waterloo and the eastern portion of Wilmot township.

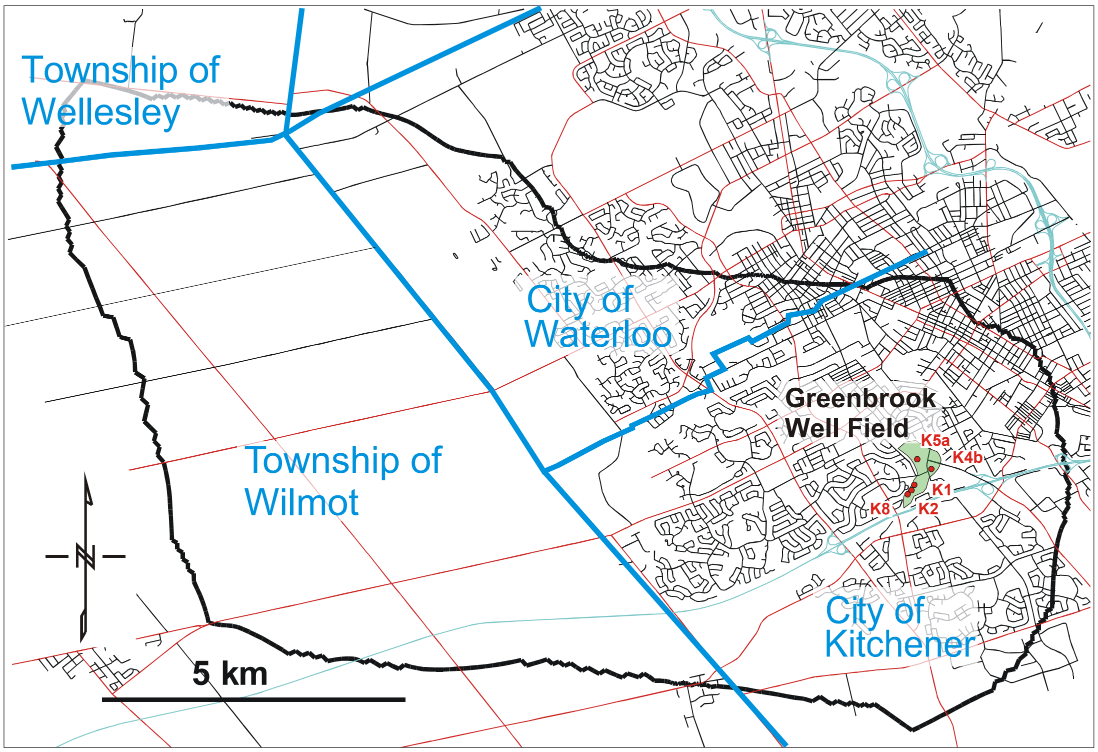

Figure 3.2. Greenbrook study area.

The conceptual model for the current study is derived from that of the Waterloo Moraine model [*Martin and Frind*, 1998] and is composed of a four-aquifer, four-aquitard system (Figure 3.3). Geology and hydrogeology of the area are described in Section 1.3. The Greenbrook wells are screened within the middle confined aquifer (Aquifer 2); however, hydrostratigraphic windows in the bounding till layers (Figure 3.4) provide numerous pathways for contaminants.

With this conceptual model, *Martin and Frind* [1998] simulated the 3D steady-state flow system of the Waterloo Moraine, using the finite element model WAT-FLOW [*Molson et al, 2002*]. The system was resolved vertically using 30 grid layers, and was calibrated using hydraulic head and streamflow data [*GLL et al.*, 1998]. This existing flow system is used for the current transport study. Three-dimensional capture zones for each of RMOW's well fields, including the Greenbrook wells, have also been identified [*Frind et al.*, 2001].

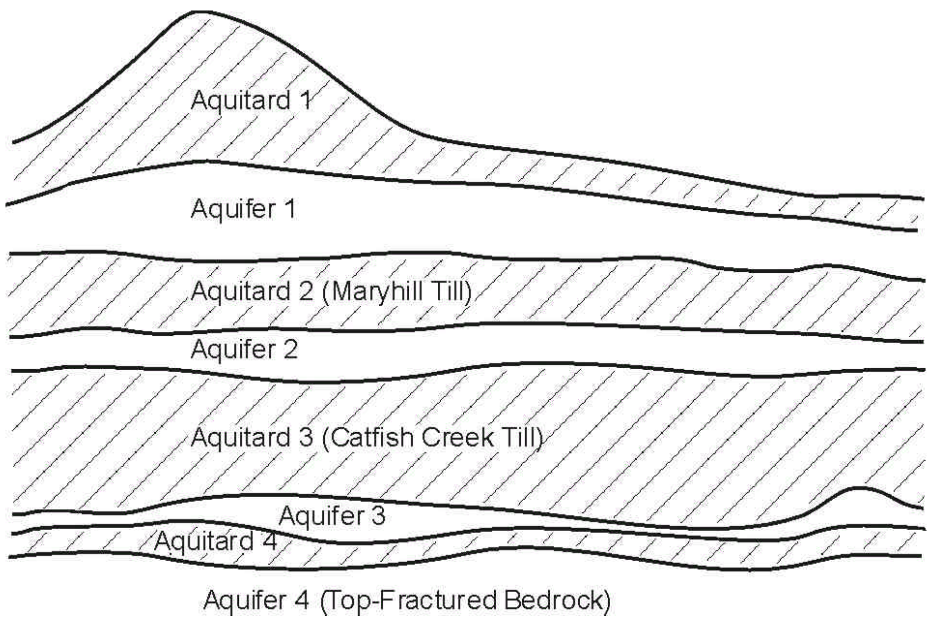

Figure 3.3. Stratigraphic conceptual model for the Greenbrook well field.

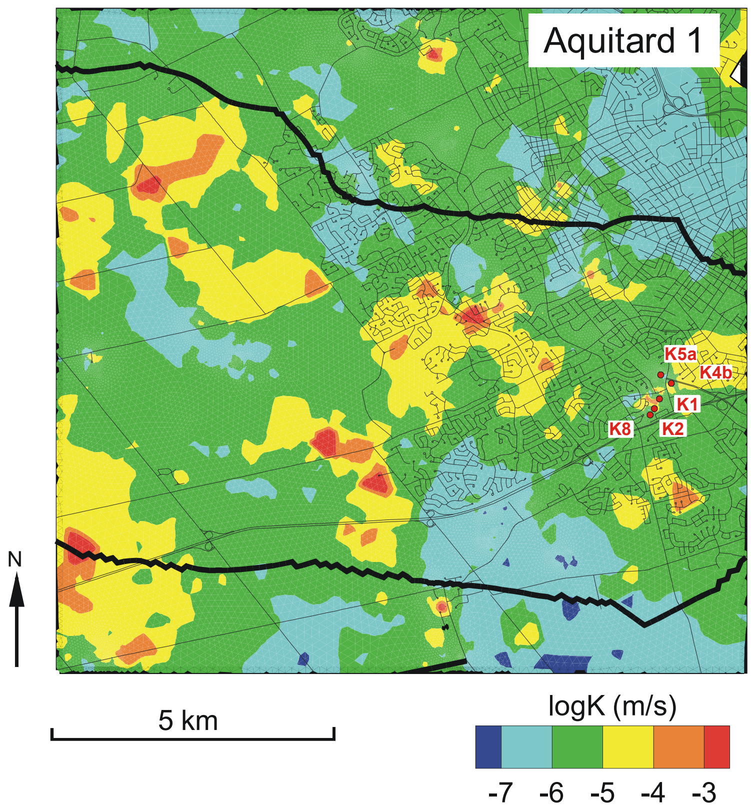

Figure 3.4. Hydraulic conductivity of Aquitard 1 showing high-conductivity windows. Model extents are outlined in black.

3.2.3 Finite Element Mesh

As stated previously, the Greenbrook finite element mesh was created by selecting a suitable subset grid from the Waterloo Moraine model (Figure 3.5). The resultant grid is 114.8 km^2 in area. Using 30 nodal surfaces (Figure 3.6) representing the main stratigraphic units in the model domain, the 2D triangular grid was projected in the vertical dimension to form a three-dimensional prismatic grid. The grid was then refined, especially in the vicinity of the pumping wells where refinement was 8x that of the original extracted mesh. The final 3D mesh includes 560,310 nodes and 1,105,830 elements (Figure 3.7).

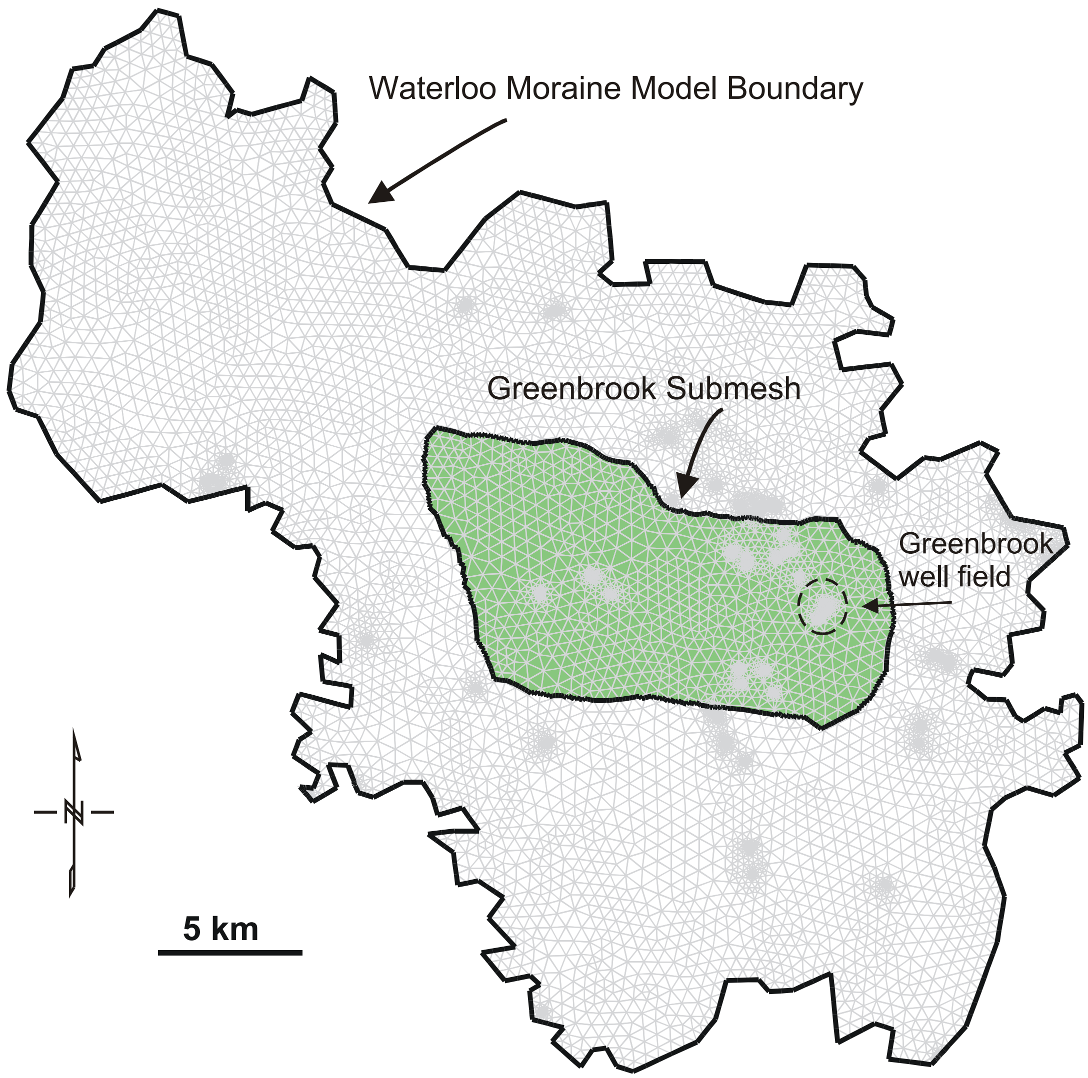

Figure 3.5. Waterloo Moraine model mesh [after *Martin and Frind*, 1998] and extracted Greenbrook submesh. The submesh is further refined (not shown) to satisfy the accuracy and stability constraints of the transport simulation.

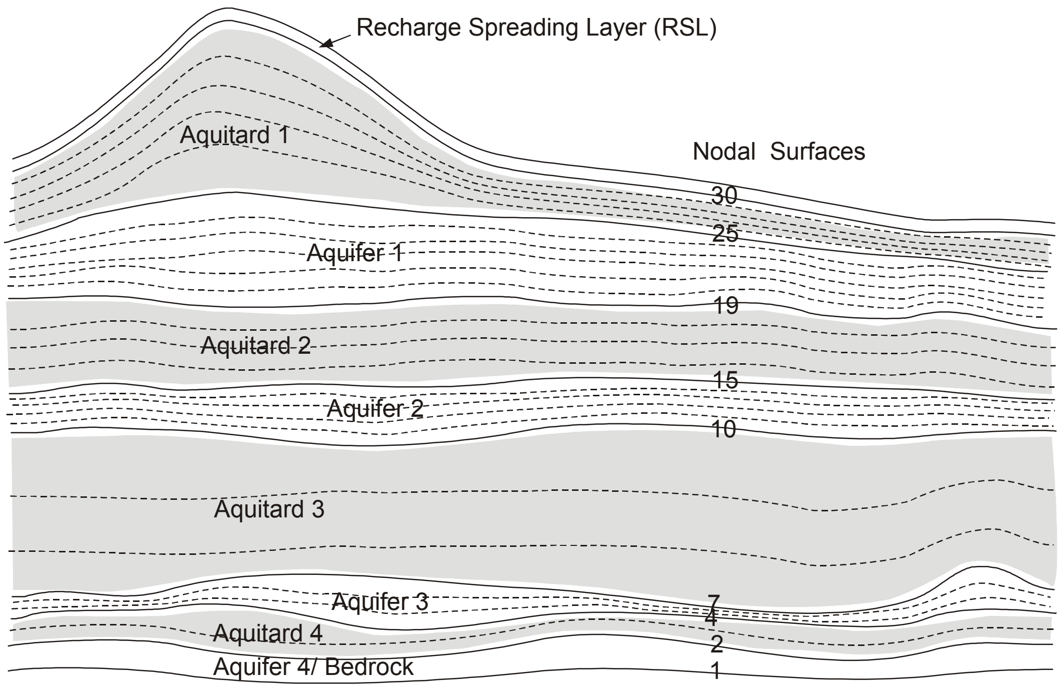

Figure 3.6. Finite element layering scheme [modified from *Callow*, 1996].

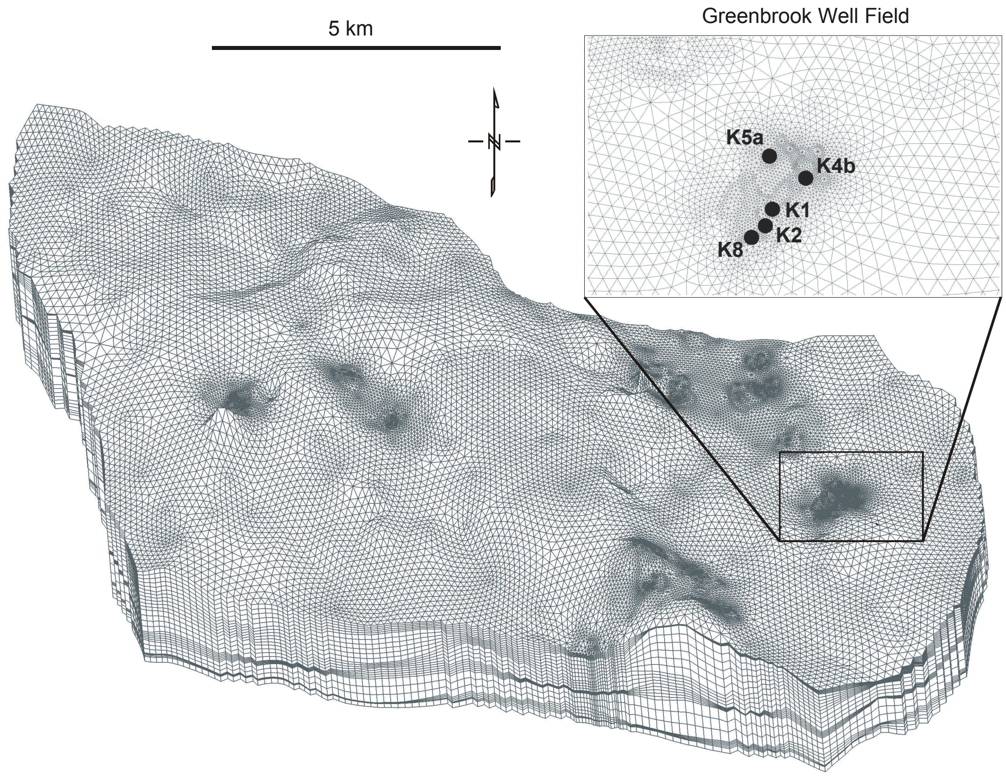

Figure 3.7. 3D Greenbrook mesh.

3.2.4 Transport Parameters

In this research, the elemental velocity, v, is obtained from the steady state flow solution of the Waterloo Moraine model [*Frind et al, 2001*]. The transport simulations were completed using a time-step of 10 days and using dispersivities of 20 m, 5 m, and 0.02 m in the longitudinal, transverse horizontal and transverse vertical directions respectively. The dispersivities are consistent with the transport scale, which is on the order of 10-15 km and are sufficient to maintain stability constraints with the grid discretization used. The low vertical dispersivity was critical to prevent smearing of the plume across the lower conductivity aquitards.

Initial conditions for chloride concentrations within the study area were set at 10 mg/L. This value is a good estimate of background chloride within the groundwater observed from monitoring wells in the Greenbrook area [*Stantec*, 2001], and in southern Ontario in general [*Jones et al*, 1986].

3.2.5 Road Network

Space- and time-variable source loading was input into the model based on the road network maps combined with the salt loading data. There are 5 types of road for which a different concentration is prescribed: private, municipal, regional, township and provincial. While these road types are usually serviced by the agency which has jurisdiction of them, it is not uncommon for selected roads to be serviced by an alternative agency. For instance, regional roads within the city of Kitchener may be salted by the city rather than by the RMOW. In addition, due to the number of agencies involved in snow removal, there has been no uniformity in reporting protocols. Although considerable effort was made to determine the spatial and temporal distribution of road salt loading in the Greenbrook area, pre-1995 data of de-icing salt usage have considerable gaps. Therefore, estimates have to be made based on recorded sand/salt mixtures (see Section 1.4) and data extrapolation backwards-in-time from post-1995 data.

Changes in the road network itself have been accurately recorded through air photos since 1945. Datasets of the road network in 5-year intervals from 1945-2000 were created using Geographic Information Systems (GIS) software and by analysing air-photos over the study area. These GIS datasets are separated into the five road-type categories mentioned above. Figure 3.8 shows the extent of the road growth in the Greenbrook area over this 55-year period; detailed datasets can be found in Appendix B. Road growth within the study area has been quite substantial since the 40's, particularly with the addition of the expressway in the south in 1970 and urbanization towards the west of the well field. The total road length has increased by as much as 2.5 times within the study area. Table 3.1 shows the road type and road length for each 5 year interval from 1945 until 2000.

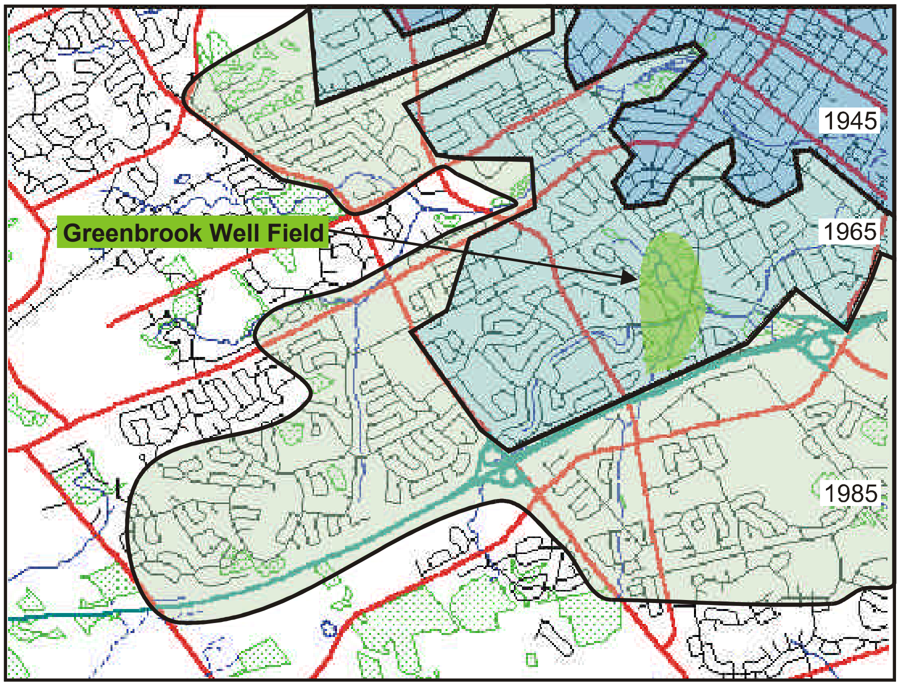

Figure 3.8. 2000 road network surrounding Greenbrook well field showing major growth stages at 1945, 1965, and 1985.

Initially, simulations were performed using a concentration of 1000 mg/L along all road types, based on work done by *Muhammad* [2000] which assumed an average application of 30 tonnes NaCl per 2-lane km road length. These values were then scaled for each road type based on literature for 2000 road salt application values [*Stantec,* 2001] and extrapolated backwards as mentioned above in this section. Table 3.2 shows the annual distribution of road salt concentration estimates based on this scaling procedure.

These estimates allow for a rough starting point from which to calibrate the loadings to target concentrations of chloride in the Greenbrook wells. Across the ground surface of the transport model, these concentrations are entered as a mass-flux (Cauchy) boundary condition. In this approach, the mass influx is dependant on both the space- and time-variable source concentrations and local recharge to the boundary. Local recharge was obtained from the existing 3D flow model calibration, which applied an initial uniform surface recharge of 530 mm/yr. Of this potential recharge, approximately 260 mm/yr discharges directly to streams through a surficial, high-permeability layer referred to as the Recharge Spreading

	Road Length (km)					
Year	**Private**	**Municipal**	**Township**	**Regional**	**Provincial**	**Total**
1945	8.22	89.49	32.12	82.27	0	212.12
1950	8.22	98.60	32.12	82.27	0	221.22
1955	8.22	116.15	30.15	82.27	0	236.79
1960	9.09	139.19	26.92	83.30	0	258.51
1965	9.28	157.32	26.92	83.30	0	276.82
1970	9.28	185.43	26.92	88.54	13.08	323.26
1975	9.28	217.99	28.89	91.19	22.01	369.37
1980	9.84	244.93	28.89	95.18	22.01	400.76
1985	9.84	257.68	28.89	94.92	22.01	413.34
1990	9.55	301.30	25.29	100.44	22.01	458.59
1995	9.55	319.51	25.29	99.99	22.01	476.36
2000	9.55	338.22	25.29	99.44	22.01	494.47

Table 3.1. Summary of road lengths for each road type and year.

	Chloride Concentration (mg/L)				
Year	**Private**	**Municipal**	**Township**	**Regional**	**Provincial**
1945	58.3	184.2	154.9	455.0	0.0
1950	58.3	184.2	154.9	455.0	0.0
1955	58.3	184.2	154.9	455.0	0.0
1960	58.3	184.2	154.9	455.0	0.0
1965	116.6	368.3	309.9	809.9	0.0
1970	233.3	736.7	619.9	1820.0	436.1
1975	233.3	736.7	619.9	1820.0	1296.6
1980	233.3	736.7	619.9	1820.0	1296.6
1985	233.3	736.7	619.9	1820.0	1296.6
1990	233.3	736.7	619.9	1820.0	1296.6
1995	233.3	736.7	619.9	1820.0	1296.6
2000	233.3	736.7	619.9	1820.0	1296.6

Table 3.2. Chloride concentration applied for each road type and year.

Layer (RSL). The rest, about 250 mm/yr recharges to the lower aquifer.

In the transport model, the vertical Darcy flux q_o in Eqn. 3.10 is obtained from the element layer immediately below the RSL (which is removed from the transport grid). This flux varies spatially depending on the local conductivity and flow system.

3.2.6 Assumptions and Limitations

In this work, the major assumptions in the transport model are that the flow field is at steady state and chloride is applied uniformly over time, rather than through seasonal pulses. In addition, this research assumes that present-day pumping rates, the road network and road salt application do not change in the future.

One limitation was that actual road growth could only be represented in 5-year intervals due to the range of data (i.e. air photos) that was available. Similarly, road salt application has only been recorded for 1997-2002, so historical values had to be initially estimated from "word-of-mouth" sources.

Assumptions and limitations applicable to the Waterloo Moraine flow model and capture zone delineation for the Greenbrook well field can be found in *Frind et al* [2001].

3.2.7 Calibration

In flow modelling, calibration is typically achieved by adjusting hydraulic conductivity and/or recharge to simulate hydraulic heads and base flows observed in the field. Calibration of large-scale flow models, however, are typically not sensitive to local scale changes in hydraulic conductivity. Errors in the simulated conductivity field near pumping wells, for example, may go unnoticed during the flow model calibration whereas they may have profound effects on the transport simulation.

In this thesis, the transport model simulation was based on adjusting the road-salt boundary concentrations and source locations. Calibration of the transport model to observed chloride data at each of the five Greenbrook wells was difficult to achieve since the transport domain is approximately an order of magnitude smaller than the flow model, and plume behaviour is very sensitive to the magnitude and variability of the local velocity field.

Instead of calibrating to individual well data, the transport model calibration is based on the simulated and observed average concentration of the five wells, each weighted according to their individual pumping rates. The individual observed well data and weighted average of this data is presented in Figure 3.9. Because the concentrations for each well were reported at different monitoring dates, each data set had to be approximated via a fitting curve, and these new interpolated concentrations at each time point back-calculated and averaged. For calibration, this weighted average is herein referred to as the calibration target. This averaging of the pumping wells into one calibration target is further justified by the fact that in reality each well contributes to the reservoirs. The reservoirs are then used as the municipal water supply, and therefore water used by the public does not reflect the quality from an individual well, but from the weighted average.

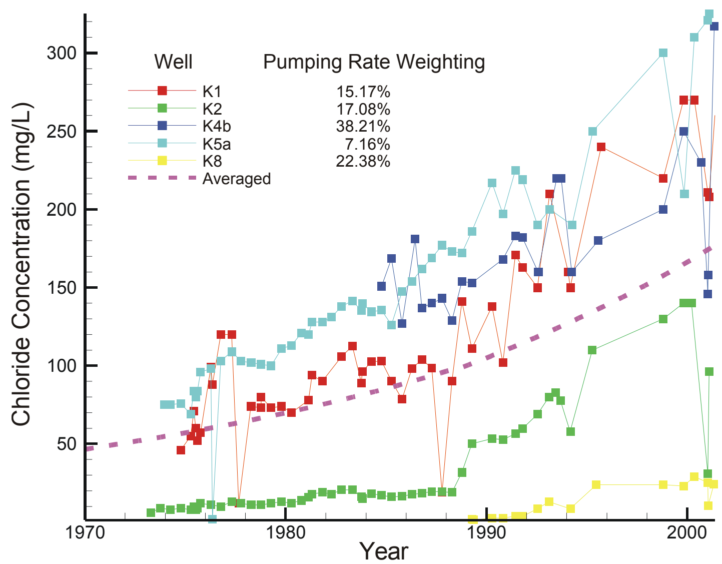

Figure 3.9. Observed and weighted average of observed chloride concentrations in the Greenbrook production wells.

Calibrated values of source loadings (Table 3.3) show a smooth gradient in the loading function compared to the initial source loadings presented in Table 3.2. Figure 3.10 shows that the final weighted average of the modelled concentration agrees well with the weighted average of the observed concentrations. Discrepancies between the two curves at the beginning and the end of the time series can be attributed to the interpolative function of the fitting curves rather than an error in data. Small discrepancies between the two curves can be attributed to small errors in the road network or source loading, or due to errors or non-uniqueness in the flow calibration.

	Calibrated Chloride Concentrations (mg/L)				
Year	**Private**	**Municipal**	**Township**	**Regional**	**Provincial**
1945	75	237	200	587	0
1950	83	261	220	645	0
1955	86	273	230	675	0
1960	97	308	260	763	0
1965	101	321	270	792	0
1970	116	368	310	910	651
1975	143	453	382	1121	802
1980	170	539	454	1332	953
1985	201	636	536	1573	1125
1990	225	712	600	1761	1260
1995	240	758	638	1872	1339
2000	320	910	770	2163	1562

Table 3.3. Calibrated chloride concentration for each road type and year.

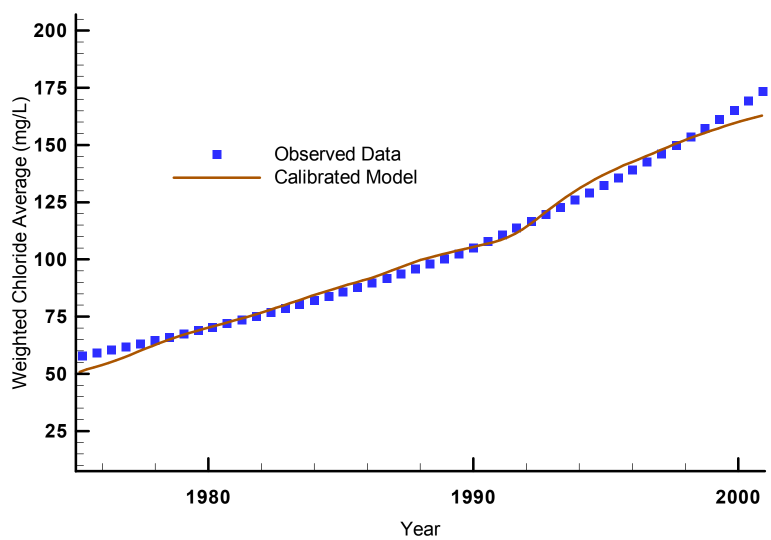

Figure 3.10. Model calibration showing observed and simulated breakthrough curves of weighted average concentrations at the Greenbrook wells.

Three-dimensional simulation results for the year 2002 show clearly defined plumes (Figures 3.11 to 3.13) originating from heavily-treated roads that are known to be major transit corridors in the study area. These results also show the impact of minor city streets in the form of smeared, less-defined plumes. While the well field is obviously at a disadvantage due to its urban location as opposed to any rural well field to the west of the city, it also benefits from the fact that it is located within parklands as seen in Figure 3.11. Other areas in this figure that show little or no chloride contamination are Westmount Golf and Country Club, located at the top left of the inset box, and other small parks or "green" areas scattered throughout the city.

Areas with less road cover that are saved from high chloride contamination are quite obvious upon closer view. The outline of the Ottawa Street Landfill site, located in the southeast corner of the figure, is clearly outlined by the lack of chloride contamination near ground surface. The high chloride contours generally follow the road pattern, however in some areas these contours appear "jagged", a problem directly attributed to the individual element size in the mesh and the lack of resolution through areas of coarse mesh. In such cases, the road salt is applied onto nodes with effective "road widths" on the order of 20-30 m. Although mass is conserved, it is important to keep in mind that real plumes may be even more distinct.

Deeper within the subsurface (Figure 3.12), aquitard "windows" and other primary pathways in plan view play a part in transporting solute to the deeper layers. The plumes at this depth no longer reflect ground surface source concentrations, indicating that they have moved laterally in overlying aquifers, only to reach discontinuities in the till layers in between the aquifers and migrate downwards. This figure reflects the heterogeneity of the system, as each individual well shows varying degrees of contamination, even though they are all within 1 km of each other.

Figure 3.13 shows a chloride plume approaches well K4b results from the east. Another plume approaches well K5a from the west, as can be seen in Figure 3.12 and Figure 3.13. Other plumes, such as that arising from Homer Watson Blvd., show small "local-scale" flow systems. In each of these figures, the location of the "windows" in the confining layers (Figure 3.4) can be seen by the patterns of plume migration as they reach the lower aquifers. Whether or not these windows reflect reality is left to individual interpretation. For instance, chloride reaching certain well screens (i.e. K8) has arrived there not because it is located in a highly salted area, but because of the proximity of a high conductivity window in the overlying aquitard. However, the hydraulic conductivity was calibrated using the regional Waterloo Moraine flow model, and due to the non-uniqueness of the model, it is not meant as a direct representation of the true hydraulic conductivity on a local scale, therefore individual well concentrations may also be inaccurate. Overall, the calibrated simulations are a satisfactory starting point to begin scenario analyses.

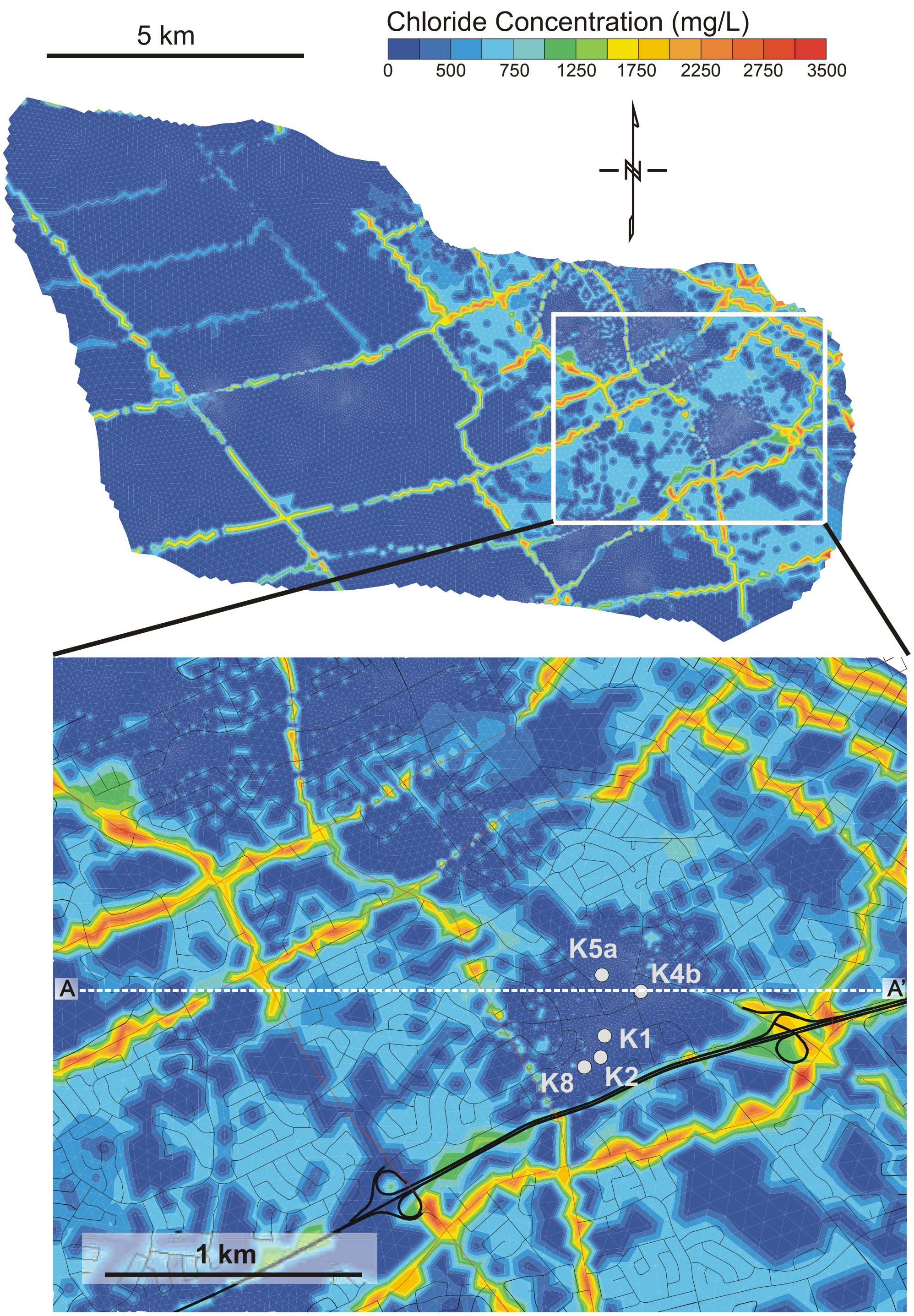

Figure 3.11. Simulated chloride concentrations at ground surface, year 2002.

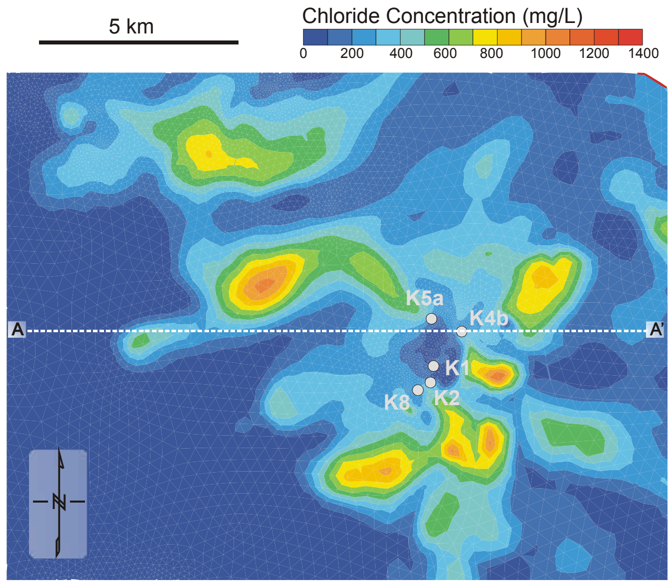

Figure 3.12. Simulated chloride distribution near the Greenbrook well field for year 2002, well screen layer (Aquifer 2).

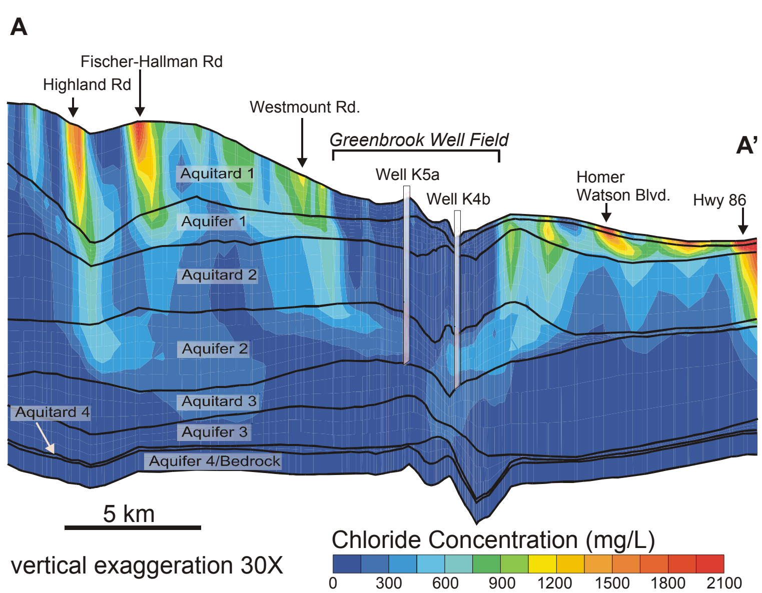

Figure 3.13. Simulated chloride concentrations within cross-section A-A', year 2002.

3.3 Simulation Results

Using the previously calibrated simulation, several predictive scenarios were continued from either 2002 or 2003 until the year 2041 and are described in table 3.4.

Scenario	Title	Description
1.	Base Case	Continued from the calibrated model, this scenario simulates a base case situation from 2003-2041 in which both the road network and the chloride loadings remain constant, implying a "do nothing" approach.
2a.	25% Reduction - Gradual	Chloride application onto all roads reduced at year 2002, gradually reaching a 25% reduction by 2007.
2b.	25% Reduction - Immediate	Chloride application reduced by 25% at 2002.
3.	100% Reduction within 5-year Capture Zone	Chloride application within the 5-year capture zone discontinued at year 2003.
4.	100% Reduction within 10-year Capture Zone	Chloride application within the 10-year capture zone discontinued at year 2003.
5.	Elimination of Secondary Roads	Chloride application onto private and municipal roads (secondary city streets) discontinued at 2003.
6.	100% Reduction within Entire Study Area	Chloride application onto all roads discontinued at 2003.

Table 3.4. Predictive scenarios.

3.3.1 Base Case

The distribution of chloride at ground surface in 2041 resulting from the base-case scenario (Scenario 1) shows that high chloride concentrations strongly mimic the prevailing road patterns (Figure 3.14). Areas with no roads, such as the park in which the well field is situated, show a lack of high chloride concentrations in the upper aquifer.

A cross-section in the vicinity of Well K4b is shown in Figure 3.15. Some of the chloride plumes can be seen reaching the well screens in Aquifer 2 through "windows" in the low conductivity layers. In addition, there are high chloride concentrations encroaching from Aquifer 3 towards the well screen of K4b, possibly entering this aquifer from a direction perpendicular to the cross section.

In Figure 3.16, chloride concentrations in the well screen layer (Aquifer 2) are shown. A comparison with the top surface concentrations (Figure 3.14) shows that heavy contamination occurs by horizontal migration of the chloride through the aquifers and through high conductivity windows in the aquitards, because contaminants are present in the vicinity of the wells at a lower depth, whereas at ground surface for the same $x - y$ locations they are not.

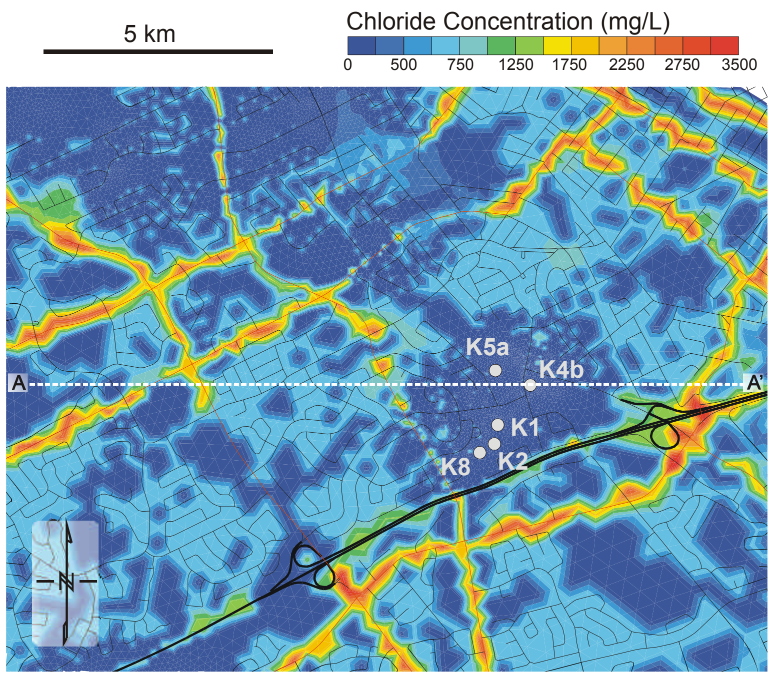

Figure 3.14. Simulated chloride distribution at ground surface, year 2041, Scenario 1.

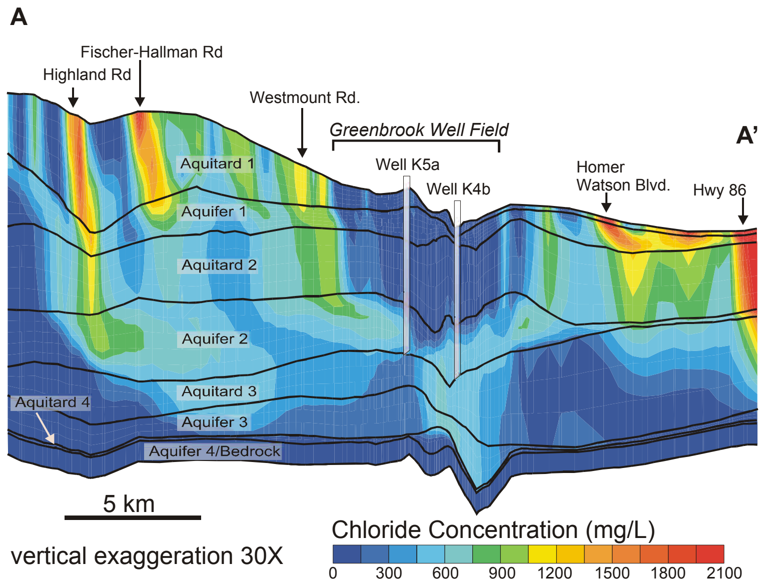

Figure 3.15. Simulated chloride concentrations within cross-section A-A' for year 2041, Scenario 1.

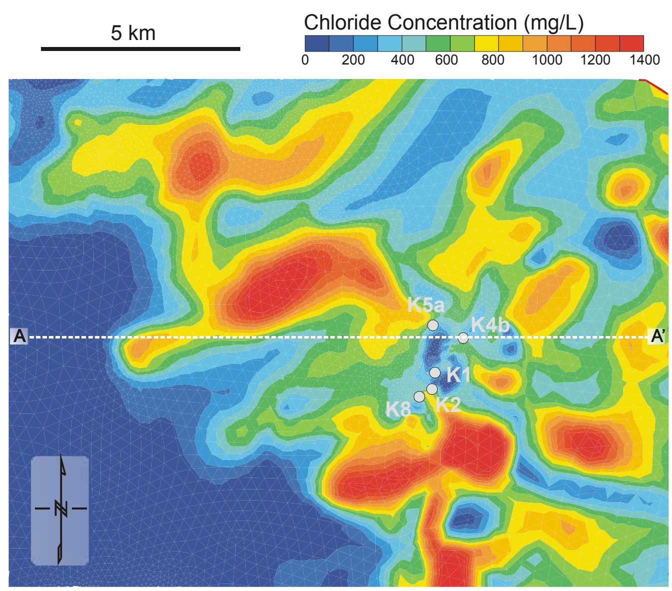

Figure 3.16. Simulated chloride distribution in the screened aquifer (Aquifer 2), year 2041, Scenario 1.

3.3.2 Remediation Options

For each scenario, results are presented as plan view plots at ground surface (Figure 3.17), cross sections through well K4b (Figure 3.18), as well as plan view plots of the screened aquifer layer(Aquifer 2)(Figure 3.19). K4b was chosen because of its high chloride levels in both the observed data and the calibrated model and because of its importance to the water supply, providing 38% of the total water pumped into the reservoirs. Breakthrough curves for Scenarios 2-6 are presented for individual discussion and comparison with the base-case results. These curves are combined in the form of weighted averaged well concentrations for each scenario and are presented in the discussion (Section 3.4) for further scenario comparisons. As mentioned earlier, these averaged concentrations can also be assumed to represent the concentration of the Greenbrook reservoirs.

Scenario 2 - 25% Reduction within Study Area

In the next two scenarios, chloride application is reduced by 25% within the entire study area, assuming first a gradual reduction, then an immediate reduction. The reduction begins in 2002 rather than 2003 since the RMOW has already begun salt reduction measures. These measures include better record-keeping (thus avoiding double applications), conservative use and pre-wetting which aids in keeping salt crystals from refracting off of the pavement and onto pervious areas [*RMOW, pers. comm*, 2002]. The RMOW has estimated that these measures would result in a 25% reduction, however, it is unknown how long it will take until the measures will be fully implemented. Therefore, 2 sub-scenarios were designed; the first of which simulates a gradual linear decrease of chloride application, beginning at year 2002 and ending at year 2007. The second sub-scenario shows the effect of immediate 25% reduction beginning at year 2002.

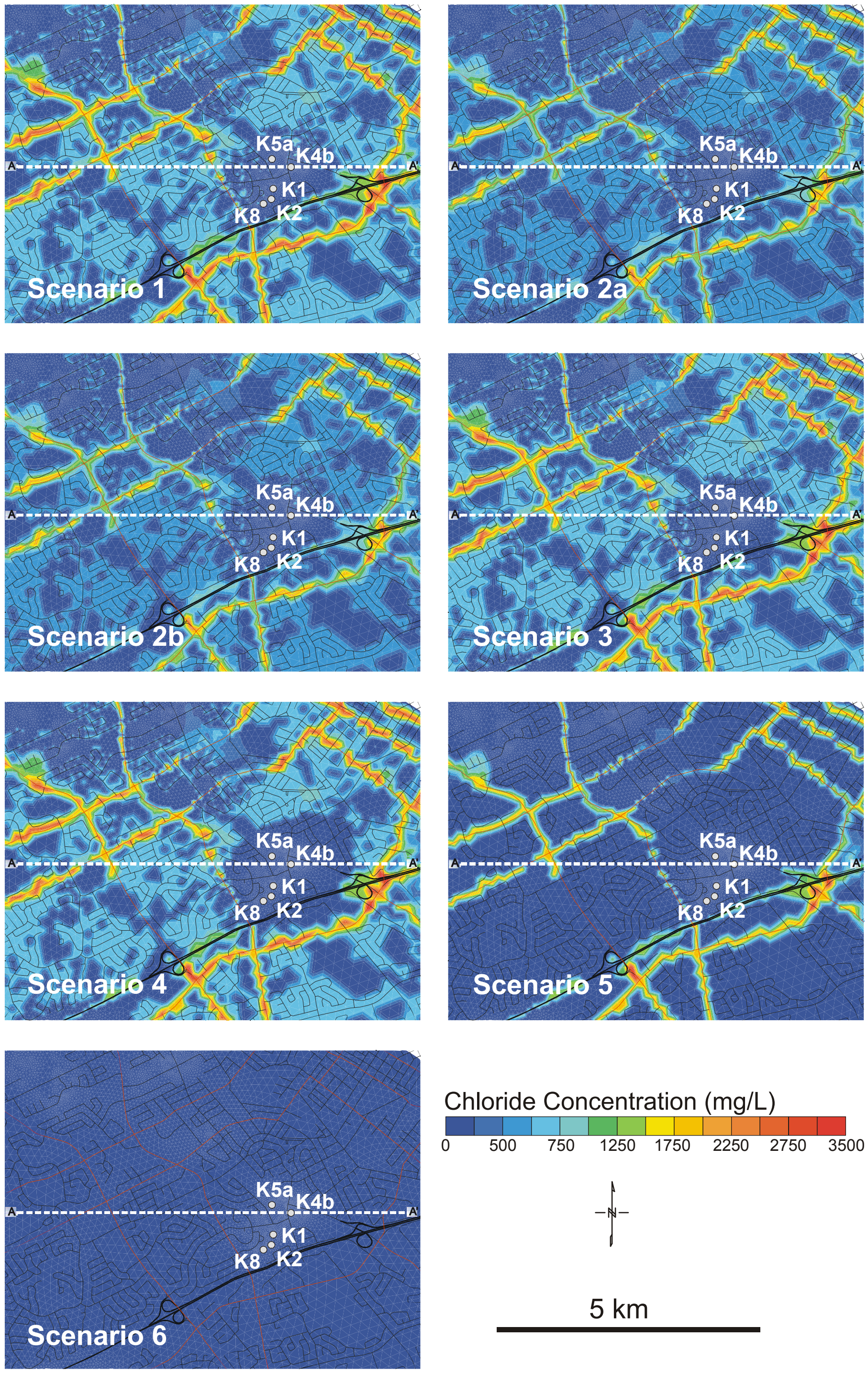

Figure 3.17. Simulated chloride distribution at ground surface, year 2041, all scenarios.

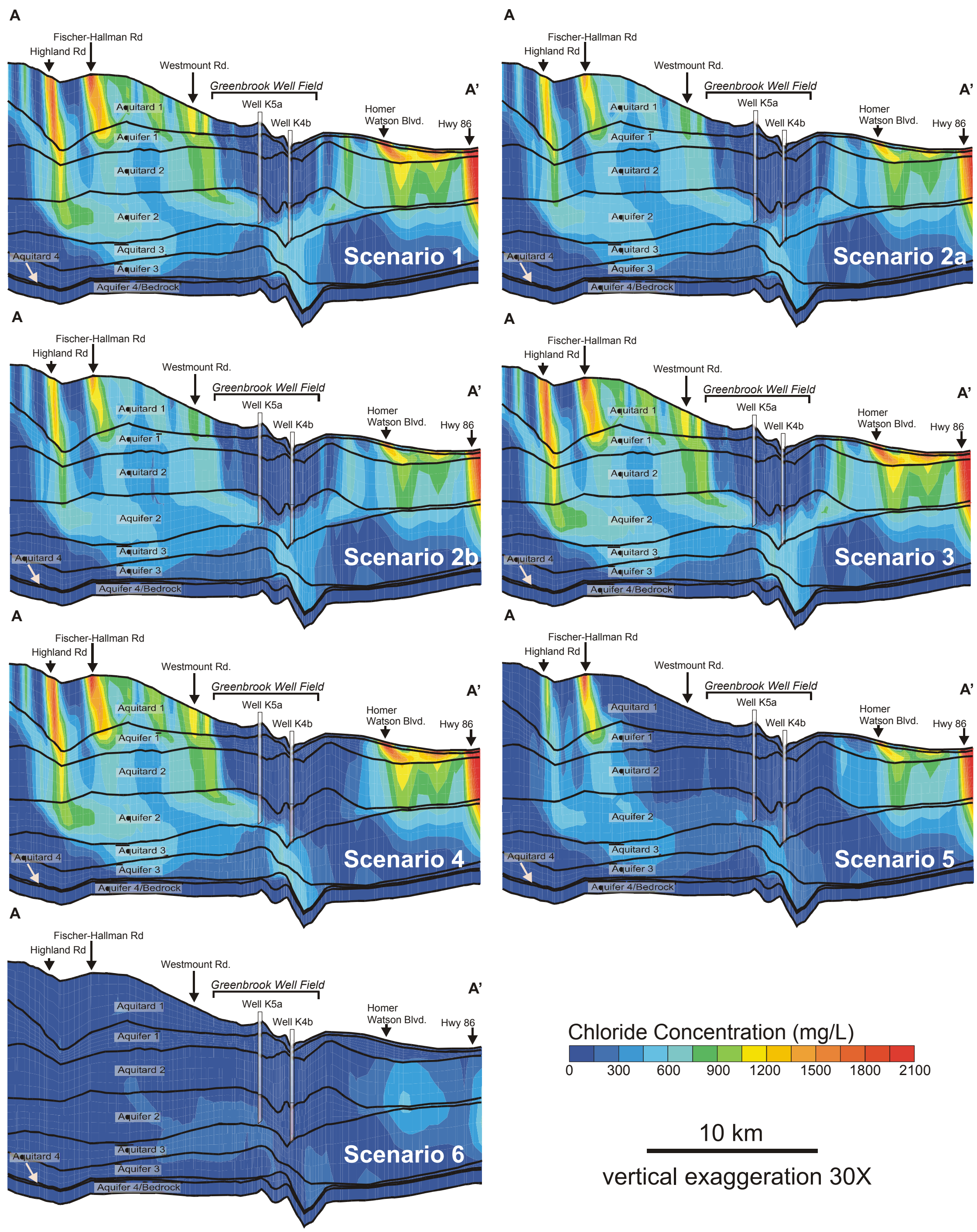

Figure 3.18. Simulated chloride concentrations within cross-section A-A' for year 2041, all scenarios.

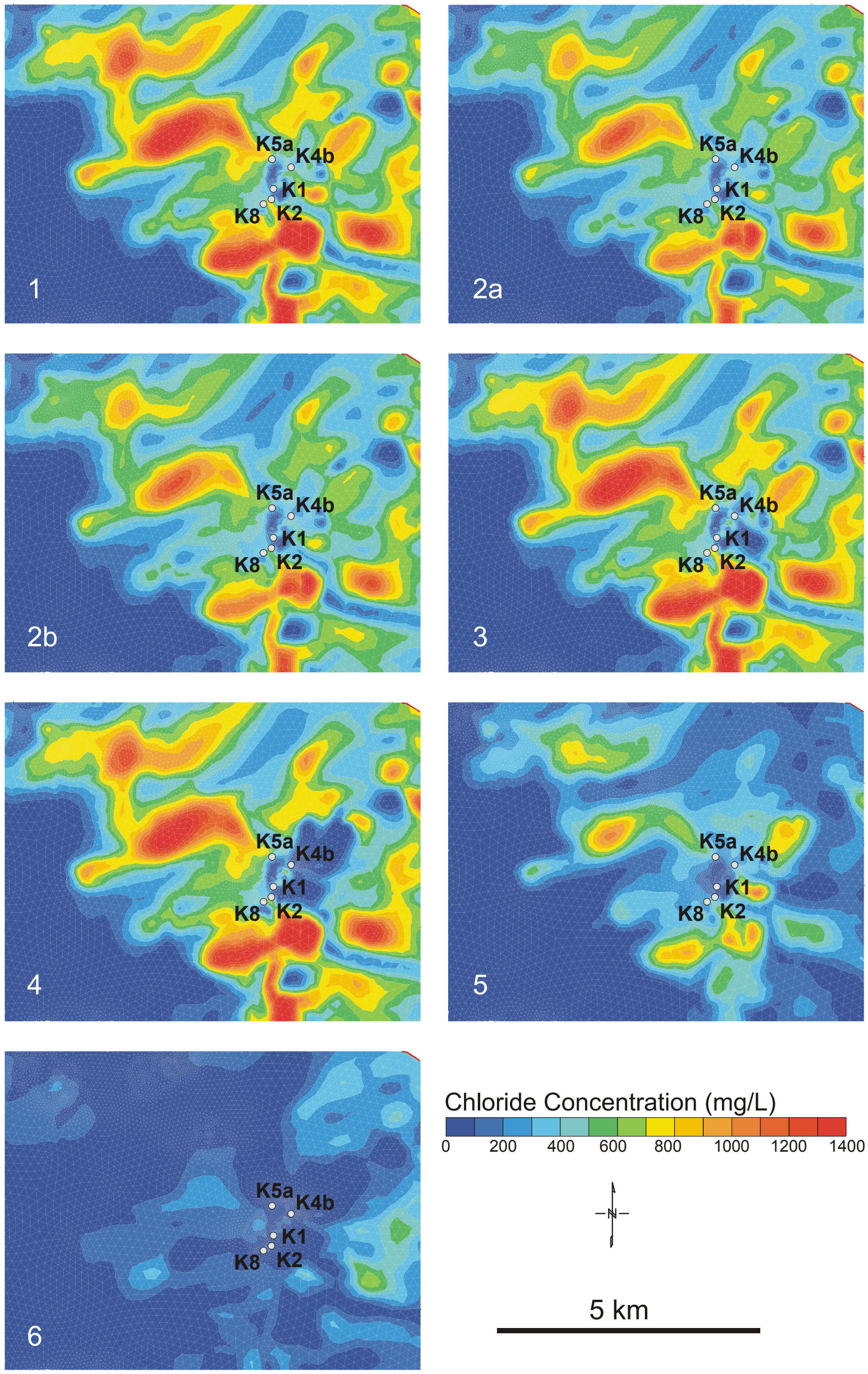

Figure 3.19. Simulated chloride distribution in the screened aquifer (Aquifer 2), year 2041, Scenarios 1-6.

Scenario 2a - Gradual Reduction

Breakthrough curves of chloride in the wells (Figure 3.20) show improvement within 2 years of reduction, although substantial improvement (>5%) does not occur for 4 years for 3 of the 5 wells. K4b shows the most significant improvement, possibly due to the fact that it has the highest pumping rate and responds faster to changes in source loading. While the reduction does decrease the chloride levels in K4b to below drinking water standards (250 mg/L), concentrations in both K4b and K1 are still rising at 2040, whereas concentrations in K5 and K8 appear to be leveling off.

The chloride concentrations near ground surface can be seen in planview in Figure 3.17-2a, and a cross-section through well K4b can be seen in Figure 3.18-2a. In these plots, overall reduction of chloride can be seen as compared to the base case. In 3.18-2a, heavy chloride plumes from Highland Rd. and Westmount Rd. remain trapped in Aquitard 2, compared to the base case (Figure 3.17-1) where these plumes have already reached Aquifer 2. In Figure 3.19-2a, the individual plumes affecting each well can be seen. The plume in the south, approaching K2 and K8 seems to have been abated by the reduction.

Scenario 2b - Immediate Reduction

Breakthrough curves of chloride in this scenario (Figure 3.21) show a faster improvement than in Scenario 2a, but that the chloride concentrations in K4b are still indeed rising, albeit to a lesser degree. In fact, by the year 2041, the chloride levels are at about the same levels as those in Scenario 2a. This is also evident in Figures 3.17-2b 3.18-2b and 3.19-2b, which show concentration distributions at 2041 to be almost identical to those of Scenario 2a. In both scenarios, this indicates that chloride in the wells had not yet reached steady-state as more mass arrives from pre-2002.

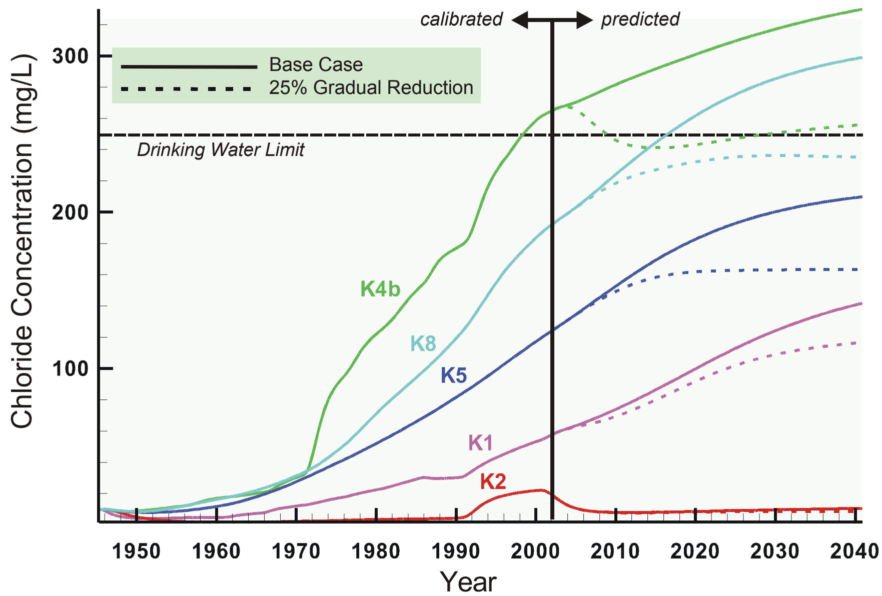

Figure 3.20. Breakthrough curves at wells showing effect of 25% gradual chloride reduction, Scenario 2a.

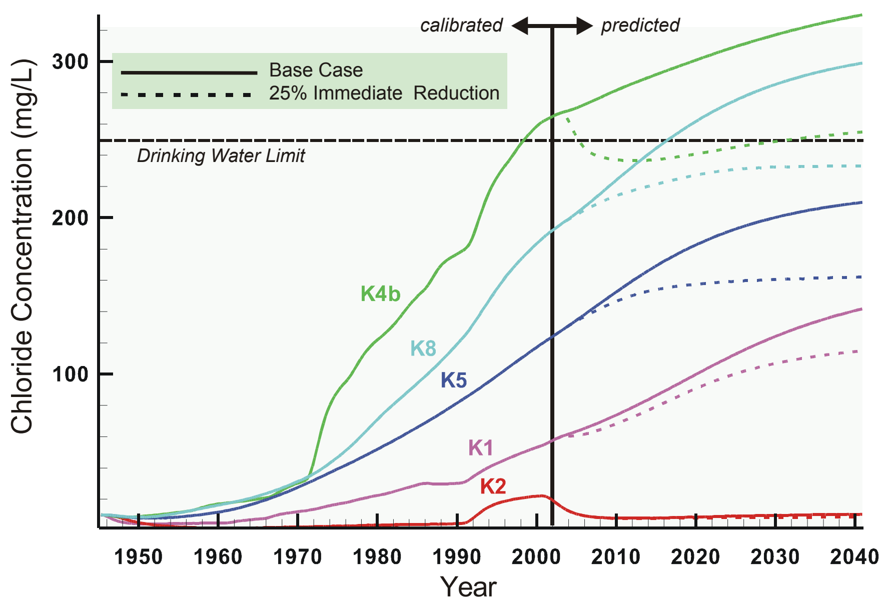

Figure 3.21. Breakthrough curves at wells showing effect of 25% immediate chloride reduction, Scenario 2b.

Scenario 3 - 100% Reduction within 5-year Capture Zone

In this scenario, chloride was reduced 100% within the 5-year capture zone (Figure 3.22) defined by *Frind et al* [2001]. This scenario, as well as Scenario 4, presents the remediation option of replacing NaCl with a de-icing agent that is less harmful to the environment.

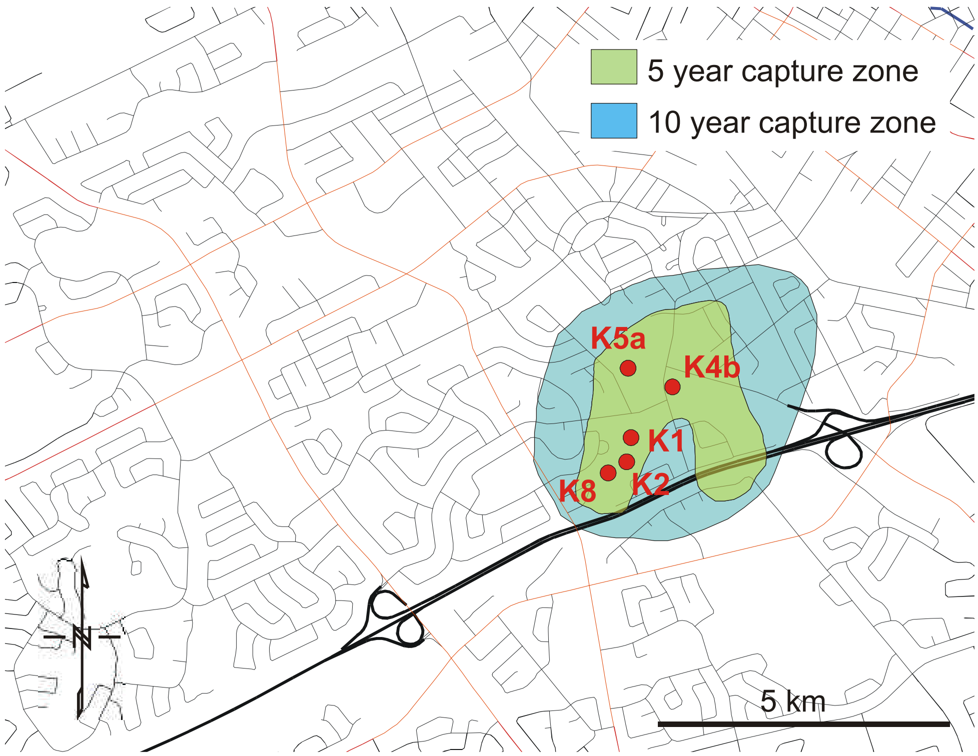

Figure 3.22. 5- and 10-year capture zones for the Greenbrook wells [*Frind et al*, 2001].

Breakthrough curves for the wells (Figure 3.23) show an immediate response to the reduction, as fresh water infiltrates within the 5 years and allows the chloride to be diluted. However, after 5 years, solute from outside the 5-year capture zone arrives at the wells, and mixing with fresh water from recharge within the capture zone is not sufficient to keep the chloride levels from rising within the wells. Removal of chloride from within the capture zone is marginally evident in Figure 3.17-3, however the 5-year capture zone does not contain many roadways, therefore the difference between the plan view of this scenario and that of the base case is insignificant. Similarly, a comparison of the cross-section A-A' for both the base case (Figure 3.18-1) and this scenario (Figure 3.18-3) and the well-screen layer (Figure 3.19) show very little difference.

Scenario 4 - 100% Reduction within 10-year Capture Zone

Similar to Scenario 3, eliminating chloride application from within the 10-year capture zone dramatically decreases chloride concentrations in the wells (Figures 3.24, 3.17-4 and 3.18-4). Within 10 years, chloride levels begin to rise again, but contrary to the level of rising in Scenario 3, the concentrations in the wells appear to be levelling off by the year 2041. Also, the chloride concentration in well K4b significantly decreases in comparison to the other wells, even more so than in the base case. Upon closer inspection of the plumes in the well screen layer (Figure 3.19-4), it appears that this decrease in well K4b is due to the abatement of a small plume to the north-east of the well. This plume originates from within the 10-year capture zone, whereas the other plumes in Aquifer 2 originate from outside the 10-year capture zone.

Scenario 5 - Elimination of Salt from Secondary Roads

When chloride application is limited to only primary transit corridors throughout the area (Figure 3.17-5), chloride concentrations dramatically decrease in the wells (Figure 3.25) and continue to do so until year 2041. Due to this elimination of chloride, the cross-section (3.18-5) shows dilution of the residual plumes in Aquifers 1 and 2 and Aquitards 1 and 2. As more fresh water enters the system, chloride continues to be diluted. Figure 3.19-5 shows a significant decrease in the chloride plumes approaching the wells. Plumes emanating from major roadways dominate the system, but these roads are located far enough away from the wells to interact and mix thoroughly with the fresh water entering closer to the well field.

Scenario 6 - 100% Reduction within Study Area

The breakthrough curves in Figure 3.26 show the response of the wells to 100% chloride reduction within the entire study area. Although this scenario is unrealistic in an urban area, it does illustrate a "best-case" remediation scenario to compare aquifer/aquitard characteristics. Figures 3.18-6 and 3.19 show that chloride is no longer a threat to any of the wells, but still remains trapped within the aquitard.

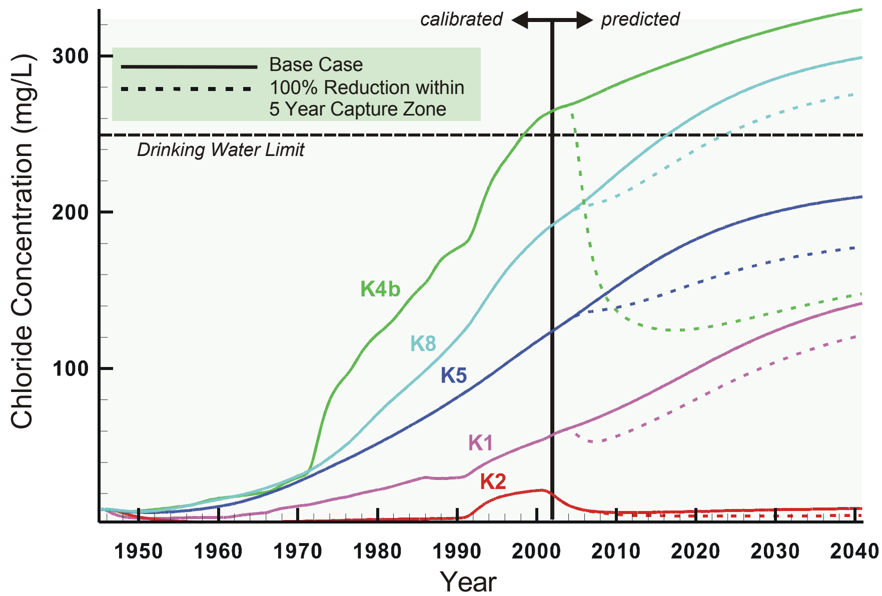

Figure 3.23. Breakthrough curves for wells, Scenario 3.

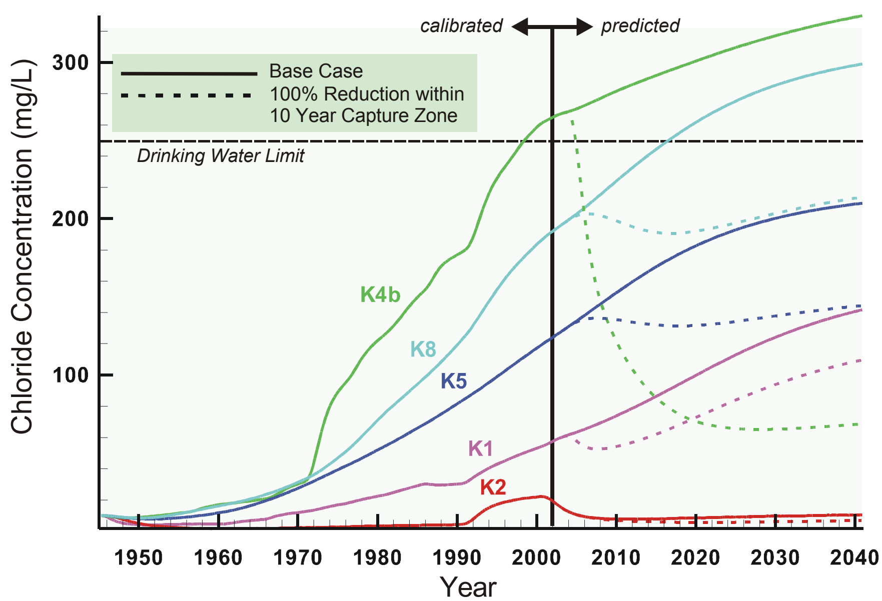

Figure 3.24. Breakthrough curves at wells, Scenario 4.

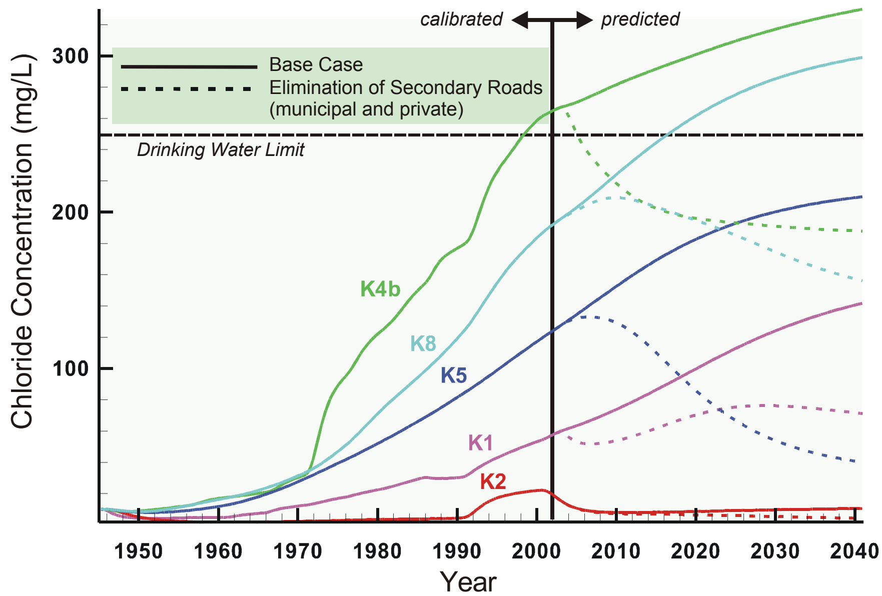

Figure 3.25. Breakthrough curves, Scenario 5.

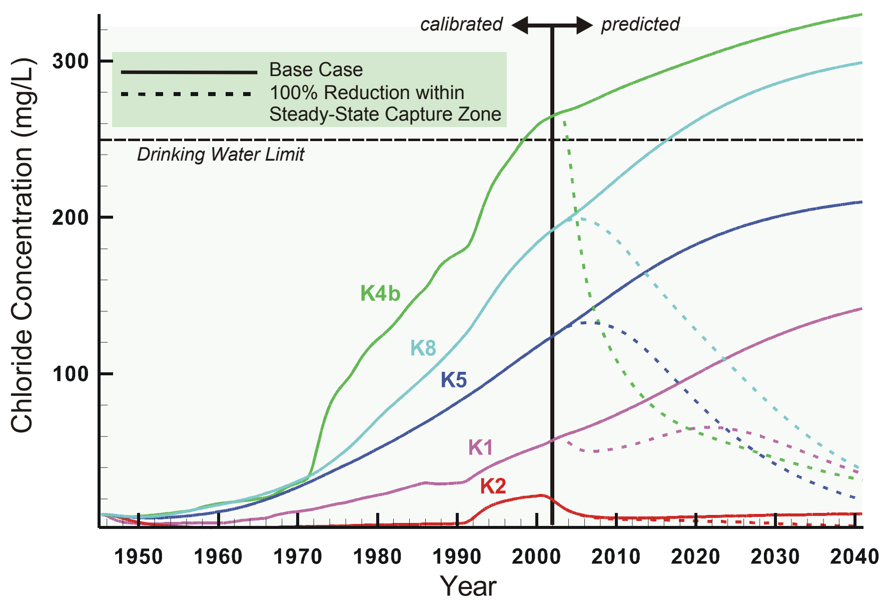

Figure 3.26. Breakthrough curves for Scenario 6.

3.4 Discussion

The observed increase in chloride concentrations at the Greenbrook wells was reproduced with acceptable accuracy by the transport model assuming reasonable chloride loading rates applied to a growing road network. These 57-year simulation results show that the well field is protected to some degree by the fact that it is located in a park, but high conductivity fields within the protecting aquitards allow pathways for chloride to migrate from surface sources to the middle pumped aquifer. Further, the simulation results suggest that some wells may not have reached their maximum chloride concentrations. After 57 years of road salt application, large quantities of chloride remain in the top aquitard, moving very slowly through it.

The effect of eliminating the chloride source at years 2002 or 2003 and projected to the year 2041 have been examined. In all scenarios, recharge entering the domain at the surface allows fresh water to flush through the upper aquifer, reducing the chloride concentrations. As well, the plumes in the deeper layers have the time to mix with fresh water and dilute the overall chloride plumes to some degree. Nevertheless, in all of the simulations, significant amounts of chloride remain within the lower conductivity aquitards.

Well K4b showed the most sensitive response to the source elimination and the approaching plumes that were previously a threat to this well are diluted significantly with fresh water. The sensitivity of well K4b shows both the effect of the higher pumping rate of this well in comparison to the others, and also that the plume that threatens this well is hydraulically well-connected to the surface. As such, well K4b shows the most sensitive response to sudden increases or decreases in the source function. Other wells show similar, although delayed responses. Although it is difficult to resolve the individual characteristics of the simulated responses in each well, the simulations suggest that chloride concentrations of wells with higher pumping rates respond rapidly.

Each scenario showed varying degrees of response to chloride reduction (Figure 3.27). These responses are measured collectively by using a weighted average of the wells in regard to their pumping rates for each scenario. This weighted average could also be recognized as the concentration of the water in the Greenbrook reservoir. Reducing overall chloride application by 25%, either immediately at 2002, or gradually from 2002-2007, resulted in decreased concentrations of chloride in the wells, but over time these concentrations are still increasing, indicating that the plumes have not reached steady-state conditions. Reducing chloride within the 5- and 10-year capture zones resulted in an even more dramatic reduction in chloride at the wells, however chloride originating from a source outside of each of the capture zones reaches the wells at the end of the 5- or 10-year travel time frame and chloride concentrations begin to rise again. A study of mass input into the model (Table 3.5) also reveals that these two scenarios inject more mass into the system than the 25% reduction scenarios, indicating that much more chloride mass has yet to reach the wells.

On the other hand, elimination of road salt application on secondary roads, or elimination of road salt application from the entire study area results in a decreasing trend in chloride levels in the wells. Although eliminating chloride from secondary roads would be difficult to accomplish, this scenario does illustrate that secondary roads have a dramatic effect on the amount of chloride mass in the subsurface. This may be attributed to the fact that although less chloride per 2-lane km is applied onto secondary roads than onto primary roads, they make up for a substantial portion of the total road length. In any case, further reduction and limited use of chloride on municipal and private roads could aid in the remediation of the Greenbrook wells. Although the 57-year simulation results (1945-2002) show that the problem of road salt contamination in the wells is serious, source cut-off results (2002-2041) show that the water quality can be mitigated with a viable remediation strategy in place.

Year Ending	S 1	S 2a	S 2b	S 3	S 4	S 5	S 6
2000	1.3327	1.3327	1.3327	1.3327	1.3327	1.3327	1.3327
2002	1.4641	1.46408	1.46395	1.46410	1.46410	1.46334	1.46230
2003	1.5291	1.52720	1.51771	1.52910	1.52908	1.50004	1.46230
2010	1.99670	1.91067	1.87489	1.99275	1.98785	1.75659	1.46230
2020	2.67070	2.41850	2.38175	2.66110	2.64910	2.12377	1.46230
2041	4.08790	3.48240	3.44540	4.06650	4.03970	2.89500	1.46230

Table 3.5. Total chloride mass (10^8 kg) input into the 3D model (not including background mass)

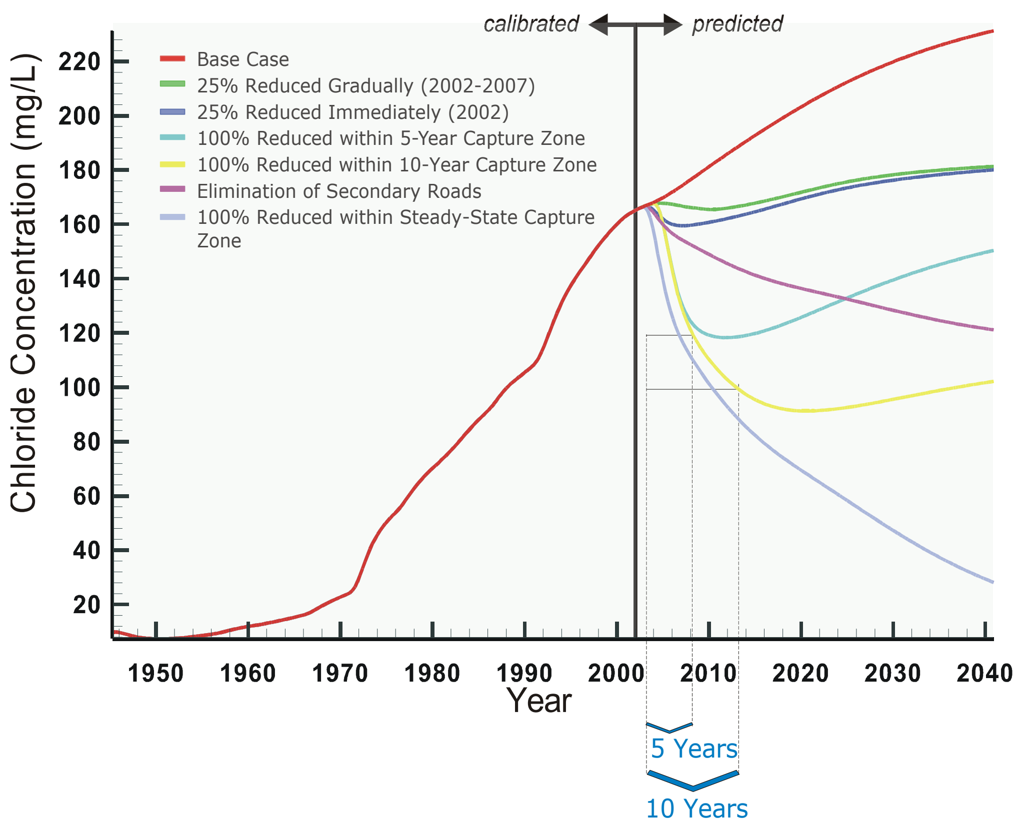

Figure 3.27. Weighted average of breakthrough curves for all scenarios.

Chapter 4

Conclusions

4.1 Summary

The two objectives of this thesis were to characterize the migration of chloride in the unsaturated zone under seasonal influences of variable recharge and variable chloride loading, and to examine a variety of remediation scenarios for the Greenbrook wells through 3-D modelling. This research has provided new insights into the behaviour of chloride contamination in groundwater through the development of a 2D variably-saturated flow and transport model and an advanced 3D full-scale transport model.

The first objective was accomplished by utilizing the 2D unsaturated-saturated model SWMS_2D. In order to characterize the behaviour of chloride in this way, the code was modified to incorporate variable source loading and variable atmospheric conditions. Simulations showed strong influxes of chloride during the spring season when precipitation and road salt applications are high. Chloride reached the water table within 150 days of travel, however the bulk of the chloride concentrations remained suspended in the unsaturated zone, consistent with findings in the field.

Simulations also showed that as the system reaches steady-state, chloride "pulses" due to seasonal fluctuations are dampened with depth. Near the surface, breakthrough curves largely reflect chloride and precipitation variations. However, closer to the water table, these responses are less prominent, and loading to the water table is more or less uniform. It is therefore concluded that long-term chloride modelling (the second phase of this research) can neglect seasonal variations in source input to the water table.

The second objective of examining the effect of different chloride reduction strategies within the Greenbrook steady-state capture zone was accomplished by incorporating a temporal and spatial type-3 source loading to the top boundary of a 3D transport model. The transport simulation was made by solving the advection-dispersion equation, using the velocity field simulated using the larger Waterloo Moraine model [*Frind and Molson, 2002*]. The observed increase in chloride concentrations at the Greenbrook wells was reproduced with acceptable accuracy by the transport model assuming reasonable chloride loading rates applied to a growing road network within the steady-state capture zone.

Seven scenarios, representing various remediation options were simulated. Chloride reduction impacts were quantified by both breakthrough curves of the concentrations at the wells, and mass input to the water table. It was found that for a rapid decline in chloride concentrations in all the wells, replacing NaCl with a less harmful de-icing agent within the 5- or 10-year capture zone is the best solution. However, this solution will not stop the chloride concentrations from increasing again after the 5 or 10 year time period. To control the rise in chloride, reducing chloride application by 25% will suffice, keeping the average concentration below 250 mg/L until the end of the simulation period at 2041 days.

4.2 Recommendations for Implementation of Remediation Strategies

In order to reduce chloride contamination in the Greenbrook wells, it is recommended that salting of secondary roads be eliminated wherever possible, or de-iced with a salt/sand mixture, as these secondary roads make up a large portion of the mass of chloride within the subsurface. Combinations of the remediation scenarios could easily mitigate chloride contamination in the Greenbrook wells. In particular, eliminating salting on some minor streets in addition to the 25% reduction strategy already in place, combined with eliminating road salt application from within the 10-year capture zone is recommended. However, it is unknown whether or not eliminating application is cost effective; using an alternative de-icer in this area would require special equipment and salting procedures, which may not be worth implementing in such a small area.

The simulation results also suggest that the well field is protected to some degree by the fact that it is located in a park, but high conductivity fields within the protecting aquitards allow pathways for contaminants to migrate from surface sources to the middle pumped aquifer. These results have implications for other well fields, such as those located in rural areas, and highlight the need to protect these well fields from urbanization.

Although individual well remediation was not studied, it is clear that those with higher pumping rates react rapidly to changes in chloride loading. This should be considered when evaluating the water quality of each well and future decision-making.

Although the simulation results show that the problem of road salt contamination in the wells is serious, source cut-off results show that the problem is fixable with a viable remediation strategy in place. It should be noted, however, that these simulations are not meant to be used as absolute predictions, but should be used to gain insight to the relative differences of each remediation solution as a tool in an overall cost-benefit analysis.

4.3 Recommendations for Further Study

It is recommended that the unsaturated model presented here be further developed to reproduce a 2D "real-life" site-characteristic of the Greenbrook well field, and calibrated using field work completed by *Stantec* [2001]. Processes such as evapotranspiration, root uptake, freeze/thaw mechanisms of the soils, delayed loading due to snowpack accumulation, and possibly even reduced porosity in the unsaturated zone due to "crusting" of the salts in the subsurface should be considered to enhance understanding of these processes and their importance on chloride migration to the water table.

It is recommended that further research be conducted to verify the source loadings used in this model. For example, a number of distinctive years where the application rates were known to have changed significantly could be chosen and the application rates could accurately be quantified by accessing archived road salt requisition forms for each jurisdiction. Although this would be too exhaustive to accomplish on a yearly basis, it may be valuable to research a select number of years to compare to the modelling results in this research and scale concentrations accordingly. In addition, it may be worthwhile to account for surface water in the study area, or in future study areas for simulations of this type.

In this work, impacts to individual wells were difficult to assess because of the inability to calibrate to them. This is due to the use of the hydraulic conductivity field that was calibrated using the larger Waterloo Moraine model, for which localized detail of the aquifer material near the Greenbrook wells was not available.

To improve this, it is recommended that the flow model be recalibrated using not only observed head data, but also chloride concentration data, with local hydraulic conductivity and recharge re-evaluated.

Bibliography

Bear, J., *Dynamics of fluids in porous media*, Dover Publications Inc., New York, NY, 1972.

Beckers, J., and E. O. Frind, Simulating groundwater flow and runoff for the Oro Moraine aquifer system: 2. Automated calibration and mass balance calculations, *Int. J. Num. Anal. Meth. Geom. in Submission*,, 2000.

Béland, A., Management of the Greenbrook Well Field, M.Sc. Thesis, Department of Earth Sciences, University of Waterloo, 1977.

Burnett, R. D., and E. O. Frind, Simulation of contaminant transport in three-dimensions: 1. The Alternating Direction Galerkin Technique, *Water Resour. Res.*, *23*(4), 683–694, 1987.

Callow, I. P., Optimizing Aquifer Production for Multiple Wellfield Conditions in Kitchener, Ontario, M.Sc. Thesis, Dept. of Earth Sciences., University of Waterloo, 1996.

Canadian Council of Ministers of the Environment (CCME). Canadian water quality guidelines (rev. ed.), 1997.

Celia, M. A., E. T. Bouloutas, and R. L. Zarba, A general mass-conservative numerical solution for the unsaturated flow equation, *Water Resour. Res.*, *26*(7), 1483–1496, 1990.

CEPA. Canadian environmental protection act, 1999.

Ch2M-Hill Engineering Ltd., Technical Report, Draft - Annual Report for Greenbrook Well Field Monitoring Program, 1995.

Chapman, L. J., and D. F. Putnam, *The physiography of southern Ontario*, Ontario Geological Survey, Special Volume 2, 1984.

Davis, L. A., and S. P. Neuman, UNSAT2 - Variably Saturated Flow Model, Technical Report WWL/TM-1791-1, Water, Waste and Land, Inc., Ft. Collins, Colorado, 1983.

Environment Canada, Atmospheric Environment Service, Canadian Climate Normals - Ontario, 1961-1990, 1993.

Environment Canada, Technical Report, Priority Substances List Assessment Report: Road Salts, Environment Canada and Health Canada, 2001.

Farvolden, R., and M. Weitzman, Technical Report, Greenbrook Well Field Study, University of Waterloo, Waterloo, Ontario, 1980.

Frind, E. O., D. S. Muhammed, and J. W. Molson, Delineation of three-dimensional well capture zones for complex multi-aquifer systems, Submitted to Ground Water, August 15, 2001.

Fritz, S. J., R. J. Drimmie, and P. Fritz, Characterizing Shallow Aquifers Using Tritium and ^{14}C: Periodic Sampling Based on Tritium Half-Life, *Applied Geochemistry*, *6*, 17–33, 1991.

Frost, L. R., S. J. Pollock, and R. F. Wakelee. Hydrogeologic Effects of Highway De-Icing Chemicals in Massachusetts, 1981.

Gartner Lee Ltd., M. M. Dillon. Ltd., J. W. Molson, and E. O. Frind. Detailed Delineation of Capture Zones, Greenbrook Well Field, Kitchener, Ontario, 1998.

Gerber, R., and K. Howard, *Groundwater to the Oak Ridges Moraine*, 173–192. St. John's, Newfoundland, Geological Association of Canada, 1997.

Gutiw, P., and Y. C. Jin, Roadside Salinity Changes Generated by Pavement Deicing Practices on a Saskatchewan Highway, in Deicing and Dustbinding - Risk to Aquifers, edited by T. Nystén, and T. Suokko, 23–30, Finnish Environment Institute, P.o. Box 140, FIN-00251, Helsinki, Finland., 1998.

Howard, K. W. F., J. I. Boyce, S. J. Livingston, and S. L. Salvatori, Road Salt Impacts on Groundwater Quality - The Worst is Still to Come!, *GSA Today*, *3*, 301,319–321, 1993.

Howard, K. W. F., and J. Haynes, Urban Geology 3. Groundwater Contamination Due to Road De-Icing Chemicals - Salt Balance Implications, *Geoscience Canada*, *20*, 1–8, 1993.

Huling, E., and T. Hollocher, Groundwater Contamination by Road Salt: Steady-State Concentrations in East Central Massachusetts, *Science*, *176*, 288–290, 1972.

Jones, P. H., B. A. Jeffrey, P. K. Watler, and H. Hutchon. Environmental Impact of Road Salting - State of the Art, Ministry of Transportation and Communications, Downsview, Ontario, 1986.

Kivimäki, A.-L., Road Salting and Groundwater - A Risk Assessment Model, in Salt Groundwater in the Nordic Countries, Proceedings of a Workshop, Sept. 30 - Oct. 1, 1992, Number NHP Report No. 35, Saltsjäbaden, Sweden, 1994.

Locat, J., and P. Gélinas, Infiltration of De-Icing Road Salts in Aquifers: The Trois-Riverières-Ouest Case, Quebec, Canada, *Can. J. Earth Sci.*, *2193*, 2186, 1989.

Martin, P. J., and E. O. Frind, Modeling a Complex Multi-Aquifer System: The Waterloo Moraine, *Groundwater*, *36*(4), 679–690, 1998.

McConnell, H., and J. Lewis, Add salt to taste, *Environment*, *14*(9), 38, 1972.

Mendoza, C. A., R. Therrien, and E. A. Sudicky. *ORTHOFEM User's Guide, Version 1.02*. Waterloo Centre for Groundwater Research, Waterloo, Ontario, 1991.

Molson, J. W., J. Beckers, P. J. Martin, and E. O. Frind. *A Three-Dimensional Groundwater Flow Model with Modules for Automated Calibration and Parameter Sensitivity Analysis*. Waterloo, Department of Earth Sciences. WATFLOW/3D Version 2.0, 2002.

Mualem, Y., A new model for predicting the hydraulic conductivity of unsaturated porous media, *Water Resour. Res.*, *12*(3), 513–522, 1976.

Muhammad, D., Methodologies for Capture Zone Delineation for the Waterloo Moraine Well Fields, M.Sc. Thesis, Dept. of Earth Sciences, University of Waterloo, 2000.

Neuman, S. P., Finite element computer programs for flow in saturated-unsaturated porous media, Second Annual Report, Part 3 Project No. A10-SWC-77,87p., Hydraulic Engineering Lab., Technion, Haifa, Israel, 1972.

Neuman, S. P. Saturated-unsaturated seepage by finite elements. J. Hydraul. Div., ASCE, 99 (HY12), 2233-2250, 1973.

Neuman, S. P., *Galerkin Approach to Saturated-Unsaturated Flow in Porous Media*, John Wiley and Sons, London, 1975.

Neuman, S. P., R. A. Feddes, and E. Bresler, Finite element simulation of flow in saturated-unsaturated soils considering water uptake by plants, Third Annual Report A10-SWC-77, Hydraulic Engineering Lab., Technion, Haifa, Israel, 1974.

Novotny, V., D. W. Smith, D. A. Kuemmel, J. Mastriano, and A. Bartošová, Urban and highways snowmelt: Minimizing the impact of receiving water, Technical Report Project 94-IRM-2, Water Environment Research Foundation, 1999.

Nystén, T. Personal Communication, 2001.

Paine, L., Chlorides in the don river watershed resulting from road de-icing salt, Technical Report Working Paper Pub. No. SIC-3, University of Toronto, Institute of Environmental Studies Snow and Ice Working Group, 1979.

Perchanok, M. S., D. G. Manning, and J. J. Armstrong, Highway de-Icers: Standards, Practice and Research in the Province of Ontario., Technical Report MAT-91-13, Ontario Ministry of Transportation, Research and Development Branch, 1991.

Pilon, P., and K. Howard, Contamination of subsurface waters by road de-icing chemicals, *Water Pollution*, *22*, 157–171, 1987.

Pollock, S., Remediating Highway De-Icing Salt Contamination of Public and Private Water Supplies in Massachusetts, *Resources, Conservation and Recycling*, *7*, 7–24, 1992.

Regional Municipality of Waterloo. Personal Communication, 2002.

Sanford, B. V., Geology; Toronto-Windsor Area; Ontario, Map 1263A, *Geological Survey of Ontario, Department of Energy, Mines and Resources*,, 1969.

Silliman, S. E., B. Berkowitz, J. Šimúnek, and M. Th. Van Genuchten, Fluid Flow and Solute Migration Within the Capillary Fringe, *Ground Water*, *10*(1), 76–84, 2002.

Šimúnek, J., T. Vogel, and M. Th. Van Genuchten, Technical Report, The SWMS 2D code for simulating water flow and solute transport in two-dimensional variably saturated media, Version 1.1, U.S. Salinity Laboratory, USDA, ARS, Riverside, CA, 1994.

Stantec Consultants Ltd., Technical Report, Road salt management and chloride reduction study, phase 1: Road salt management study, Kitchener, Ontario, 2001.

Toler, L. G., and S. J. Pollock, Retention of Chloride in the Unsaturated Zone, *Jour. Research U.S. Geol Survey*, *2*(1), 119–123, 1974.

Van Genuchten, M. T., A closed-form equation for predicting the hydraulic conductivity of unsaturated soils., *Soil Science Society of America Journal*, *44*, 892–898, 1980.

Vogel, T., SWMII - Numerical Model of Two-Dimensional Flow in a Variable Saturated Porous Medium, Technical Report Research Report No.87, Dept. of Hydraulics and Catchment Hydrology, Agricultural University, Wageningen, The Netherlands, 1987.

Woeller, R. M., and R. N. Farvolden, The Past, Present and Future of Groundwater Development in the Tri-Cities of Kitchener, Waterloo and Cambridge, Ontario, Canada, in Proceedings of the NWWA FOCUS Conference on the Regional Groundwater Issues, Kitchener, Ontario, 1989.

Appendix A:

.

Road Network Growth 1945-2000

A total of 12 plan-view maps were created to represent the different stages of road growth within the study area. Five-year intervals from 1945 to 2000 were recreated and are given on the following pages.

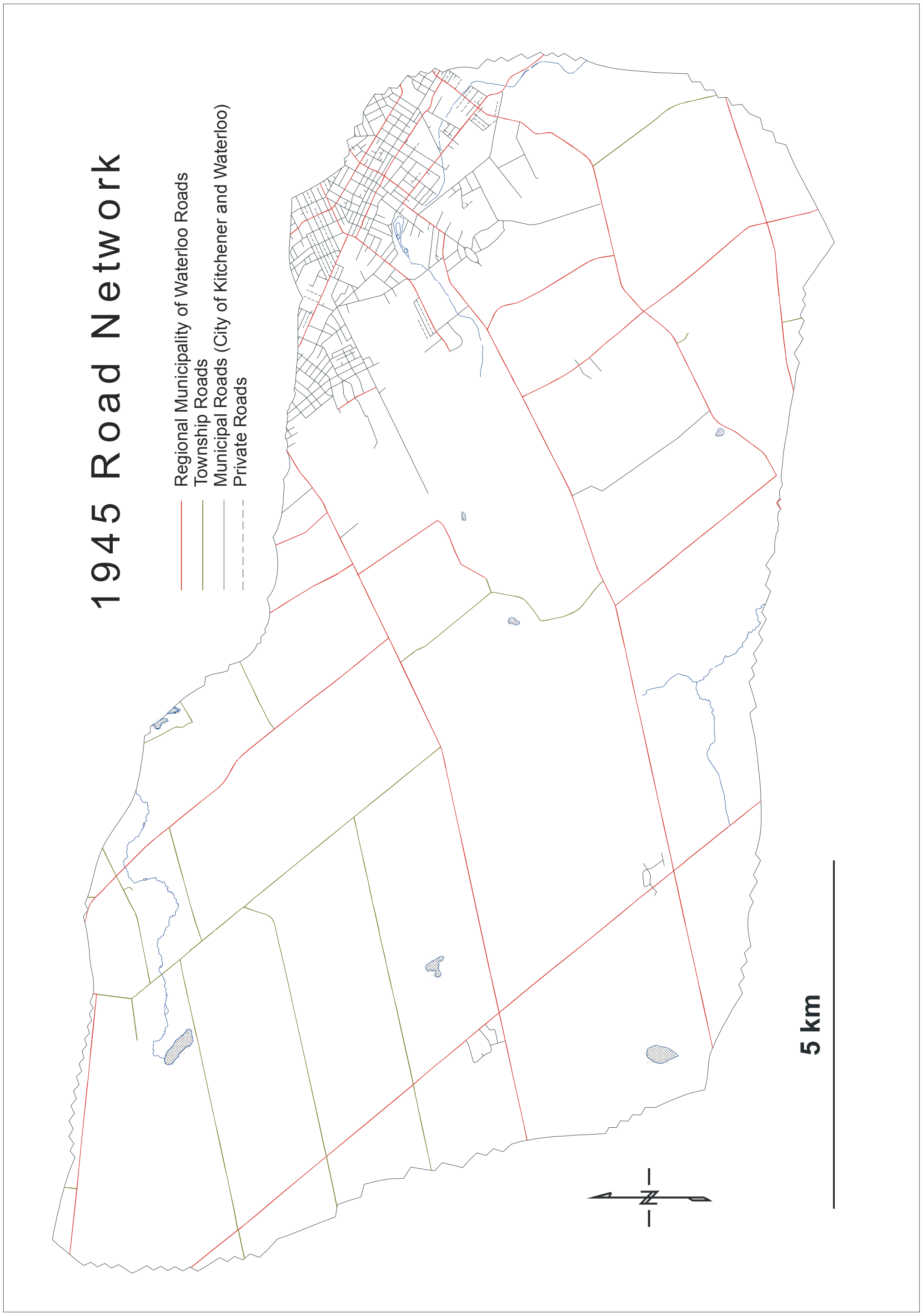
1945 Road Network
Regional Municipality of Waterloo Roads
Township Roads
Municipal Roads (City of Kitchener and Waterloo)
Private Roads
5 km
N

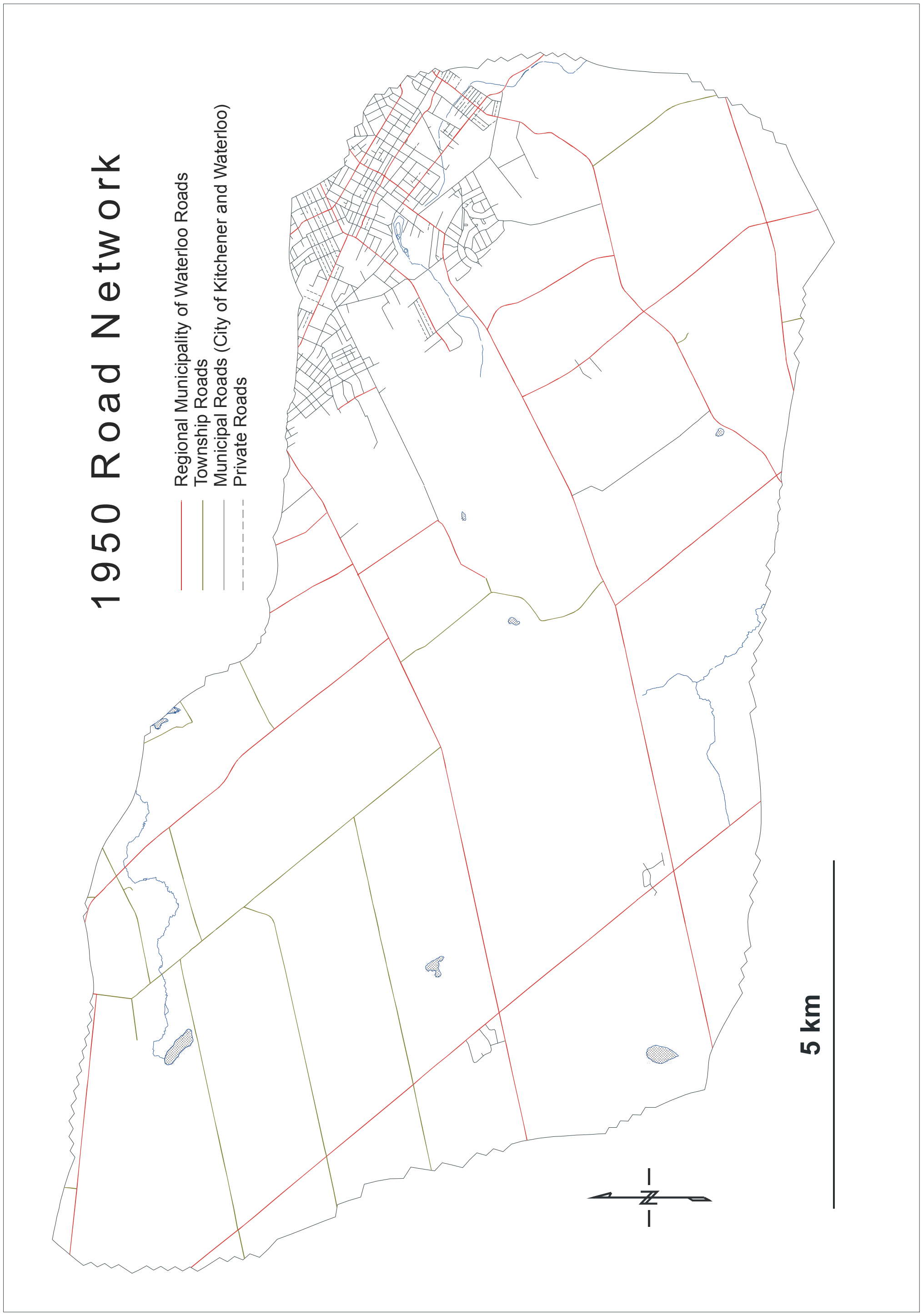
1950 Road Network
Regional Municipality of Waterloo Roads
Township Roads
Municipal Roads (City of Kitchener and Waterloo)
Private Roads
5 km
N

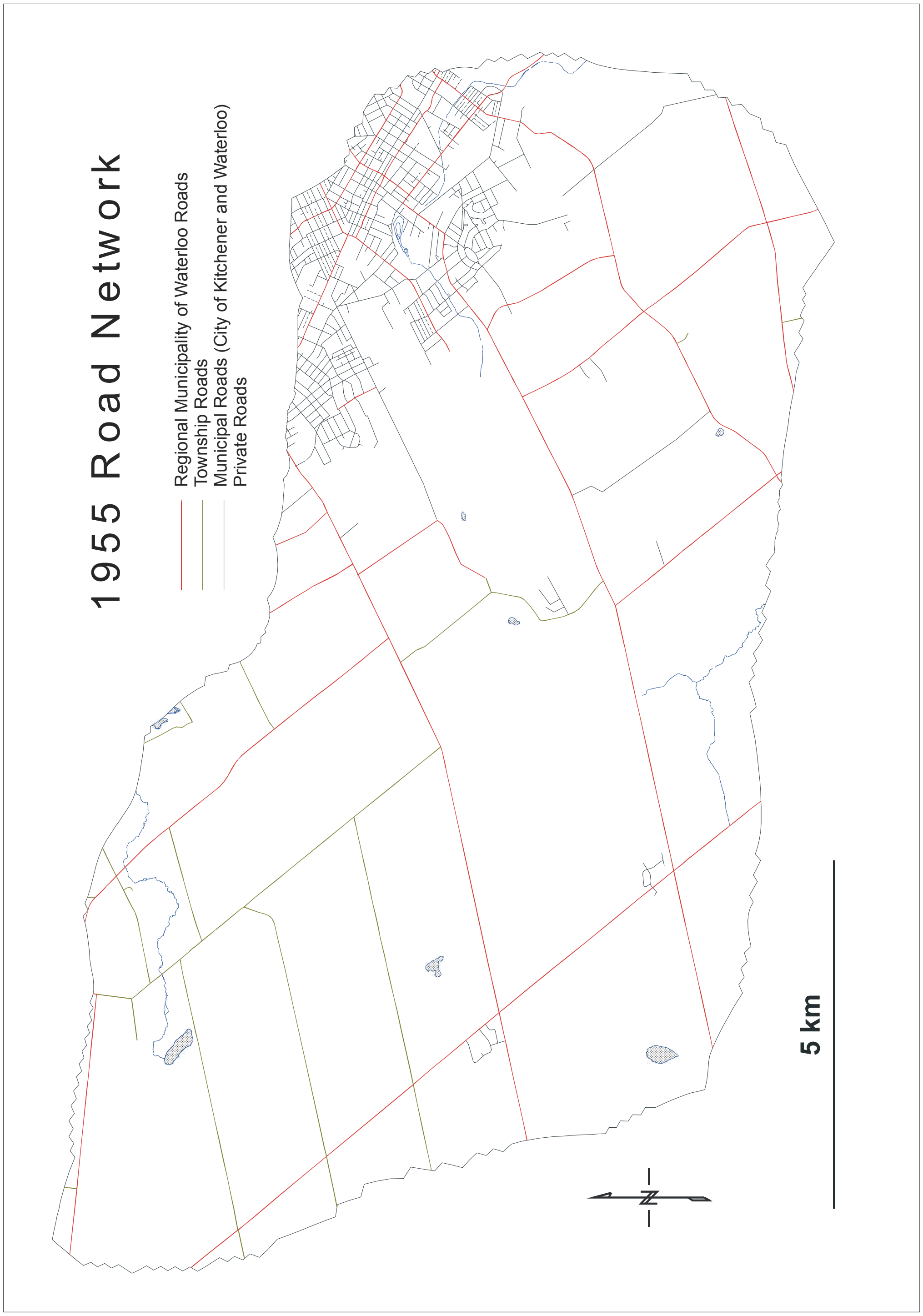
1955 Road Network
Regional Municipality of Waterloo Roads
Township Roads
Municipal Roads (City of Kitchener and Waterloo)
Private Roads
5 km
N

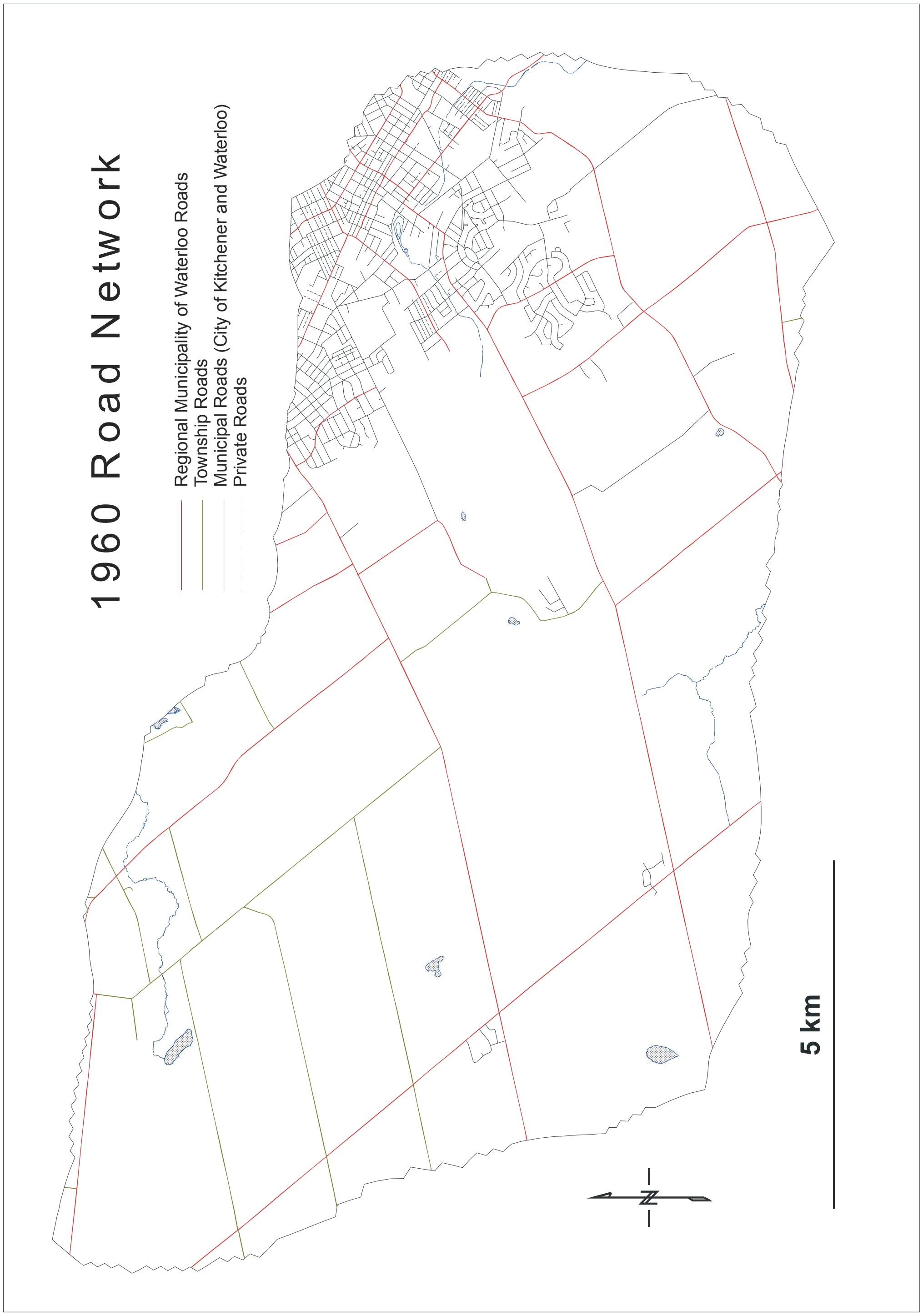
1960 Road Network
Regional Municipality of Waterloo Roads
Township Roads
Municipal Roads (City of Kitchener and Waterloo)
Private Roads
5 km

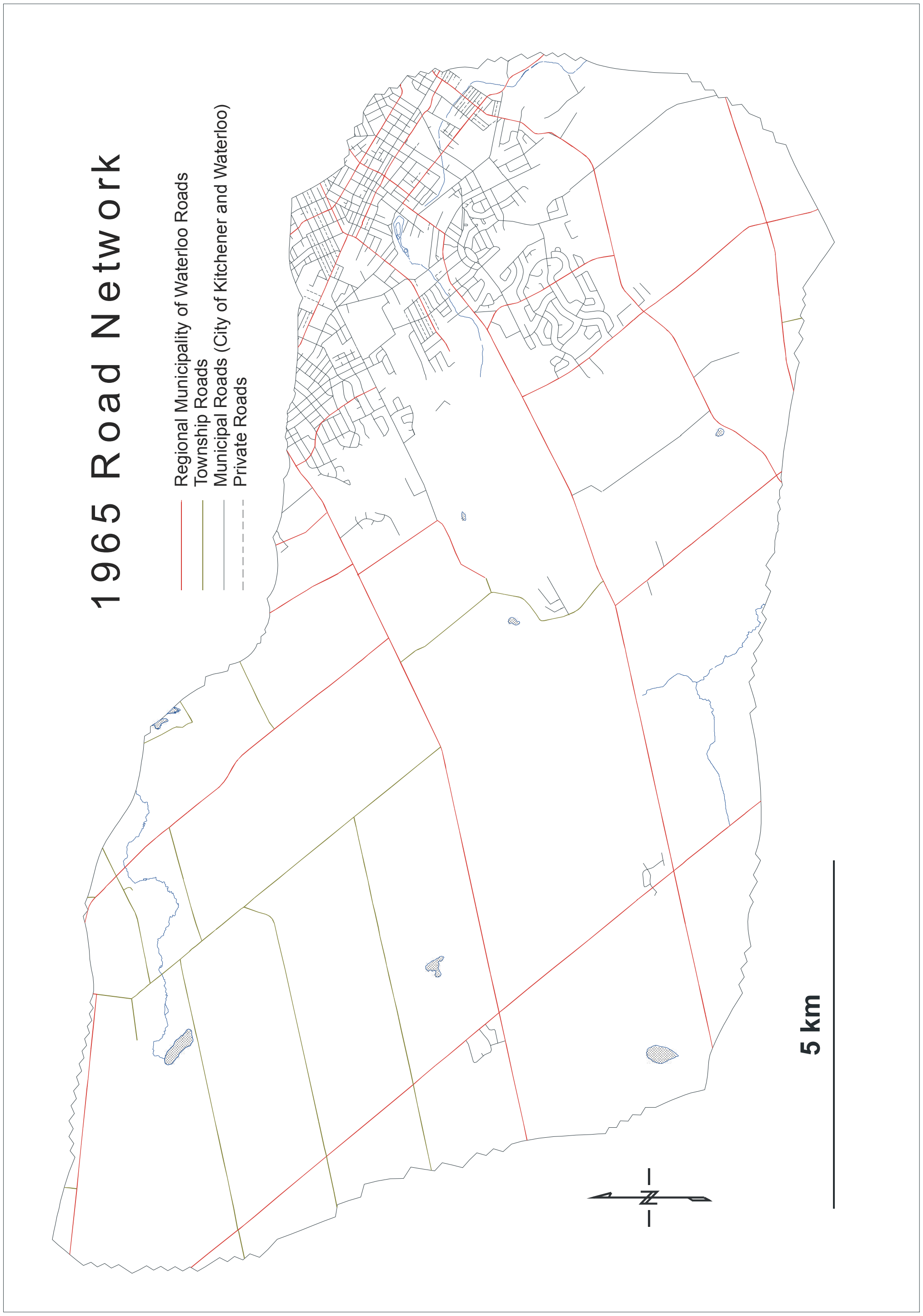
1965 Road Network
Regional Municipality of Waterloo Roads
Township Roads
Municipal Roads (City of Kitchener and Waterloo)
Private Roads
5 km
N

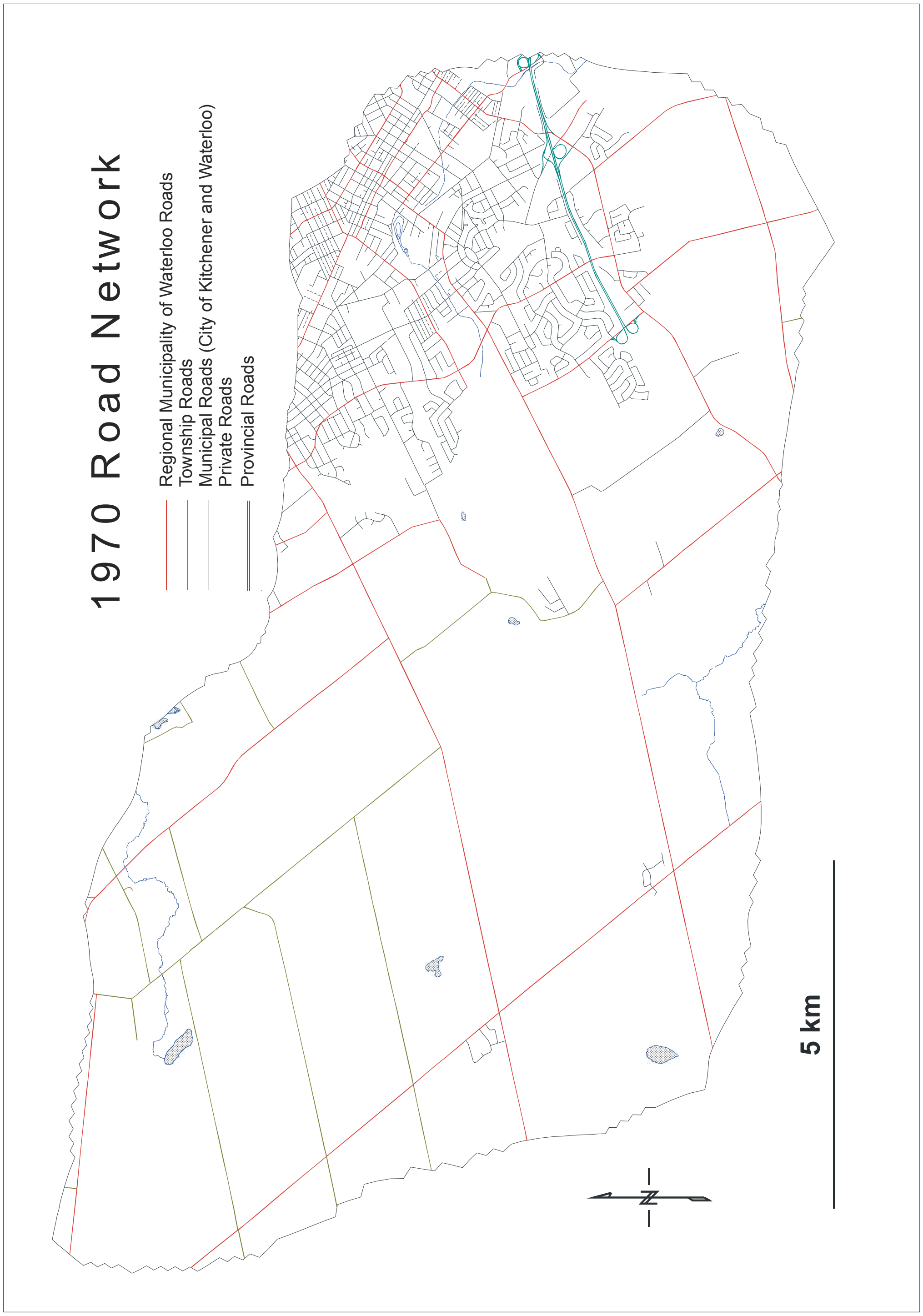
1970 Road Network
Regional Municipality of Waterloo Roads
Township Roads
Municipal Roads (City of Kitchener and Waterloo)
Private Roads
Provincial Roads
N
5 km

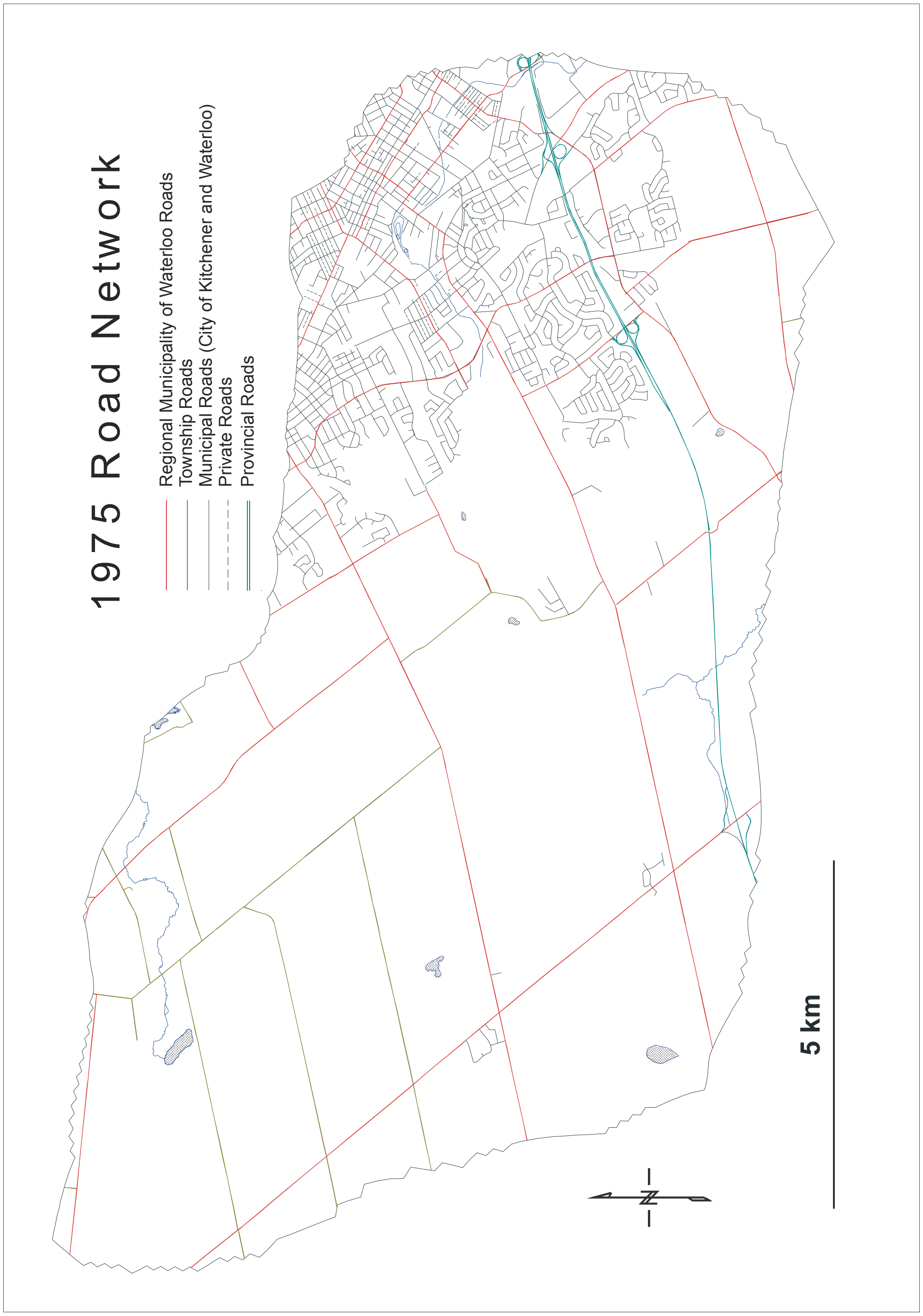
1975 Road Network
Regional Municipality of Waterloo Roads
Township Roads
Municipal Roads (City of Kitchener and Waterloo)
Private Roads
Provincial Roads
N
5 km

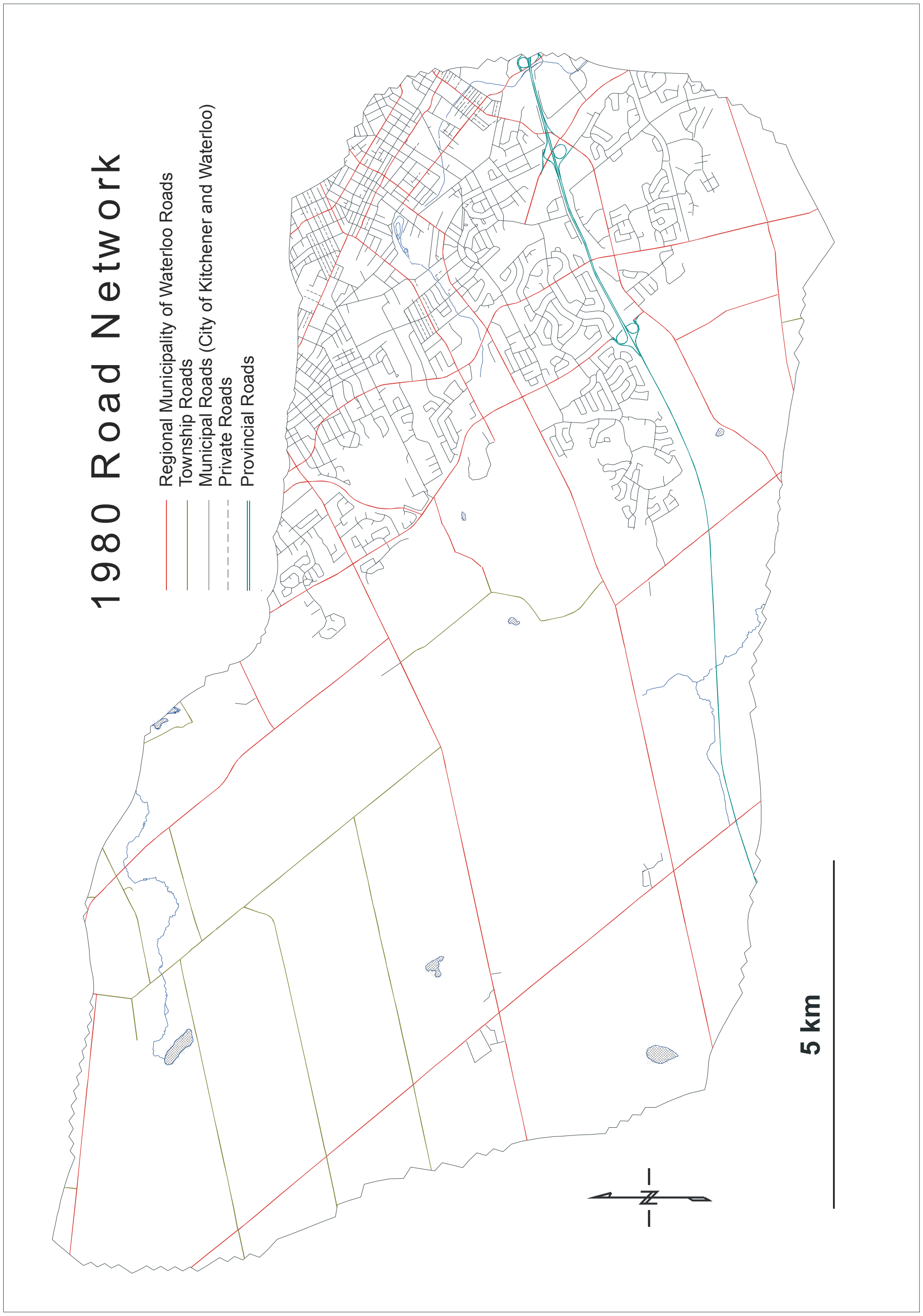
1980 Road Network
Regional Municipality of Waterloo Roads
Township Roads
Municipal Roads (City of Kitchener and Waterloo)
Private Roads
Provincial Roads
N
5 km

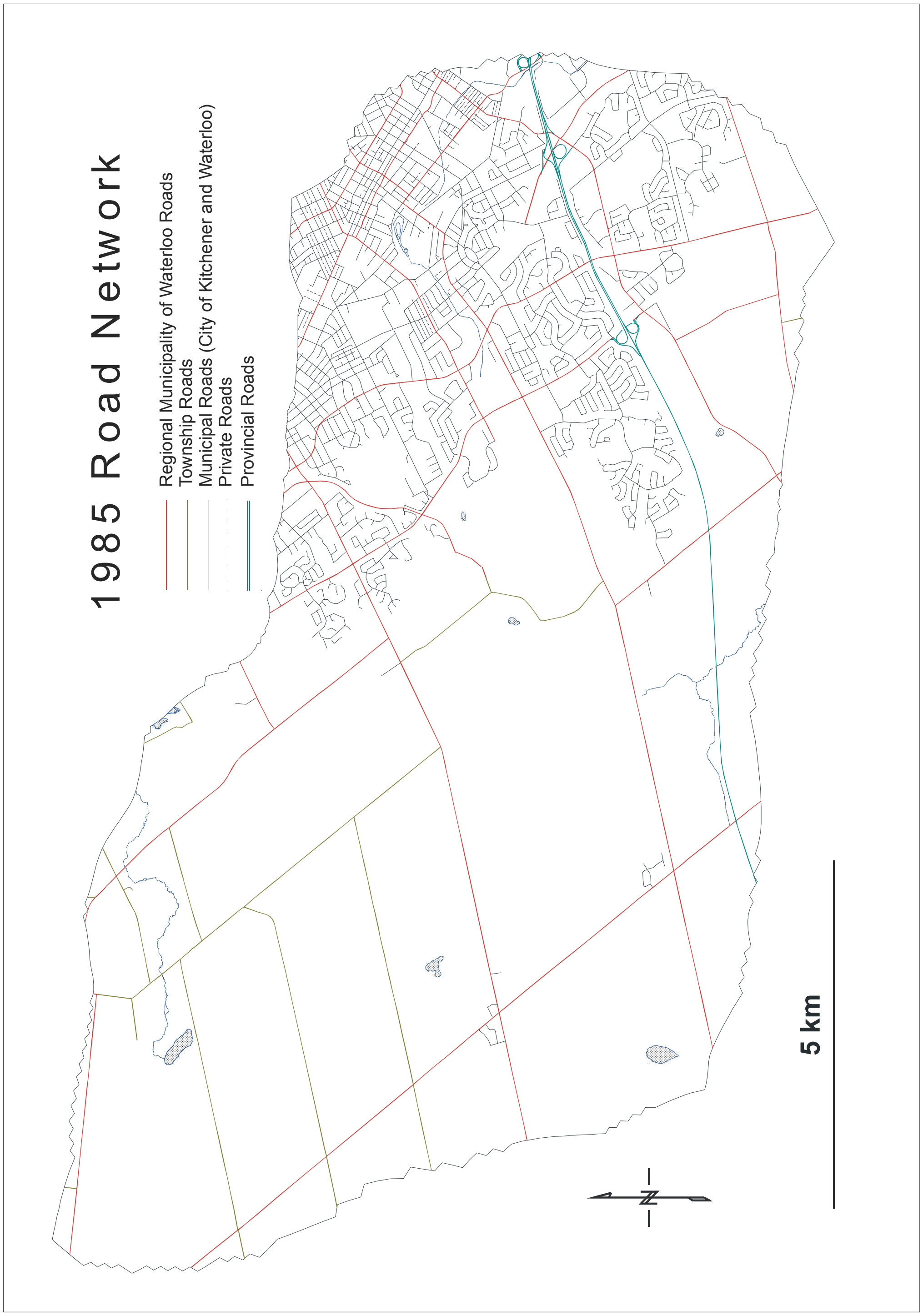
1985 Road Network
Regional Municipality of Waterloo Roads
Township Roads
Municipal Roads (City of Kitchener and Waterloo)
Private Roads
Provincial Roads
N
5 km

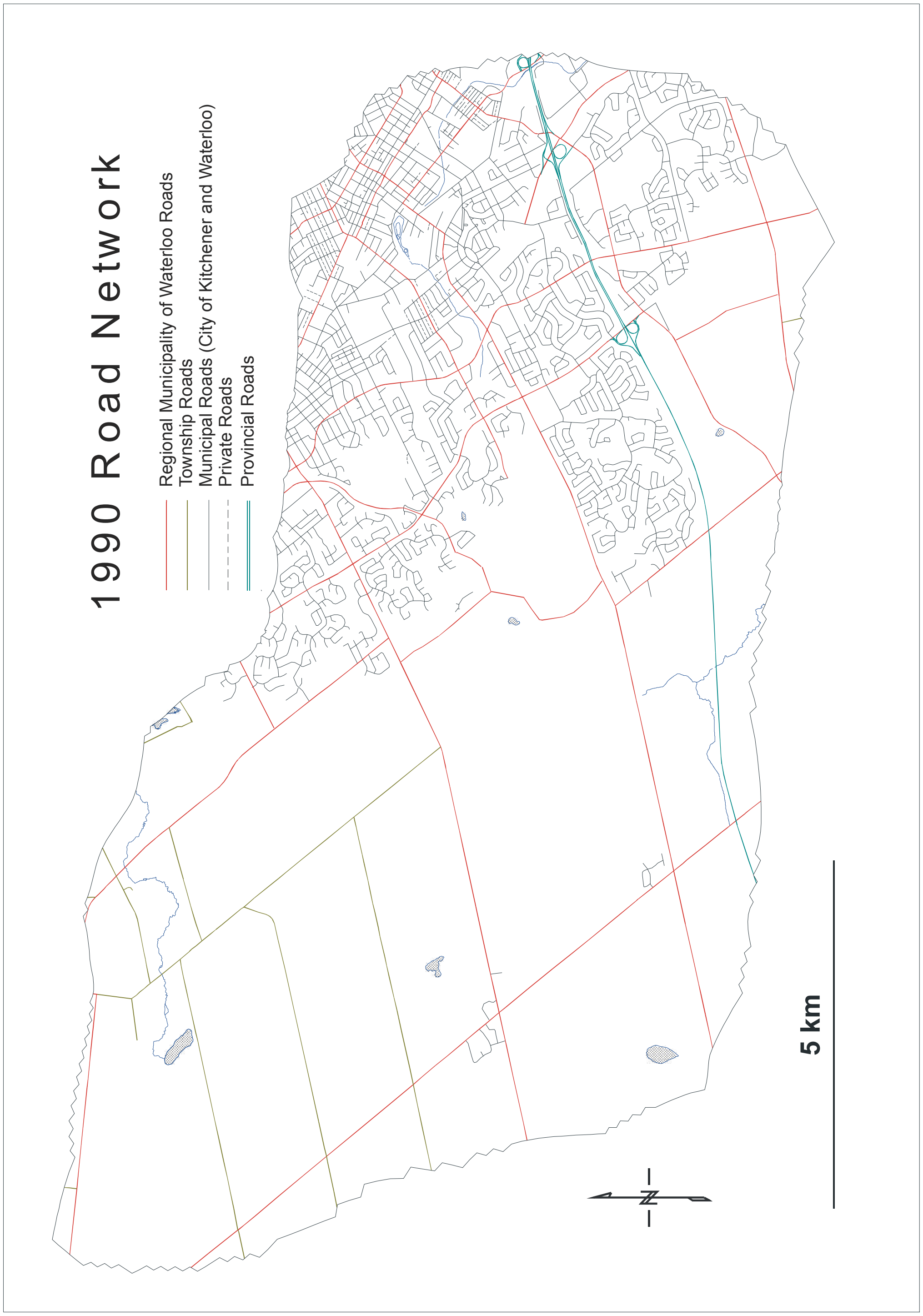
1990 Road Network
Regional Municipality of Waterloo Roads
Township Roads
Municipal Roads (City of Kitchener and Waterloo)
Private Roads
Provincial Roads
N
5 km

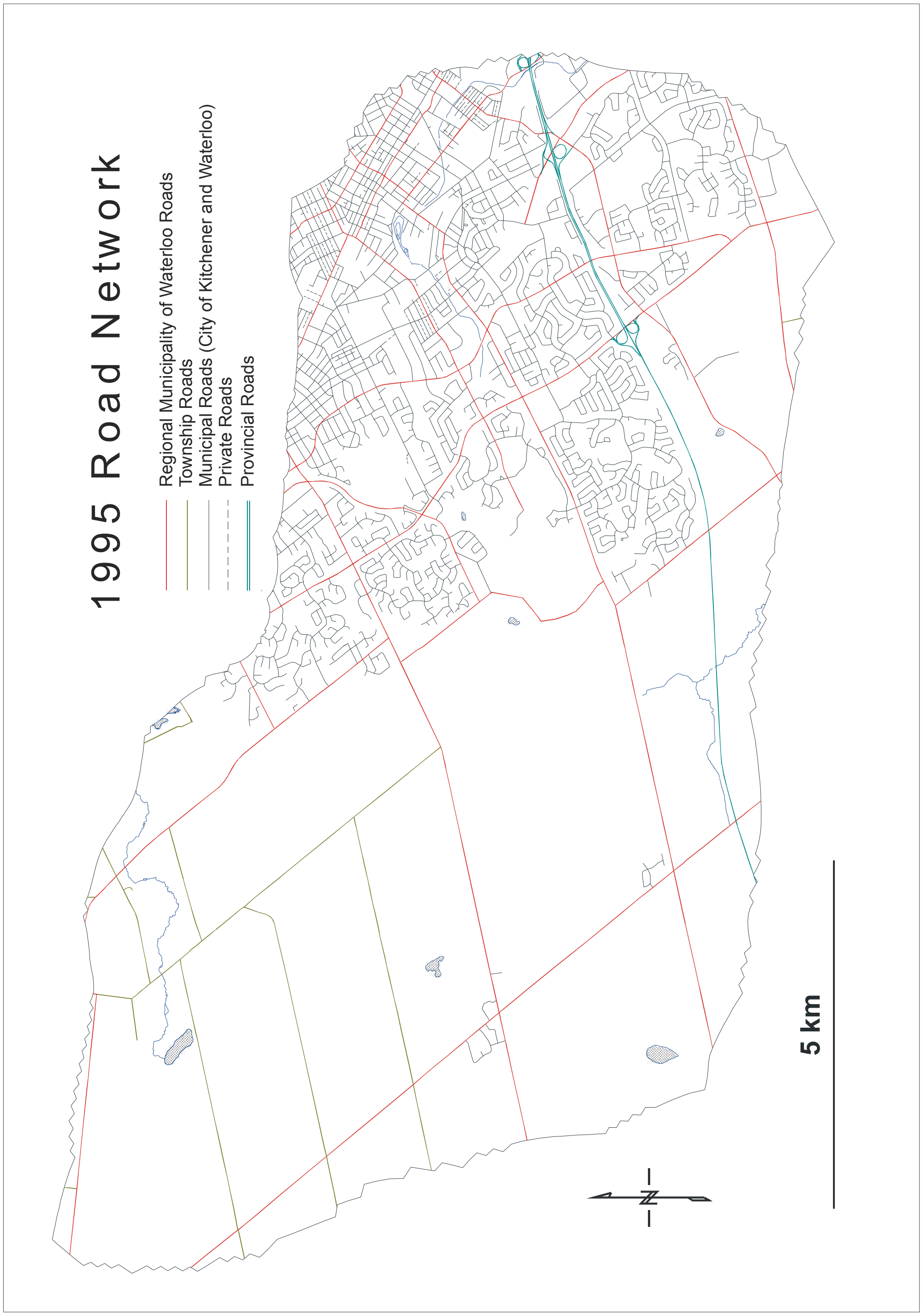
1995 Road Network
Regional Municipality of Waterloo Roads
Township Roads
Municipal Roads (City of Kitchener and Waterloo)
Private Roads
Provincial Roads
5 km
N

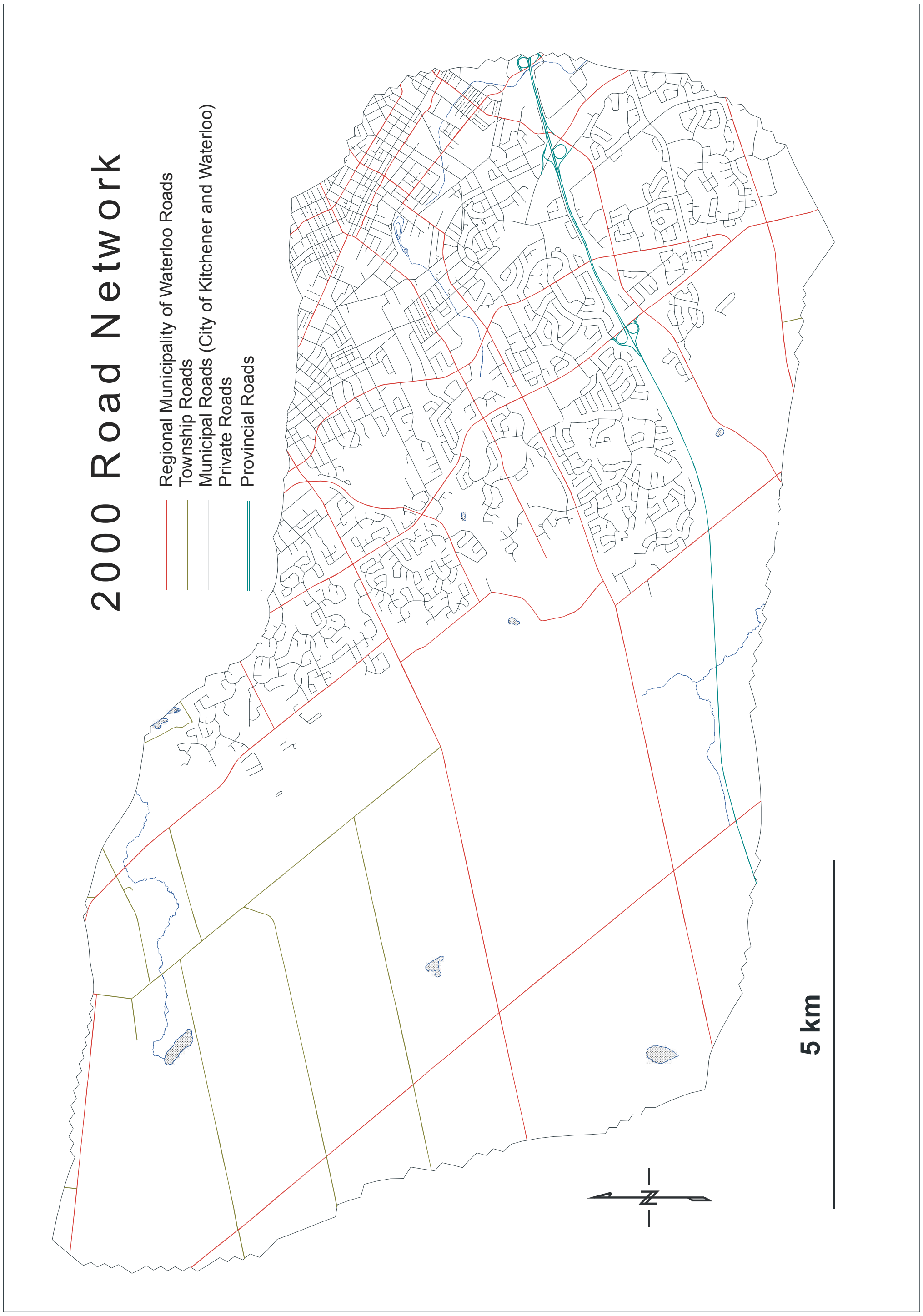
2000 Road Network
Regional Municipality of Waterloo Roads
Township Roads
Municipal Roads (City of Kitchener and Waterloo)
Private Roads
Provincial Roads
5 km
N